DURABILITY OF CONCRETE MADE WITH WASTE GLASS: A SOUTH AFRICAN PERSPECTIVE

BY
LEON MINNIES

A thesis submitted to the Faculty of Engineering and the Built Environment
Department of Civil Engineering and Geomatics
in fulfilment of the requirements for the degree of
Master of Engineering: Civil Engineering at

Cape Peninsula University of Technology

Supervisor: Dr Patrick Bukenya
Co-supervisor: Dr. Philemon Arito

Cape Town
02 October 2025

DECLARATION

I, Leon Minnies, declare that the contents of this thesis represent my own unaided work and that the thesis has not previously been submitted for academic examination towards any qualification. Furthermore, it represents my own opinions and not necessarily those of the Cape Peninsula University of Technology.

October 02, 2025

Signed

Date

DEDICATION

This research is dedicated to God who gave me health and strength to complete this work. To my mother, who taught me that the most useful knowledge is that which is ought for its own sake, and that nothing worthwhile can be accomplished without sacrifice. Lastly, to my supervisors for teaching me that even the largest tasks can be completed step by step.

ABSTRACT

The surge in urban development has driven extensive industrial growth and spurred numerous construction projects, particularly in the provision of affordable housing for low- and middle-income communities. Urbanisation has brought about an increase in the demand of concrete and its constituent materials such as sand. This has resulted in a reduction in the quantity of available natural sand. Urbanisation brings about a demand for concrete and its constituent materials. However, the supply of constituent materials such as sand is limited. Places such as Cape Town have limited resources. As a result, glass has to be sourced from far. And because Glass has to be sourced from fire and is limited, it means that the cost of construction and producing concrete is going to increase. However, something like glass has the same properties as sand, so glass can be used as a partial replacement. In addition to that, glass is also non-biodegradable, therefore incorporating it into concrete as a partial replacement for sand also will help to address municipal solid waste management challenges.

A controlled experiment using laboratory-made concrete mixes was conducted. Three replicates were used throughout the testing. Waste glass was used as a partial replacement for sand – at replacement levels of 10% and 20% – in concrete mixes with w/c ratios of 0.50 and 0.66. Fresh concrete properties that were investigated comprised slump, flow, and vebe time. The hardened properties that were investigated comprised compressive strength at 3, 7, 14, and 28 days, surface resistivity, accelerated drying shrinkage and durability indexes (oxygen permeability index and water sorptivity index). Microstructural and mineralogical analyses of the hardened concrete were also undertaken using scanning electron microscopy, X-ray fluorescence, and X-ray diffraction.

The effect of glass content on the workability of concrete is dependent on w/c ratio. An increase in glass content resulted in a corresponding reduction in slump, a reduction in flow and an increase in vebe time in mixes with a w/c ratio of 0.50; and an increase in slump, an increase in flow, and a reduction in vebe time in mixes with a w/c ratio of 0.66. An increase in glass content also resulted in a corresponding reduction in density (fresh and hardened), and compressive strength of the density of concrete at all ages and drying shrinkage. Glass did not result in a significant increase in the surface resistivity of concrete. The effect of glass on OPI, WSI and macroporosity was not well-defined. The addition of glass in concrete improved the density of the interfacial transition zone and the overall microstructure of the matrix. Glass was observed to densify the concrete microstructure, with a glass content of 10% producing the best microstructure. The matrix of concrete mixes containing glass was also characterised by microcracks. The incorporation of waste glass in concrete holds much potential for use in concrete and would significantly reduce overdependence on natural sand in concrete production,

contribute to efficient municipal solid waste management, and promote environmental sustainability. However, further research on the effect of waste glass – at various water/cement ratios – on hydration, durability, reinforcement corrosion, alkali silica reaction and an in-depth life cycle analysis and life cycle costing is required to evaluate the economic, environmental and long-term performance of glass in concrete.

ACKNOWLEDGEMENTS

I would like to extend my heartfelt gratitude to all the individuals and organisations that contributed to the completion of this thesis:

- My supervisors, Dr Patrick Bukenya and Dr Philemon Arito, for their exceptional guidance and support throughout this project. Their doors were always open whenever I needed advice, and I deeply appreciate their wisdom and inspirational leadership during this journey.
- My mentor, Dr Maphole Loke, for her unwavering confidence in me and her support and encouragement during challenging times.
- Cape Peninsula University of Technology for their financial assistance.
- The Concrete Materials and Structural Integrity Research Unit (COMSIRU), the Department of Civil Engineering, and the University of Namibia's Civil Engineering Department for their invaluable help with laboratory testing.
- PPC Cement, Western Cape, for providing their laboratory facilities and invaluable support and assistance with the laboratory testing.
- AECI Much Asphalt, Western Cape, for their support in supplying materials.
- The staff of CPUT: Mr Snell and Mrs Heuvel, for their invaluable assistance with laboratory preparations, materials procurement, and conference attendance arrangements.
- Dr Orlette Mkhari from the Department of Chemistry at CPUT, for his support in the chemistry laboratory.
- My friends and family for their prayers and emotional and motivational support.
- Lastly, my sincere gratitude goes to God Almighty for giving me strength, courage, and wisdom. I owe the Lord my life for all He has done for me.
- To the many others who have contributed in various ways, though too numerous to mention individually, I am deeply indebted to you all.

Table of Contents

List of figures

List of tables

Nomenclature

Constants

A	Cross-sectional area of test cube (mm²)
a	Probe spacing (cm)
BD	Bulk density of the aggregate particles, expressed in kilograms per cubic meter (kg/m³)
d	Average specimen thickness (mm)
F	Line of best-fit [g/√h]
F	Load at failure (N)
g	Gravitational acceleration = 9.81 m/s²
I	Electrical current (Amps)
L	Length of the specimen at the measured age (mm)
L_0	Initial length of the specimen after curing (mm)
L_1	Initial length of the specimen (measured at 24 hours after casting) (mm)
L_2	Length of the specimen at the measurement age (e.g., 16 days) (mm)
m	Mass of the aggregate in the container (kg)
M_1	Mass of the saturated surface-dry test sample (g)
M_2	Mass of the saturated test sample in water at 25 °C (g)
M_3	Mass of the oven-dried test sample (g)
M_5	Mass of the oven-dried sample (g)
M_6	Mass of the saturated sample (g)
m_a	Mass of the saturated surface-dry aggregate (g)
m_b	Mass of the oven-dried aggregate (g)
m_c	Mass of the pycnometer plus aggregate and water (g)
m_d	Mass of the pycnometer filled with water (g)
Ms_0	Initial mass (g)
M_{sv}	Vacuum saturated mass (g)
M_{wti}	Mass at any given time (g)
n	Number of data points
P_0	Pressure at time t_0 (kPa)
P_{CR}	Cumulative percentage retained.
P_P	Percentage passing
P_t	Pressure reading taken at time t after t_0 (kPa)
t	Time (s)
t_i	Time corresponding to the mass gain reading (h)
V	Electrical potential (Volts)

v	Volume of the container (m^3)
W_{ABS}	Water absorption percentage
z	Slope of the regression line

Greek letters

δ	Bulk density, in (kg/m³)
δ_{pd}	Apparent bulk particle density of the aggregate, in kilograms per cubic metre (kg/m³)
δ_{wT}	Density of the water at the test temperature, T, in kilograms per cubic metre (kg/m³)
ε	Drying shrinkage strain (microstrain)
$\boldsymbol{\theta}$	Absolute temperature (K)
$\boldsymbol{\omega}$	Molar mass of oxygen = 32 g/mol
ρ	Density of concrete in kg/m³
v	Volume of cube in m³

Acronyms and abbreviations

AASHTO	American Association of State Highway and Transportation Officials
ACI	American Concrete Institute
ASTM	American Society for Testing and Materials
BD	Bulk density of the aggregate particles, expressed in kilograms per cubic meter (kg/m^3)
$Ca(OH)_2$	Calcium hydroxide
CaO	Calcium oxide
CBD	Compacted bulk density
CEM	Cement
CG	Coarse glass
CSF	Condensed silica fume
CSH	Calcium silicate hydrate
CO_2	Carbon dioxide
DEA	Department of Environmental Affairs
DI	Durability index
FA	Fine aggregates
FG	Fine glass
FM	Fineness modulus
ITZ	Interfacial transition zone
kN	Kilonewton
kPa	Kilopascals
kg	Kilogram
kg/m^3	Kilogram per cubic meter
mm	Millimetre
MPa	Megapascals
NaCl	Sodium chloride
NaOH	Sodium hydroxide
N/mm^2	Newton per square millimetre
OPC	Ordinary Portland cement
OPI	Oxygen permeability index
P_{CR}	Cumulative percentage retained
P_P	Percentage passing
PPC	Pretoria Portland cement
PSD	Particle size distribution
R	Universal gas constant = 8.313 Nm/K mol
SABS	South African Bureau of Standards

SANS	South African National Standards
SEM	Scanning electron microscopy
SiO_2	Silicon dioxide
UCT	University of Cape Town
UNAM	University of Namibia
UWC	University of the Western Cape
w/c	Water to cement ratio
WG	Waste glass
WGS	Waste glass sand
W_{ABS}	Water absorption percentage
WSI	Water sorptivity index
XRD	X-Ray diffraction

Chapter 1 - Introduction

1.1 Introduction

The surge in urban development, rapid industrialisation and population growth has led to an increase in the generation of waste materials such as glass. Glass, like any other waste, harms the environment by polluting the soil and water. To combat pollution, the glass processing industry has adopted the reuse and processing of waste glass into recycled glass products. Some of the common applications of waste glass comprise glassphalt, fibreglass, cullet, sand-blasting, and aggregate substitute in concrete (Chen et al., 2002; Poon and Wong, 2007; Qaidi et al., 2022). In the construction industry, waste glass is primarily utilised for manufacturing asphalt material for roadworks, geotextiles in pipe laying, manufacturing of paving bricks, decorative aggregate in architectural moulds, and increasingly for concrete production. The use of recycled glass reduces the need to extract natural raw materials for building and frees up landfill space when combined with other recycled materials like fibre and rubber (Rakshvir and Barai, 2006). Glass waste recycling reduces environmental and health risks, including the amount of waste that ends up in municipal landfills.

Waste glass is considered a weaker material in concrete applications primarily due to its lower compressive strength and less effective bonding with the cement matrix, leading to potential durability issues (Meyer, 2001; Poon and Wong, 2007). However, the use of waste glass as a replacement for fine or coarse aggregates in concrete production has gained significant attention over the last decade (Olofinnade and Ede, 2018; Afshinnia and Rangaraju, 2021; Limbachiya, 2009; Abdallah et al., 2014; Kavyateja et al., 2016; Kim et al., 2018; Upreti and Mandal, 2021). Research on the use of glass in concrete production has mainly focused on the effects of waste glass on mechanical strength, durability, workability, thermal insulation, and aesthetics (Harrison et al., 2020; Khan et al., 2020; Poon and Wong, 2007). Olofinnade and Ede (2018), for instance, demonstrated that sustainable eco-friendly concrete can be produced by using waste glass as a partial replacement for sand, achieving optimal results with replacement levels below 25%. Additionally, Afshinnia and Rangaraju (2021) emphasised the influence of ground recycled glass on reducing alkali-silica reaction (ASR) in mortars, highlighting its potential to enhance durability when incorporated correctly. However, it has been found that ASR and compressive strength are negatively impacted by concrete with recycled glass (Meyer, 2001).

In South Africa, there has been an increased research focus on the use of waste glass as a substitute for fine aggregates in concrete. For example, Steyn et al. (2021) observed an improvement in workability and durability of concrete resulting from the replacement of fine aggregates with glass. Sasanipour and Aslani (2020) found that incorporating waste glass as a partial replacement for traditional aggregates in concrete can enhance certain durability properties, such as resistance to chloride ion penetration, while potentially negatively affecting other characteristics like compressive strength.

The incorporation of waste glass in concrete aligns with South African environmental goals, given the significant generation of waste glass and low recycling rates, as detailed by the South African State of Waste Report (Department of Environmental Affairs, 2018). This study therefore investigates the potential use of waste glass as a partial replacement for fine aggregates, with a specific focus on the durability and long-term performance of South African infrastructure. Specific fresh concrete properties (slump, flow, vebe time), hardened concrete properties (drying shrinkage, surface resistivity and compressive strength) and durability indexes (water sorptivity and oxygen permeability index), are investigated.

1.2 Research problem

The increasing demand for affordable housing and infrastructure projects in South Africa has led to significant urbanisation and industrialisation, particularly in cities catering to poor and middle-class populations (Abrananth, 2020). Urbanisation and infrastructure development has increased the demand for concrete in large-scale projects and a corresponding depletion of natural resources such as sand. With the ever-increasing demand for concrete as a primary construction material, these natural aggregates are being rapidly depleted, leading to unsustainable practices that drive up project costs.

Recent studies have reported varied results regarding the performance of concrete containing glass aggregates. For instance, Morrison (2023) argued that post-consumer glass can enhance the durability and mechanical properties of concrete while simultaneously reducing landfill waste. However, Kumar et al. (2023) raised concerns about the long-term durability of glass aggregate concrete under certain environmental conditions.

In response to the challenges of resource depletion, escalating material costs, and environmental degradation, there is a need to explore alternative materials that can partially or wholly replace

natural fine aggregates in concrete production. One promising alternative is the use of glass waste as a substitute for sand. Incorporating glass waste not only addresses resource depletion but also offers environmental benefits by reducing the volume of waste sent to municipal landfills. However, the effects of incorporating glass waste on concrete properties must be thoroughly understood before widespread adoption in concrete production, particularly regarding strength development and durability characteristics. This study therefore investigates the potential use of waste glass as a partial replacement for sand in concrete production, focusing on how glass content affects selected fresh and hardened properties such as workability, compressive strength, durability properties, shrinkage and surface resistivity.

1.3 Research questions

The key questions that this research intends to answer comprise the following:

1. Is waste glass a viable substitute for fine aggregate for use in concrete production in South Africa?
2. How does the content of waste glass affect compressive strength, surface resistivity, accelerated drying shrinkage, and the water sorptivity index and oxygen permeability index of concrete?
3. What is the mineralogy of waste glass and how do these minerals affect the aforementioned concrete properties in (2)?

1.4 Objectives of the study

The main objective of this study is to investigate the effect of waste glass on selected fresh and hardened properties of concrete. This study also aimed to achieve the following sub-objectives:

1. To assess the effect of glass of fresh concrete properties such as slump, flow and vebe time of fresh concrete.
2. To assess the effect of glass on hardened concrete properties such as compressive strength, surface resistivity, drying shrinkage, and durability indexes (water sorptivity and oxygen permeability index).
3. To analyse the mineralogy and microstructure of concrete containing glass.

1.5 Scope and limitations

1.5.1 Scope

1. Waste glass particles ranging between 75 μm and 2 mm.
2. Glass replacement levels of 10% and 20% by mass of sand.
3. Testing under a controlled laboratory environment.
4. Selected fresh and hardened properties such as slump, flow, vebe time, compressive strength, water sorptivity index, oxygen permeability index, surface resistivity and accelerated drying shrinkage.

1.5.2 Limitations

This study is limited to the following:

1. Concrete making materials readily available in the Western Cape Province of South Africa, namely:
    a. Portland limestone cement, CEM II/A-L, 42.5 N as the primary binder.
    b. Fine aggregates: Hornfels crusher dust (7.1 mm).
    c. Coarse aggregates: 20 mm Hornfels stone.
2. Two water-to-cement ratios of 0.50 and 0.66.
3. Short-term laboratory tests done at the following organisations/institutions:
    a. Cape Peninsula University of Technology (CPUT).
    b. University of Cape Town (UCT).
    c. University of Namibia (UNAM).
    d. University of the Western Cape (UWC).
    e. Pretoria Portland Cement (PPC, Cape Town).
4. investigating the mechanical properties of waste glass, not the cost analysis.

1.6 Assumptions of the study

The following key assumptions have been made in this study:

1. The selected water:cement ratio falls within the range commonly used in practice in South Africa, making it suitable for evaluating the effects of waste glass on concrete properties.
2. The chosen durability tests (surface resistivity, drying shrinkage, WSI, and OPI) will effectively assess the long-term performance of concrete that incorporates waste glass.

1.7 Significance of the research

This study is significant as it will:

1. Contribute to the body of knowledge on the effect of glass content on selected fresh and hardened concrete properties such as flow, vebe time, slump, compressive strength, surface resistivity, water sorptivity index, oxygen permeability index and drying shrinkage.
2. Contribute to efficient municipal solid waste management by reducing the rate of opening up new sites due to the reduction in the volume of glass being dumped.
3. Contribute to conservation of natural resources such as sand.
4. Contribute to the production of affordable concrete that could be used for low-cost housing and non-structural applications.
5. Contribute to the realisation of the United Nations Sustainable Development Goals 9, 11, 12, 13 and 15 and the United Nations 2030 Agenda for Sustainable Development.

1.8 Context of the research

This research falls within the discipline of Building Materials (Concrete) in the Faculty of Engineering and The Built Environment. The study is important as it will investigate the effect of waste glass on selected fresh and hardened concrete properties such as flow, vebe time, slump consistency, compressive strength, surface resistivity, drying shrinkage, microstructure, mineralogy and durability (water sorptivity index and oxygen permeability index). The research aligns with sustainable engineering design practices in concrete manufacture, aiming to reduce the environmental effect of concrete production.

1.9 Expected outcomes

This study evaluates the feasibility of waste glass as a partial replacement for fine aggregate (Philippi dune sand) in concrete production. The evaluation will focus on the microstructure, mineralogy, and selected fresh and hardened properties that dictate the durability and performance of concrete in service. The study is expected to consolidate and/or advance existing knowledge on the effect of waste glass on selected fresh and hardened concrete properties such as Oxygen Permeability Index (OPI), Water Sorptivity Index (WSI), surface resistivity workability and compressive strength. This research will also provide valuable insights that can be used to assess the viability of waste glass as an effective replacement material for fine aggregate. The incorporation of waste in glass in concrete will further contribute to environmental sustainability, improved municipal solid waste management, conservation of natural resources and reduced construction costs. The findings of the study can inform policy and decision making.

1.10 Organisation of thesis

A general summary of the chapters in this thesis is hereby presented:

1. Chapter 1 is an introduction to the study. The chapter presents information regarding the background of study, problem statement, key research questions, objectives, scope, limitations and significance of study.
2. Chapter 2 presents a literature review on the use of waste glass in concrete production. Literature on the effects of glass on fresh and hardened concrete properties, including durability has been reviewed. Knowledge gaps are also highlighted.
3. Chapter 3 presents an in-depth description of the methodology used in this study. Specific details regarding the experimental design, variables, casting and testing are presented.
4. Chapter 4 discusses the results of the experiments that were conducted. Important inter-relationships among the results and literature are highlighted.
5. Chapter 5 presents the conclusions derived from the study. A list of recommendations for further research is also presented.

Chapter 2 - Literature review and theory

2.1 Introduction

Concrete is the second most consumed material globally after water (Gagg, 2014). It plays a crucial role in the construction of a wide array of civil engineering projects, including buildings, bridges, dams, roads, schools, hospitals, and homes. The primary constituents of concrete are cement, water, and aggregates (fine and coarse). Concrete derives much of its strength and durability from aggregates. Aggregates can constitute up to 60-75% of the total volume of the concrete mix (Tamanna et al., 2020). The type and quality of aggregates used would thus significantly affect the performance of concrete.

In recent years, the construction industry has experienced rapid growth, particularly in developing and emerging economies. This growth has increased the demand for natural aggregates such as sand, gravel, and stone. However, the ongoing extraction of these materials has led to their depletion in many parts of the world, including India, China, the United States, Singapore, and countries in the Middle East and Africa (Ametepay and Ansah, 2014). The extraction of natural materials from the earth poses severe environmental challenges, such as habitat destruction, soil erosion, and land degradation. The over-reliance on natural resources also threatens the sustainability of the construction industry and calls for urgent measures to mitigate its environmental impact.

Over the last 30 years, the construction industry has resorted to the use of recycled materials du to the increased depletion of natural resources.. Recycling materials conserves natural resources and reduces the volume of waste sent to municipal landfills, thereby mitigating pollution and other environmental harm. Landfills, often filled with non-biodegradable materials – including construction waste like concrete, bricks, and glass – are a growing concern for many local authorities and municipalities. Landfills contribute to land occupation, pollution, and greenhouse gas emissions from decomposing organic materials. Addressing these concerns requires reducing landfill usage and promoting material reuse.

Recycled waste glass holds much potential for use in construction, particularly in concrete production. Glass, a non-biodegradable material, can persist in landfills for thousands of years, contributing significantly to long-term environmental pollution (Olofinnade et al., 2018). In South Africa, for example, the State of Waste Report (Department of Environmental Affairs, 2018)

revealed that approximately 42 million tonnes of waste were generated in 2017, with 5.4 million tonnes classified as construction and demolition waste (Department of Environmental Affairs, 2018). Unfortunately, only 6% of this waste was recycled, with the remaining being sent to landfills.

Landfills remain the most common disposal method for most glass waste worldwide (Byars et al., 2004). This situation presents significant challenges for municipalities. Substantial volumes of single-use glass exacerbate the problem and put a strain on fragile ecosystems. The indefinite lifespan of glass waste poses several challenges as it occupies space within material recovery facilities and waste disposal facilities, space that could otherwise be used for biodegradable waste. This issue underscores the significant environmental impact of glass, given the large volumes generated worldwide each year. Consequently, this contaminated glass is classified as waste glass, with more than 90% ending up in landfills or being stockpiled as shown in Figure 2.1 (located in Bellville South, Cape Town)

Figure 2.1: Landfilling of waste glass

There have been significant research efforts on the potential of glass as a substitute for coarse and fine aggregates and cement in concrete production. These efforts have primarily focused on maintaining and improving the compressive strength of concrete. The primary concerns that have been observed with the incorporation of glass in concrete are twofold: the maintenance or improvement of compressive strength and the management of alkali-silica reaction (Meyer, 2001).

Impurities and the costs associated with recycling have hindered the widespread use of recycled glass (Shi and Zheng, 2007). Post-consumer glass is glass that has been used by consumers and is no longer needed, such as bottles, jars, and containers that are thrown away. This waste glass can be reused, recycled into new glass products, or used in making construction materials. However, recycling it into new glass products is complicated due to difficulties in sorting, cleaning, and melting. The challenges of recycling waste glass – such as sorting and contamination – combined with increasing amounts ending up in landfills, and its non-biodegradable nature, have led the USA to seek alternative methods for recycling waste glass, particularly in construction (Tamanna et al., 2013). In South Africa, there is currently insufficient information to demonstrate that glass can be effectively utilised in the concrete construction sector. This, therefore, hinders the development of standards and best practices regarding the use of recycled materials in South Africa.

This chapter presents a literature review on the use of glass waste in the construction industry, highlighting the physical and chemical properties of glass, its use as a partial replacement for aggregates (coarse and fine) and cement in concrete production.

2.2 Use of waste glass in the construction industry

The glass waste stream in South Africa includes a variety of glass types, encompassing both packaging glass like bottles and jars, and flat or sheet glass such as windows, windscreens, and mirrors (Department of Environmental Affairs, 2018). According to Sobolev et al., (2007), glass does not lose it quality even after recycled which makes it a potential substitute for any of the concrete constituents (sand, coarse aggregates and cement) The use of glass waste in the building industry significantly contributes to the conservation of natural resources and carbon emission reduction. This in turn leads to employment of sustainable construction which is responsible for the drop of greenhouse gas emissions.

From the year 1960, many studies have been conducted on the effect of glass as a coarse aggregate substitute on compressive strength and alkali silica reaction of concrete (Pike et al., 1960; Schmidt and Saia, 1963; Phillips and Cahn, 1972; Johnson, 1974; Figg, 1981; Polley et al.,

1998; Shayan and Xu, 2004; Shi and Zheng, 2007; Oliveira et al., 2008; Abdallah and Fan, 2014). Experimental results showed that concrete produced with glass waste as a coarse aggregate substitute is susceptible to alkali-silica reaction (ASR) which results into compressive strength reduction. ASR takes place between the minerals (sodium and silica) in the waste glass and alkalis (Na_2O and K_2O) in cement. This reaction between glass and cement results in excessive expansion when moisture is present. This results into the reduction of concrete durability and strength due to the creation of pressure cracks. Furthermore, when glass particles greater than 4.5 mm are used as coarse aggregates, the presence of ASR expansion is evident Rajabipour et al.,(2010) stated when glass aggregates are crushed, tiny cracks appear at their edges.

The high silica and sodium content in recycled post-consumer glass used as both fine and coarse aggregate replacements can facilitate this reaction. Interestingly, the presence of chromium in green-coloured recycled post-consumer glass is believed to have less impact on alkali-silica reaction (Pellegrino et al., 2019).

Glass has the same properties as natural sand when crushed and screened to pass through a 4.75 mm sieve. Waste glass (WG) can be used as an aggregate replacement in concrete at levels of up to 30% (Romero et al., 2013; Atoyebi et al., 2018). However, a study by Bisht and Ramana (2018) reported that replacing 21% of fine aggregate with WG increased concrete compressive strength by 9.04% and 9.90% after 28 and 90 days, respectively. The study also showed that incorporating WG improved the densification of the concrete matrix, which increased its compressive strength.

2.3 Sustainable perspective of waste glass in concrete

The production of glass involves several steps, beginning with the selection and preparation of raw materials, followed by mixing and melting these materials, and finally, the formation of the desired glass products as illustrated in Figure 2.2. Once these glass products reach the end of their useful life and become unusable, they are typically discarded into glass recycling containers. At the recycling facility, the discarded glass undergoes processes such as washing, cleaning, and sorting to prepare it for reuse. However, if the glass particles are contaminated with organic materials or other substances that cannot be easily removed, they become inappropriate for reintroduction into the glass production process. Waste glass refers to the glass material that remains after the recycling process in glass recycling facilities and factories. It cannot be reused for producing new glass products. Even though glass can theoretically be recycled indefinitely

without compromising its quality, there is a portion of the recycled glass that becomes unsuitable for reuse.

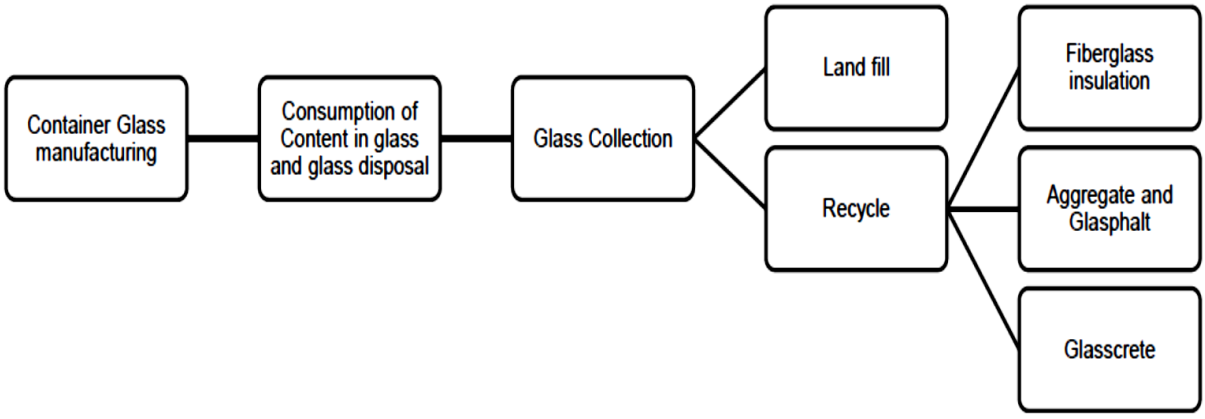

Figure 2.2: The recycling process (Gebremichael, 2022)

The waste glass is typically crushed into small particles resembling the size of sand, allowing it to partially substitute natural sand in concrete mixtures (Shayan and Xu, 2004; Malvar and Lenk, 2006; Prezzi et al., 1997). The utilisation of waste glass as an aggregate in concrete offers potential benefits to the economy and the environment. Glass, from an environmental perspective, is non-biodegradable. The repurposing of waste glass would thus reduce the demand for new and raw materials and their extraction from the earth's crust. Economically, the use of waste glass in concrete production is attractive because it reduces costs and additional time associated with conventional aggregate extraction processes. Despite the fact that adding glass waste in the production of concrete can negatively impact the mechanical properties of concrete, studies have shown otherwise, i.e., an improvement in some concrete properties (Corinaldesi et al., 2005; Meyer et al., 2001; Shayan and Xu, 2004; Malvar and Lenk, 2006; Prezzi et al., 1997; Ismail and Al-Hashmi, 2009).

2.4 Properties of glass

In the construction industry, there are several applications where this versatile material is being used. Section 2.4 discusses the different properties of glass (physical and chemical).. This will be helpful in determining which applications in construction are suitable for glass and making sure this material is handled, processed and used appropriately.

2.4.1 Physical properties

Singh et al., (2015) reported that workability of concrete was affected by the shape and texture of glass waste used as fine aggregate substitute, for example angular shaped and spherical shaped glass particles result in the reduction and increase of workability of concrete respectively.. Smaller particles resulting from additional crushing tend to exhibit less angularity and fewer flat and elongated particles. Proper crushing effectively eliminates sharp edges, mitigating safety hazards during handling.

2.4.2 Chemical properties

Glass-forming elements, when combined with oxygen, can be converted into glass. Silicon dioxide (SiO_2), used in the form of sand, is the most prevalent glass-forming component. Common glass contains approximately 70% SiO_2. Soda ash (anhydrous sodium carbonate, Na_2CO_3) acts as a fluxing agent in the melt, lowering the melting point and viscosity of the formed glass, releasing carbon dioxide, and assisting in stirring the melt. Other additives are also introduced to glass to achieve specific properties. Alumina, lead, and cadmium are used to increase the strength of the glass and enhance resistance to chemical attack (Patwary, 2012). The typical chemical compositions of these glasses are shown in Table 2.1.

Table 2.1: Chemical composition of different glass types (Xie and Xi, 2002)

Chemical composition, %	Soda-lime glass			Borosilicate glass	Lead glass
	Clear	Amber	Green		
SiO_2	73.2-73.5	71.9-72.4	71.3	70-80	54-65
$Na_2O_3 + K_2O$	13.6-14.1	13.8-14.4	13.1	4-8	13-15
Al_2O_3	1.7-1.9	1.7-1.8	2.2	7	0
MgO + CaO	10.7-10.8	11.6	12.2	0	0
SO_3	0.20-0.24	0.12-0.14	0.05	0	0
Fe_2O_3	0.04-0.05	0.3	0.56	0	0
Cr_2O_3	0	0.01	0.43	0	0
B_2O_3	0	0	0	7-15	0
PbO	0	0	0	0	25-30

2.4.3 Mechanical properties

Glass is an amorphous material that fractures as a result of tensile stress. Gravel-sized particles of crushed glass greater than 4.75 mm exhibit poor durability compared to conventional aggregate materials. Conversely, gravel-sized particles of crushed glass less than 4.75 mm exhibit improved durability compared to conventional aggregate materials (Patwary, 2012). The internal angle of friction, shear strength, and bearing capacity of crushed glass aggregates are high, and their compatibility is insensitive to moisture content.

2.5 Use of glass in concrete

2.5.1 Effects of glass on concrete properties

The use of waste glass as a replacement material in concrete has been extensively researched due to the growing need to address challenges pertaining to the environmental, municipal solid waste management and the depletion of natural aggregates. Glass offers potential as a sustainable alternative to traditional construction materials when recycled and incorporated into concrete. Recent studies on the potential of glass waste as a partial substitute for fine aggregate have yielded promising results. Findings from these studies have shown that the effect of colour of glass on concrete properties is insignificant (Park et al., 2004), thereby eliminating the need to sort consumer glass by colour, and consequently rendering the recycling of glass attractive. The incorporation of glass in concrete can result in both beneficial and detrimental effect of concrete properties. The subsequent subsections below present the applications of glass in concrete, focusing on its partial replacement for coarse aggregates, fine aggregates, and cement.

2.5.2 Effect of aggregates on hardened properties of concrete

Concrete structures need to be strong and stable enough to withstand applied loads without significant deformation. The strength of concrete is influenced by the surface texture, stiffness, shape, strength and toughness, and grading of the aggregates. The physical and mechanical properties of aggregates are crucial, as these properties can vary significantly within the same type of aggregate (Alexander and Mindess, 2005).

2.5.3 Partial replacement of coarse aggregates

For the last sixty years, various researchers have conducted studies on the replacement of coarse aggregates with waste glass. Early studies conducted by Schmidt and Saia (1963) and Polley et

al. (1998), laid the foundation of exploring the viability of glass cullet as a substitute for coarse aggregate. Conclusions from these studies showed that the workability of concrete does change much when glass is used as substitute of aggregates in concrete production. On another note, concrete with glass waste as aggregates is more susceptible to ASR resulting into development of cracks.. More research by Topcu and Canbaz (2004) showed that there was a reduction in the compression strength of concrete when glass is used as a substitute of coarse aggregate... The authors emphasised how crucial particle size management is in avoiding ASR-related problems. Therefore, when using waste glass as a replacement of coarse aggregates, careful consideration of compressive strength and ASR is needed.

Other studies by Ahmed et al. (2023) showed that the compressive and tensile strength of concrete reduced by 21% and 7% respectively in OPC concrete. The same authors reported a 11% to 26% and 11% to 29% decrease in compressive and tensile strength in geopolymer concrete respectively.. Ahmed et al., (2023) further reported that while there was a decrease in drying shrinkage, there was an increase in porosity, sorptivity and chloride permeability when glass waste was used. It was observed the changes in the concrete properties were due to the porous interfacial transition zone identified by microstructural investigation. . The mechanical and durability characteristics of concrete with 10% to 20% glass waste showed similar results with control samples that had only natural aggregates. This indicates that despite some studies indicating negative effects of glass waste in concrete, this material can be used as a reliable substitute up to 20% replacement for aggregates.

2.5.4 Effect of glass on fresh concrete properties

Workability of concrete is one of the most crucial fresh concrete properties that affects on how easily concrete can be mixed, poured and compacted. Singh et al., (2015) stated that workability guarantees that concrete can be handled and compacted without segregation. Olifinnade et al., (2018) observed that an increase in the amount of glass waste led to a decrease in workability. This is due to the internal friction raised in the concrete ingredients. Other studies have reported that increasing the replacement levels of waste glass up to 30% reduces the workability of concrete (Steyn et al. 2021, De Castro and de Brito 2013, Limbachiya 2009, Topcu and Canbaz 2004, and Park et al. 2004)). These changes in the workability are due to glass particle size, and the amount of glass used De Castro and de Brito (2013). However, studies by Ali and Al-Tersawy (2012) and Ibrahim (2017) concluded that there was no significant change in the workability of concrete with the addition of waste glass as a replacement of aggregates in concrete production.

Slump is another fresh concrete property which is affected by waste glass. Experimental results by Bahadur and Parashar (2023), Hadi et al. (2022), Upreti and Mandal (2021), Gupta et al. (2018), Ibrahim (2017), and Kavyateja et al. (2016) indicated that there is an increase in slump when up to 50% replacement levels of aggregates. The increase in slump is due to the fact the glass has a smooth surface that decreases friction between the surfaces, hence making it easy to mix concrete. On the contrary, Tan and Du (2013) and Ismail and Al-Hashmi (2009) concluded that slump reduced when waste glass was added. This because of the texture and shape of the glass particles that increased the ingredient friction.

.

2.6 Density

According to concrete Topçu and Canbaz, (2004); Adaway and Wang, (2015); Hunag et al., (2015); Ismail and Al-Hashmi, (2009),the fresh and dry density of concrete reduced when fine aggregates were replaced by fine waste glass The reduction in density is inversely proportional to glass content and the effect can be attributed to glass's lower particle density and specific gravity compared to traditional fine aggregates. For example, studies have shown fresh density decreasing from 2442 kg/m³ in control concrete to 2399 kg/m³ with 20% waste glass content (Hunag et al., 2015).

Ling and Poon (2012), however, observed a positive linear relationship between glass content and concrete density. They attributed this relationship to three specific factors. First, the particle size distribution of the waste glass affects how well it fills the spaces between other particles in the mix. Smaller particles can fill voids more effectively, leading to a denser concrete structure. Second, the compaction method used during mixing significantly influences density. Effective compaction techniques help eliminate air pockets and ensure that all particles are closely packed together. Third, the mix design ratio of waste glass, cement, and other aggregates affects how these materials interact and pack together, which can lead to increased density when optimised properly. The apparent contradiction in findings might be explained by differences in glass particle characteristics (size, shape), mixing and compaction techniques, overall mix design, and testing methodologies. Additionally, the shape of glass particles appears to affect workability, with slump test results showing reduction as waste glass content increases, likely due to the sharper and more irregular shapes of glass particles compared to sand (Adaway and Wang, 2015).

The addition of waste glass as a replacement for fine aggregate reduces the fresh and dry density of concrete (Topçu and Canbaz, 2004; Adaway and Wang, 2015; Hunag et al., 2015; Ismail and Al-Hashmi, 2009). The reduction in dry density has been reported by Adaway and Wang (2015), Topçu and Canbaz (2004), and Ismail and Al-Hashmi (2009) to be inversely proportional to glass content. The reduction in fresh density may be due to the lower particle density and specific gravity of glass compared to traditional fine aggregates. Replacing denser fine aggregates with glass would thus result in a reduction in the density of concrete. Ling and Poon (2012), however, observed a positive linear relationship between glass content and concrete density. They attributed the observed relationship to several factors such as the particle size distribution of the glass, the compaction method used, or the mix design employed in their study.

2.7 Compressive strength

The compressive strength test stands as a pivotal mechanical assessment for concrete. It offers insights into the effects of its mix design constituent materials. The compressive strength of concrete is sensitive to the inclusion of waste glass (Ismail and Al-Hashmi, 2009). While most studies indicate a decrease in compressive strength with increasing amounts of waste glass (De Castro and de Brito 2013), exceptions exist. For example, Park et al. (2004) found that using fine glass aggregates at varying percentages (up to 100%) reduced both flexural and compressive strength, particularly at glass contents above 20%. Similarly, Limbachiya (2009) observed that while concrete mixes with up to 30% glass maintained acceptable compressive strength, further increases resulted in decreased mix stability.

Oliveira et al. (2008) showed that finely ground waste glass could replace all the fine aggregate in concrete without reducing its strength – it could even make concrete 30% stronger. Several other researchers found similar results: Tamanna (2020), Shayan and Xu (2004), Park et al. (2004), and Lalitha et al. (2020) all reported that using up to 60% glass sand did not weaken the concrete. However, many other studies found that adding too much glass could make concrete weaker. Upreti et al. (2021) observed that while a little glass made concrete stronger, using more than 15% glass made it weaker. Many other researchers (Limbachiya, 2009; Ismail and Al-Hashmi, 2009; Turgut and Yahlizde, 2009; Gautam et al., 2012; Abdallah and Fan, 2014; Kavyateja et al., 2016; Lalitha et al., 2017) found that concrete became weaker at glass contents exceeding 20%. Al-Zubaid, Shabeeb, and Ali (2017) tested different amounts (11%, 13%, and 15%) and found 13% glass gave the strongest concrete. The effect of waste glass content on the 28-day compressive strength at various ages is shown in Figure 2.3. The trend shows that using

up to 20% WGS does not affect concrete strength but adding more leads to strength reductions. Additionally, the negative effect of WGS becomes less noticeable in stronger concrete mixes. For example, when using 50% WGS, concrete designed for 20 N/mm^2 lost 31% of its strength, while concrete designed for 40 N/mm^2 only lost 20% of its strength..

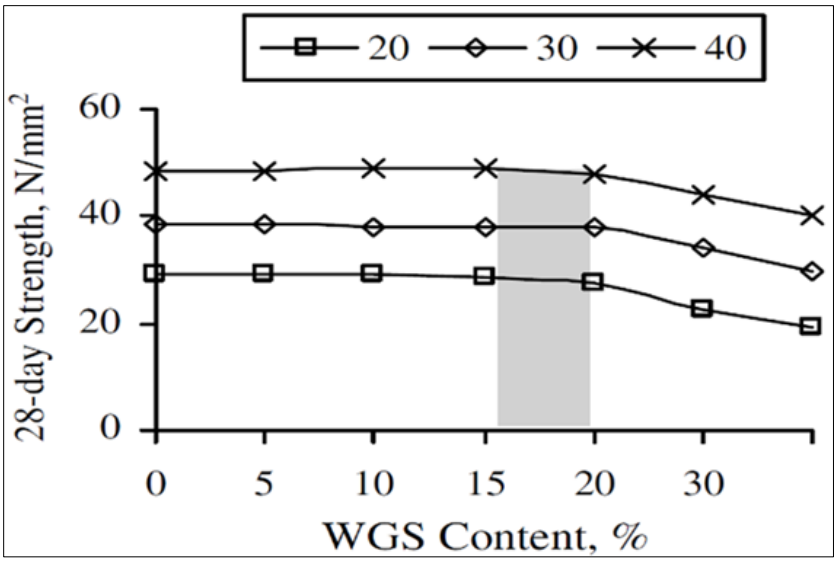

Figure 2.3: Effect of waste glass sand on 28-day strength of concrete (Limbachiya, 2009)

The observed reduction in compressive strength due to an increase in glass content can be attributed to two factors: the physical properties of glass itself and problems at the interfacial transition zone (or ITZ) (Limbachiya, 2009). The ITZ is very important for concrete strength. Because glass has a smooth surface, it does not bond well with cement. This poor bonding can lead to tiny cracks and makes it harder for stresses to spread through the concrete, which is why strength drops significantly when more than 30% glass is used. Małek et al. (2020) found that the use of glass in mortar could increase strength by 11-29% compared to normal mortar. They observed a good performance in mortars containing 20% green glass with very small particles, because smaller pieces bonded better with the cement and the green glass was harder than regular sand.

Oliveira et al. (2008) demonstrated that finely ground waste glass could be integrated into concrete as a fine aggregate replacement at rates of up to 100% without compromising compressive strength; in fact, it could even increase by up to 30%. Similar findings were observed by Tamanna (2020), who did not observe a reduction in compressive strength with glass replacing fine aggregate up to 60%. This observation was also seen by Shayan and Xu (2004), Park et al.

(2004), and Lalitha et al. (2020). However, Upreti et al. (2021) found that while the compressive strength initially increased with glass sand content, it decreased beyond a 15% replacement level. Subsequent studies by Limbachiya (2009), Ismail and Al-Hashmi (2009), Turgut and Yahlizde (2009), Gautam et al. (2012), Abdallah and Fan (2014), Kavyateja et al. (2016), and Lalitha et al. (2017) supported this observation, noting a decrease in compressive strength when glass sand content exceeded 20%. Al-Zubaid, Shabeeb, and Ali (2017) specifically tested the impact of waste glass at 11%, 13%, and 15% replacement levels, with 13% replacement yielding the highest compressive strength after various curing durations.

Małek et al. (2020) explored the effects of incorporating glass aggregate into mortar, reporting an increase in compressive strength of 11-29% compared to reference mortar, with the most significant gains achieved with 20% by mass of green glass aggregate featuring small particle sizes. This improvement was attributed to enhanced bonding at the aggregate-cement interface and the higher Mohs hardness of the green glass aggregate. Using waste glass sand (WGS) up to 20% had no effect on strength development. However, when more WGS was added, the strength began to decrease gradually, as shown in Figure 2.4. At 50% WGS content, after one year of curing, the strength difference compared to normal concrete (made with natural aggregates) was no more than 10.0 N/mm^2. These findings are similar to those from previous research on recycled glass sand concrete (Shayan and Xu, 2006; Taha and Nounu, 2008).

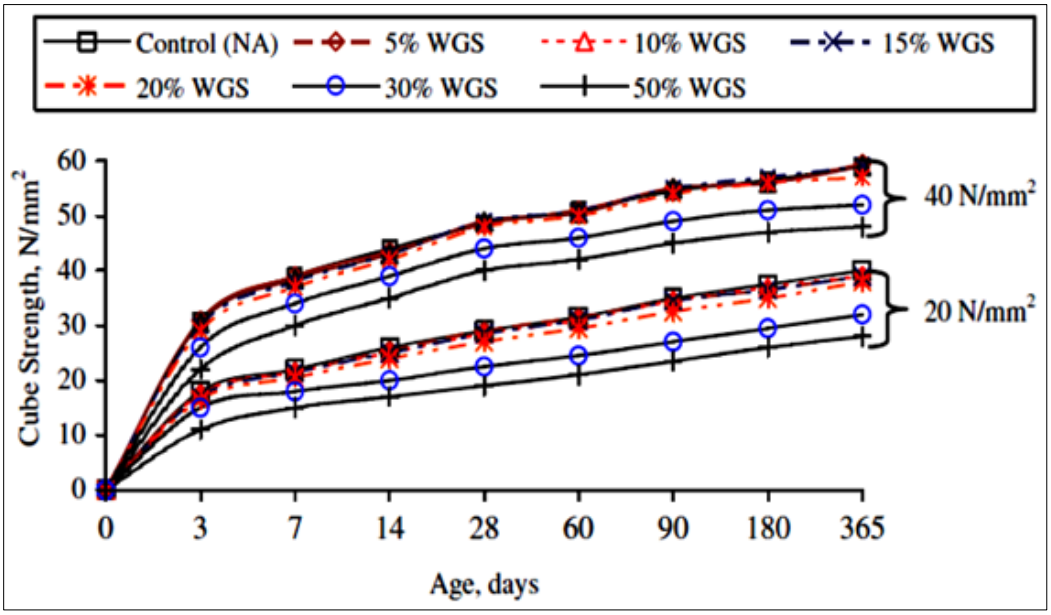

Figure 2.4: Effects of different sand replacements for waste glass on the compressive strength at various days (Limbachiya, 2009)

2.8 Accelerated drying shrinkage

The incorporation of glass in concrete has been observed to reduce shrinkage (Hunag et al., 2015). Limbachiya (2009) observed that replacing fine aggregates with mixed colour beverage waste glass up to a replacement level of 20% by mass of fine aggregate did not result in any discernible effect on drying shrinkage. They further observed a reduction in shrinkage resulting from an increase in glass sand beyond 20%. Additionally, De Castro and de Brito (2013) observed that concrete containing both fine and coarse glass aggregates exhibited lower drying shrinkage in comparison to concrete mixes containing either fine sand or coarse sand. They attributed the observed reduction in drying shrinkage to the low water absorption capacity of glass sand in comparison to natural fine sand, and the impermeable properties of glass.

2.9 Durability indexes (DIs)

To determine the penetrability of concrete, durability indexes need to be determined (Alexander et al., 2017). Examples of DIs tests that are commonly used in South African include the oxygen permeability index (OPI) and water sorptivity index (WSI) which are used in this study.

Experimental studies show that replacing sand with up to 30% waste glass produces similar results or even better than concrete without waste glass. . It was also observed that adding waste glass led to the decrease in water absorption, water permeability, chloride diffusivity, and diffusion coefficient (Oliveira et al. 2008 and Kim et al. 2018) Limbachiya (2009) reported that the partial replacement of natural sand with glass at levels exceeding 20% led to a significant decrease in concrete durability, particularly in resistance to chloride penetration and water permeability. Similarly, De Castro and de Brito (2013), Lalitha et al. (2020), and Tamanna (2020) observed an increase in porosity and a reduction in durability properties, such as sulphate resistance and freeze-thaw durability, in concrete mixes containing less than 20% recycled crushed glass.

It can be inferred from the aforementioned studies that higher replacement levels of recycled glass (beyond 20%) in concrete can have detrimental effects on its durability. However, most studies reported that the use of glass aggregates (GA) did not result in substantial alterations to the durability-related properties of concrete. In cases where variations were observed, they

typically fell within a range of ±15%, which aligns with the expected scatter of experimental results. Upreti et al. (2021) observed an improvement in durability properties (e.g., reduced water absorption and enhanced chloride resistance), workability, and strength, along with a reduction in the weight of concrete, when 5-10% of fine aggregate was replaced with waste glass.

2.10 Microstructural and mineralogical analysis

The use of WG as a partial sand replacement in concrete and mortar has been extensively studied using scanning electron microscopy (SEM) to understand its effects on material microstructure. Schwarz et al. (2008), Du and Tan (2014), Harbec et al. (2017) and Bisht and Ramana (2018) observed an improvement in the density of the interfacial transition zone (ITZ) and a corresponding improvement in microstructure, durability and mechanical properties such as strength resulting from the replacement of fine aggregates with of glass up to replacement levels of 21%. However, Singh et al. (2017) noted that higher glass replacement levels at high w/c ratios can lead to irregular void distribution. In their study about the effect of waste glass on concrete properties, Bisht and Ramana (2018) concluded that the density of the ITZ increased with the addition of waste glass as a fine aggregate substitute. The authors indicated that compressive strength and workability can increase when up to 30% of fine aggregates is replaced by waste glass. This increase in the concrete compressive strength and workability us attributed to the pozzolanic reactions between the glass particles and the cement matrix. Bisht and Ramana (2018) did warn, however that going above 20% as a replacement of fine aggregates with glass waste could result into increased porosity and decreased cement hydration. This may result into the strength and bonding interface to be affected negatively.

To understand the phase composition and crystallinity in glass-modified cementitious materials experimental tests such as X-ray diffraction (XRD) has been used The correlation between glass fineness and pozzolanic activity using XRD has been studied by Shao et al. (2000) . The results obtained demonstrated the the characteristic amorphous hump in XRD patterns. In addition, to measure the crystalline phases and monitor compositional changes as a function of curing time, Aliabdo et al. (2016) utilised XRD. Idir et al. (2011) demonstrated that XRD analysis may be used to track the The consumption of calcium hydroxide (CH), a critical indicator of pozzolanic activity. by The authors also observed that mixtures containing glass waste had lower levels of calcium hydroxide.

2.11 Chapter summary

The increase in the population has led to and increased demand for accommodation around the world. To curb this demand for housing, governments have resorted to building low cost and affordable houses for the populace. This in turn has increased the demand for more building materials to be used hence depleting the natural resources such as sand where these materials come from. Furthermore, landfills are also being filled with waste glass that is nonbiodegradable. This results into environmental pollution and degradation. .

To address the abovementioned challenges, it becomes crucial to investigate the use of recycled glass as a substitute of either fine or coarse aggregates in concrete production.. Chapter 2 has discussed different investigations on how glass waste has been used as a replacement of aggregates in concrete and how the fresh, hard and durability properties are affected.. However, there is still a research gap regarding the mechanical and durability properties of concrete incorporating waste glass as a fine aggregate, especially in the South African context. While many studies have looked at using waste glass in concrete, there is limited information on its use in low-strength concrete and the specific challenges this presents in South Africa.

The main challenge is to develop effective methods for creating this new type of concrete while keeping the original mix design and successfully incorporating waste glass. This research aims to fill that gap by providing specific insights and guidelines for producing sustainable, durable low-strength concrete with waste glass. Doing this can contribute to cost reduction in the construction industry, efficient municipal solid waste management while supporting global efforts to reduce waste and promote environmental sustainability. Chapter 3 presents the research methodology followed in achieving the objectives of this research study.

Chapter 3 – Research methodology

3.1 Introduction

The main objective of this study was to investigate the effect of waste glass on selected fresh and hardened properties of concrete. This objective was achieved through laboratory tests. A single-factor control laboratory experiment was designed to examine the impact of waste glass on specific concrete properties. Tests were conducted in laboratories at the Cape Peninsula University of Technology (CPUT), PPC (Cape Town), University of Namibia (UNAM), University of the Western Cape (UWC), and the University of Cape Town (UCT).

An overview of the testing programme that was adopted in this study is shown in Figure 3.1.

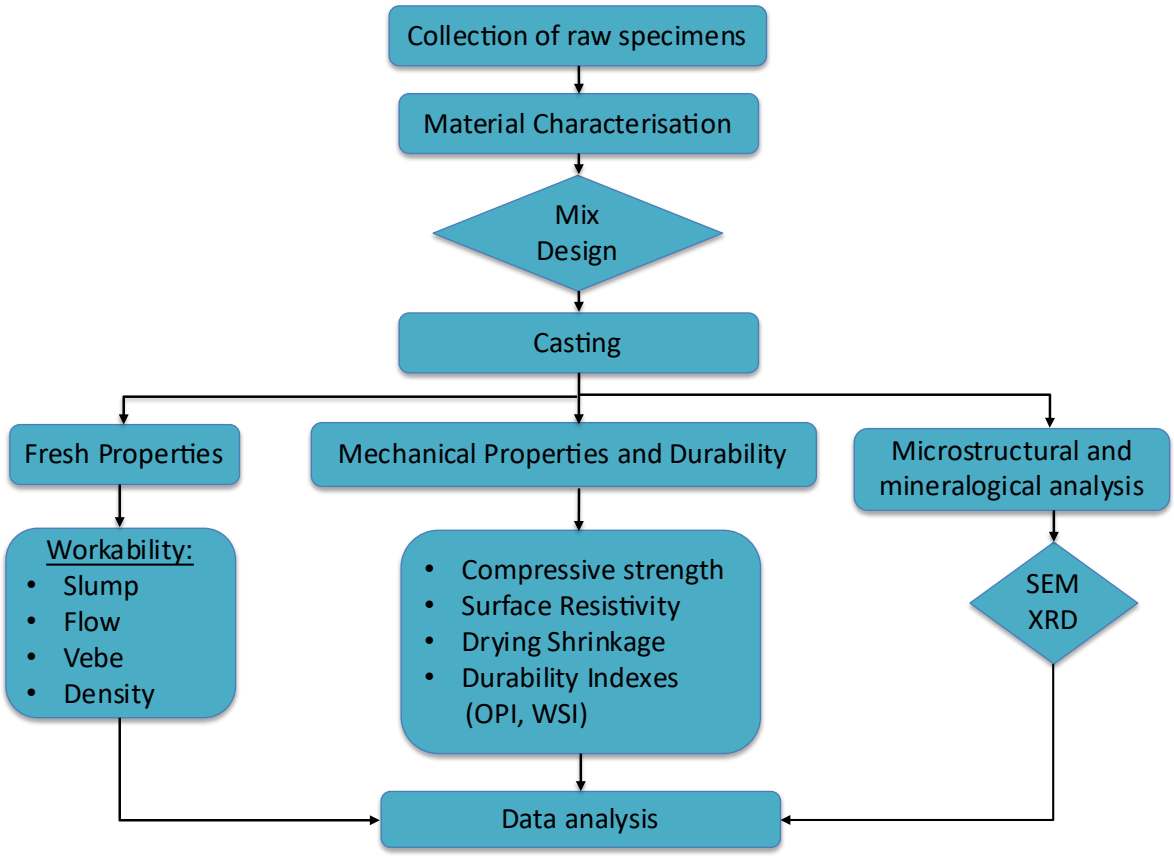

Figure 3.1: Overview of testing programme

3.2 Testing philosophy

The testing philosophy of this study was structured to ensure a systematic and rigorous approach to evaluating the effects of waste glass as a partial replacement for fine aggregate in concrete. The experimental approach was based on recognised testing standards, ensuring the reliability and reproducibility of the results.

All tests were conducted in accordance with South African National Standards (SANS). Where appropriate SANS standards were unavailable, alternative internationally recognised standards such as those from the American Association of State Highways and Transportation Officials (AASHTO) and the American Society for Testing Materials (ASTM) were employed. The adherence to standardised testing protocols ensured the validity and comparability of the results within the broader field of concrete research.

3.3 Experimental approach

Waste glass was used as a partial replacement for Philippi dune sand. The waste glass utilised in this study had a particle size distribution ranging between 0.075 and 2.0 mm and was sourced from Ardagh Glass Packaging in the Western Cape. Portland limestone cement, CEM II 42.5 N from PPC in Cape Town was used for its cost-effectiveness and suitability for general construction applications, particularly where high-strength concrete was not required.

A blend of Philippi dune sand and hornfels crusher dust was used as the fine aggregate. Specifically, 7.1 mm hornfels crusher dust and 20 mm hornfels stone were used as fine and coarse aggregates respectively. Both the coarse aggregates and dune sand were sourced from AECI Much Asphalt in the Western Cape Province, South Africa. Philippi dune sand was selected due to its widespread availability in the Cape Flats of the Western Cape Province, making its partial replacement in concrete an important step toward reducing the environmental impact of sand mining.

Two w/c ratios of 0.50 and 0.66 were used to achieve a balance between workability and strength in the concrete mix. Various studies recommend w/c ratios between 0.4 and 0.6 for high-quality concrete (Simnani, 2017; Mehta and Monteiro, 2014; Neville, 2011). A lower w/c ratio typically enhances concrete strength and durability, whereas a higher w/c ratio improves workability, facilitating mixing and placement (Neville, 2011; ACI Committee 211, 2007). Therefore, the selection of a w/c ratio of 0.50 aimed to optimize compressive strength while maintaining

adequate workability, as research indicates this ratio can yield high-performance concrete with satisfactory durability characteristics (Simnani, 2017). The higher w/c ratio of 0.66 was included to evaluate its effects on workability and overall performance compared to the lower ratio.

Waste glass was incorporated at replacement levels of 10% and 20% by mass of fine aggregate. A blend of 70% Philippi dune sand and 30% hornfels was utilised as the fine aggregate. This blend was chosen to optimise performance, as Philippi dune sand is very fine and tends to absorb significant amounts of water, which can negatively affect the mix's workability and strength if used alone. The properties of hornfels differ significantly from those of dune sand; thus, blending the two materials aimed to create a more balanced aggregate mix, enhancing the overall performance of the concrete.

By maintaining adherence to standardised testing methods and using a well-structured experimental approach, this study ensured a robust assessment of waste glass as a fine aggregate replacement in concrete production.

3.4 Materials and test equipment

3.4.1 Materials

The following materials were used in this study:

i. Portland limestone cement, CEM II/A-L, 42.5 N: supplied by PPC Cement and conforming to SANS 50197-1 specifications. The specific gravity of this cement is 3150 kg/m³.
ii. Fine aggregates:
    a. Philippi dune sand: sourced from Cape Flats and supplied by AECI Much Asphalt, Western Cape, was used as the natural fine aggregate in this study. The sand has an average particle diameter of 2.0 mm, relative density of 2.58, and a fineness modulus of 1.27. Additional details on this material and detailed test results are presented in Appendix C.2.
    b. Hornfels crusher dust: sourced from the Tygerberg Mountains and supplied by AECI Much Asphalt, Western Cape. It was used as a fine aggregate in concrete production. The material has an average particle diameter of 7.1 mm, relative density of 2.74 and fineness modulus of 3.55. Additional details on this material and detailed test results are presented in Appendix C.6.
    c. Hornfels stone: sourced from the Tygerberg Mountains and supplied by AECI Much Asphalt, Western Cape. It was used as a coarse aggregate. It has a nominal size of

20 mm, specific gravity of 2.74 and compacted bulk density (CBD) of 1420 kg/m³. Additional details on this material and detailed test results are presented in Appendix A.3 and Appendix A.9.

d. CHRYSO®Plast Omega 122 plasticiser, supplied by CHRYSO Southern Africa (Pty) Ltd, Cape Town, was used as the water-reducing admixture. It is a liquid polycarboxylate-based superplasticiser. It has a specific gravity of 1.010 (±0.020) at 25 °C, a pH of 8.0 (±1.0), chloride content of ≤ 0.1% and a viscosity of 10–20 seconds. Additional details on this material are presented in Appendix D.
e. The waste glass: sourced from Ardagh Glass Packaging, Western Cape. The glass was processed to achieve a particle size distribution ranging between 0.075 mm and 2.0 mm. It was utilised as a partial replacement for fine aggregate in concrete. It has a relative density of 2.53 and a fineness modulus of 4.34. Additional details on this material and detailed test results are presented in Appendix A.2 and Appendix C.1.

3.4.2 Test equipment

The following equipment was used in this study:

1. 50 litre concrete mixer: for mixing fresh concrete.
2. Scoop and containers: for sampling freshly mixed concrete.
3. Slump cone: for determining the slump of freshly mixed concrete.
4. Moulds of various sizes: for casting test specimens of various dimensions.
5. Curing tank: for curing test specimens.
6. Standard sieves conforming to SANS 3310-1: for particle size analysis and determination of fineness modulus.
7. Metal cylinders and tamping rod: for testing for bulk density and void content.
8. Water-tight container and wire basket: for testing for water absorption.
9. Electronic weighing scale: for measuring the mass of materials and concrete specimens.
10. Compression strength testing machine: for testing for compressive strength.
11. Oxygen permeability test assembly: for testing for OPI.
12. Vacuum saturation facility: for testing for WSI.
13. Trays: for drying materials and other tests such as WSI.
14. 4-Point Wenner probe resistivity meter: for testing the surface resistivity of concrete.

15. Strain extensometer and strain targets: for measurement of shrinkage strains.
16. Well-ventilated oven: for drying materials and specimens.
17. Vernier calliper: for measuring specimen dimensions.
18. Desiccator: for conditioning specimens for WSI and OPI tests.
19. Stopwatch: for timing various tests.

3.5 Experimental methodology

This section presents a detailed explanation of tests that were undertaken and the corresponding test standards .

3.5.1 Material characterisation

The waste glass was prepared by thoroughly washing it to remove impurities and dust particles. The materials were characterised following standard procedures. The standard procedures that were used to characterise the materials and their corresponding test standards comprise:

1. Sieve analysis (SANS 3001-AG1:2014).
2. Particle and relative densities (SANS 3001-AG23:2014).
3. Fineness modulus (SANS 3001-PR5:2024)
4. Water absorption (SANS 3001-AG21:2014).

Waste glass cullet, with a particle size less than 5.0 mm, was sourced from Ardagh Glass Packaging in the Western Cape. The glass was initially collected from post-consumer sources, including clear and green bottles. The 'as received' waste glass was thoroughly cleaned to remove impurities and contaminants. It was then crushed to smaller sizes using a rod mill apparatus to achieve the desired particle size distribution. Figures 3.2 and Figure 3.3 show the 'as received' and crush waste glass respectively.

Figure 3.2: ‘As-received’ waste glass before crushing and sieving

Figure 3.3: Crushing of waste glass to fine aggregate sizes

The as-received aggregates (fine and coarse) were first dried, prior to testing, in a well-ventilated laboratory oven maintained at a temperature of 105 ± 5 ^{o}C over a duration of 24 hours. Oven-drying was intended to remove moisture from the as-received materials. Each material was thereafter tested for each of the properties in accordance with established standard testing procedures. Each test was repeated thrice and the mean of three individual measurements was recorded as the average value of the material property of interest. The detailed test procedures

are presented in Appendices B.1, B.2, B.3, B.4, B.5, and B.6, while the corresponding results are provided in Appendix A.

3.5.1.1 Particle size distribution and fineness modulus

The particle size distribution of all aggregates – i.e., waste glass, fine and coarse aggregates – was determined in accordance with SANS 3001-AG1 (2014). Standard 300 mm diameter sieves conforming to SANS 3310 and with aperture sizes ranging between 0.075 mm and 5.0 mm were used. An automatic electronic shaker (see Figure 3.4) was also used. The mass of the material retained on each sieve after shaking was weighed using an electronic weighing scale. Each test, for a specific material, was repeated thrice and the mean of the three individual measurements recorded as the average value of the property of the specific material. The detailed test procedures are presented in Appendices B.3 and B.6, while the corresponding results are provided in Appendices C.1, C.2, C.3, C.4, and C.6. Other material properties that were obtained from the particle size distribution comprise fineness modulus and dust content.

Figure 3.4: Sieve analysis test set-up

Fineness Modulus (FM) is an important property of aggregates. It influences the water demand, workability, strength, and durability of concrete. The fineness modulus of the fine aggregates and waste glass was determined in accordance with SANS 3001-PR5 (2024). The test results of sieve

analysis were used to calculate the fineness modulus. Each material was tested thrice and the mean of the three individual measurements recorded as the average fineness modulus of the material. The detailed test procedures are presented in Appendices B.5 and B.6, while the corresponding results are provided in Appendices C.1, C.2, C.3, C.4, and C.6.

3.5.1.2 Density measurements and voids content

The particle density, bulk density, specific gravity (i.e., relative density), apparent density, compacted bulk density and voids content of the dune sand, waste glass and coarse aggregates were determined in accordance with SANS 3001-AG20 (2014), SANS 3001-AG22 (2012), SANS 3001-AG23 (2014) and SANS 5845 (2006). Each material was tested thrice and the mean of three individual measurements recorded as the average value of the property of interest for the specific material. Figure 3.7 shows the general set-up of the density measurements and voids content test. The detailed test procedures are presented in Appendices B.4 and B.5, while the corresponding results are provided in Appendix A.

Figure 3.5: Relative density test assembly

Figure 3.8 shows the general set-up for the test for bulk density.

Figure 3.6: Bulk density test set-up

3.5.2 Water absorption

The test for water absorption is crucial for evaluating the durability and performance of concrete, particularly in environments subject to high moisture. This test measures the quantity of water absorbed by concrete (as a percentage) and porosity. The test for water absorption of the dune sand, waste glass and coarse aggregate was done in accordance with SANS 3001-AG21 (2014). The test was repeated thrice and the mean of three individual measurements recorded as the average absorption of the specific material. The detailed test procedure is presented in Appendix B.1, while the corresponding results are provided in Appendix A. Figure 3.9 shows the general set-up of the water absorption test.

Figure 3.7: Water absorption test set-up

3.5.3 Concrete mix design

The concrete mixes were designed according to the C&CI method (Cement and Concrete Institute, 2011). A summary of the concrete mix design constituents and proportions that were used in this study is presented in Table 3.1.

Table 3.1: Materials content for 1 m^3 of concrete mixture

Constituent	Quantity					
	Water:cement ratio					
	0.50			0.66		
	Glass content (%)					
	0	10	20	0	10	20
Water (l/m^3)	216.00	216.00	216.00	216.00	216.00	216.00
CEM II 42.5 N (kg/m^3)	432.00	432.00	432.00	327.27	327.27	327.27
20 mm hornfels stone (kg/m^3)	1163.45	1163.45	1163.45	1163.45	1163.45	1163.45
Philippi dune sand (kg/m^3)	676.01	608.34	540.67	676.01	608.34	540.67
Hornfels crusher dust (kg/m^3)	289.98	289.98	289.98	289.98	289.98	289.98
Waste glass (kg/m^3)	0.00	67.67	135.34	0.00	67.67	135.34
Plasticizer (CHRYSO® Plast Omega 122) (kg/m^3)	0.346	0.346	0.346	0.262	0.262	0.262

3.5.4 Casting, compaction and curing

Concrete specimens were prepared in accordance with SANS 5861-3 (2006). The preparation of concrete specimens was aimed at ensuring consistency, minimising variability, accurately representing batch properties, and evaluating performance and quality. Freshly cast specimens were demoulded after 24 hours and then cured in a water bath maintained at a temperature ranging between 22 °C – 25 °C. Figure 3.10 shows test specimens in a curing tank. The duration of curing was dependent on the age at which a specific material property was required.

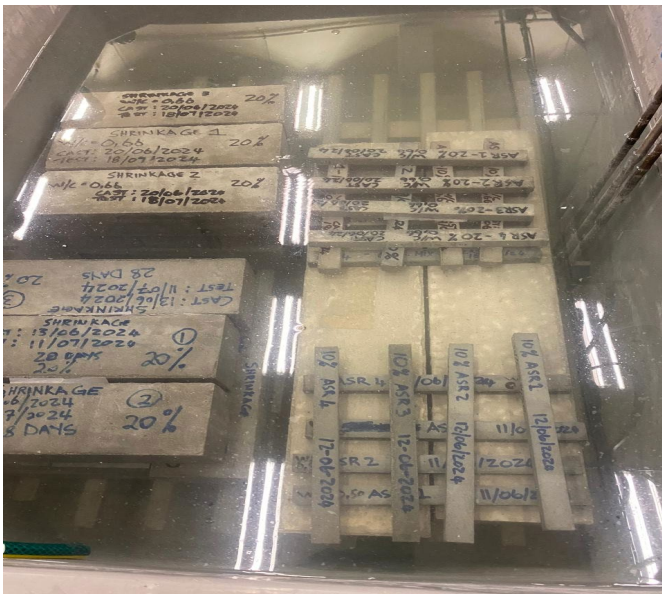

Figure 3.8: Water bath

3.5.5 Tests for fresh concrete properties

The fresh concrete properties that were tested during this study – i.e., flow, slump, vebe time and fresh concrete density – are presented in the subsequent subsection.

3.5.5.1 Slump

The slump of freshly mixed concrete was done in accordance with SANS 5862-1 (2006). The freshly cast concrete mix was tested for slump immediately after casting. A slump cone, tamping rod, steel plate and rule were used. The slump cone was filled in three approximately equal layers. Each layer was tapped gently 25 times using the rounded tip of the tamping rod. The tamps were evenly distributed. A steel rule was used to measure the slump of the specific concrete mix. Utmost care was taken during the lifting of the slump cone and the tamping of the concrete layers. The test for slump was repeated thrice and the mean of the three individual measurements recorded as the average slump of the specific mix. The detailed test procedure is presented in Appendix B.7.1, while the corresponding results are provided in Appendix C.7. Figure 3.11 shows the general set-up of the slump test.

Figure 3.9: Slump test apparatus

3.5.5.2 Flow

The test for flow was done in accordance with SANS 5862-2 (2006). A mould on a flow table was filled with fresh concrete and vibrated for 30 seconds. The diameter of the concrete spread was measured after vibration and recorded as the flow of the concrete. The test was repeated thrice and the mean of the three individual measurements was recorded as the average flow of the specific mix. The detailed test procedure is presented in Appendix B.7.2, while the corresponding results are provided in Appendix C.8. Figure 3.12 shows the general set-up of the flow test.

Figure 3.10: Flow test set-up

3.5.5.3 Vebe time and fresh concrete density

The vebe time test measures the consistency or mobility of fresh concrete or mortar mixes. This test is generally used to assess the workability of concrete mixes that are very dry. The vebe time test was done in accordance with SANS 5862-3 (2006). A vebe consistometer and a stopwatch were used. Freshly cast concrete was placed in the vebe consistometer. The time taken for the concrete in the consistometer to flow completely was measured using a stopwatch and recorded as the vebe time of the mix. The test was repeated thrice and the mean of the three individual measurements was recorded as the average vebe time of the specific mix. The detailed test procedure is presented in Appendix B.7.3, while the corresponding results are provided in Appendix C.9. Figure 3.13 shows the general set-up of the vebe time test.

Figure 3.11: Vebe consistometer apparatus

The density of the freshly cast concrete mix was determined in accordance with SANS 6250. The test was repeated thrice and the mean of the three individual measurements was recorded as the average fresh density of the specific mix. The detailed test procedure is presented in Appendix B.8, while the corresponding results are provided in Appendix C.10.

3.5.6 Tests for hardened concrete properties

3.5.6.1 Hardened concrete density

The density of the hardened concrete was determined in accordance with SANS 6251 (2006). Hardened concrete specimens (cubes and cylinders) that had been submerged in water for at least 24 hours prior to testing were weighed. The volume of each specimen was calculated from its measured dimensions (length, width, diameter, etc.). The density of each specimen was thereafter calculated from its mass and volume. The test was repeated thrice and the mean of the three individual measurements was recorded as the average fresh density of the specific mix. The detailed test procedure is presented in Appendix B.9, while the corresponding results are provided in Appendices C.11 and C.12.

3.5.6.2 Compressive strength

Compressive strength testing was done in accordance with SANS 5863. 150x150x150 mm concrete cube specimens were used. Each test specimen was removed from the curing tank, cleaned and the surface water, grit and projecting fins removed. The mass of the specimen was also determined using a weighing scale. The loading platens of the hydraulic compressive strength testing machine were cleaned, and the specimens positioned at the centre of the platens. A gradual compressive force was applied, without shock, to opposite as-cast surfaces of the specimens at a uniform rate of 0.3±0.1 MPa/second. The load at which the specimen failed was used to calculate the compressive strength of the specimen. The mass and dimensions of the specimens were used to calculate the density of the specimen. The failure pattern of each specimen was also noted.

Compressive strength testing was done at 3, 7, 14 and 28 days from the date of casting. The test was repeated thrice and the mean of the three individual measurements was recorded as the average compressive strength of a specific mix. The detailed test procedure is presented in Appendix B.10, while the corresponding results are provided in Appendix C.14. Figure 3.14 shows the general set-up of the compressive strength test. Results from this test were deemed valid if the highest and lowest recorded strength did not exceed 15% of the average value.

Figure 3.12: Compressive strength test set-up

3.5.6.3 Accelerated drying shrinkage

Drying shrinkage is the reduction in volume of concrete due to changes in moisture. Shrinkage affects the durability of concrete, especially when it results in cracks that would enhance the ingress of water/moisture, oxygen and aggressive deleterious chemical species. Cracks accelerate corrosion of steel in concrete. Drying shrinkage takes place over a long duration, with normal drying shrinkage tests taking long (in excess of 180 days) before stable measurements can be undertaken. Therefore, it was imperative, considering the limited time available for this study, that accelerate drying shrinkage be undertaken.

The test for accelerated drying shrinkage was done in accordance with SANS 6085. 100 x 100 x 300 mm square prisms were used. Testing was done under controlled laboratory exposure conditions (temperatures of 22 ^{o}C to 25 ^{o}C and a relative humidity not exceeding 60%). The magnitude of shrinkage was measured using a strain extensometer and shrinkage studs that were attached on the two opposite surfaces of each specimen along its longitudinal axis using a high contact adhesive. The gauge length of the shrinkage studs was 100 mm. Shrinkage readings were made at a frequency of 48 hours. Testing was stopped when the difference between two successive shrinkage was less than 2 µm per 100 mm nominal specimen length. The lowest shrinkage reading was recorded as the final dry measurement and used to calculate the shrinkage of the specimen. Three tests were run on each specimen and the mean of the three results was

reported as the average accelerated drying shrinkage of the concrete. The detailed test procedure is presented in Appendix B.11, while the corresponding results are provided in Appendices C.15 and C.16. Figure 3.15 shows the general set-up of the accelerated drying shrinkage test.

Figure 3.13: Drying shrinkage test set-up

3.5.6.4 Concrete surface resistivity

The surface resistivity of concrete is an indirect indicator of its durability. More specifically, surface resistivity correlates with the permeability and resistance of concrete to chloride ion penetration. The surface resistivity of concrete was determined in accordance with AASHTO T358. A 4-point Wenner probe resistivity meter was used. The specimens were tested 28 days after casting. Three tests were run on each specimen and the mean of the three results reported as the average surface resistivity of the concrete. The detailed test procedure is presented in Appendix B.12, while the corresponding results are provided in Appendix C.17. Figure 3.16 shows the general set-up of the concrete surface resistivity test.

Figure 3.14: Surface resistivity test set-up

3.5.6.5 Durability Indexes (OPI and WSI)

The test for durability indexes – oxygen permeability index (OPI) and water sorptivity index (WSI) – entailed the following:

i. The preparation of test specimens.
ii. The testing for OPI and WSI.
iii. The determination of microporosity from the WSI test specimens.

(a) Specimen preparation

Specimens were tested for OPI and WSI at the age of 28 days from the date of casting. The specimens were prepared in accordance with SANS 3001 – Part CO3-1 (2015)-3. 70 ± 2 mm diameter cylindrical cores were extracted from four 150 x 150 x 150 mm concrete cubes using a water-cooled diamond tipped core barrel attached to a coring drill. The cylindrical cores were thereafter sliced into 30 ± 2 mm thick discs. The discs were then oven-dried for seven days, and cooled in a desiccator maintained at 23 ± 2 ^{o}C prior to testing for WSI and OPI. Figure 3.17 shows the steps involved in specimen preparation.

(a) (b) (c)

Figure 3.15: (a) Extraction of cores from cubes using a drill; (b) drilled cores; (c) test specimens for WSI and OPI

(b) OPI

The OPI test provides valuable information on the durability and quality of concrete, particularly its resistance to penetration of gases such as oxygen, which can be indicative of its overall performance in various environmental exposure conditions. The test for OPI was done in accordance with SANS 3001-Part CO3-2 (2022). Four specimens from each concrete mix were tested for OPI and the mean of the four test results was reported as the average OPI of the specific mix. The detailed test procedure is presented in Appendix B.13.1, while the corresponding results are provided in Appendices C.19, C.20 and C.21. Figure 3.18 shows the general set-up of the test for OPI.

Figure 3.16: Permeameter for OPI tests

(c) WSI

The WSI test measures the unidirectional ingress of water in a preconditioned standard concrete disc specimen. The test for WSI was done in accordance with the Durability Index Testing Procedure Manual – Part 3 (2017) (University of Cape Town and University of the Witwatersrand, 2017). Four specimens from each concrete mix were tested for WSI and the mean of the four test results reported as the average WSI of the specific mix. The detailed test procedure is presented in Appendix B.13.2, while the corresponding results are provided in Appendices C.22 and C.23.

3.5.7 Microstructural and mineralogical analysis

The microstructure of concrete and the mineralogy of the constituent materials and the products formed during and after hydration is critical for the understanding of the effect of glass on concrete properties. The microstructure and mineralogy of the concrete and its constituents were analysed using a scanning electron microscope (SEM), X-ray diffraction (XRD) and X-ray fluorescence (XRF). The microscopy of the concrete products formed after the incorporation of glass was analysed using an SEM in accordance with ASTM C1723. The detailed procedure for SEM is presented in Appendix B.14.1. Figure 3.19 shows the SEM that was used in this study.

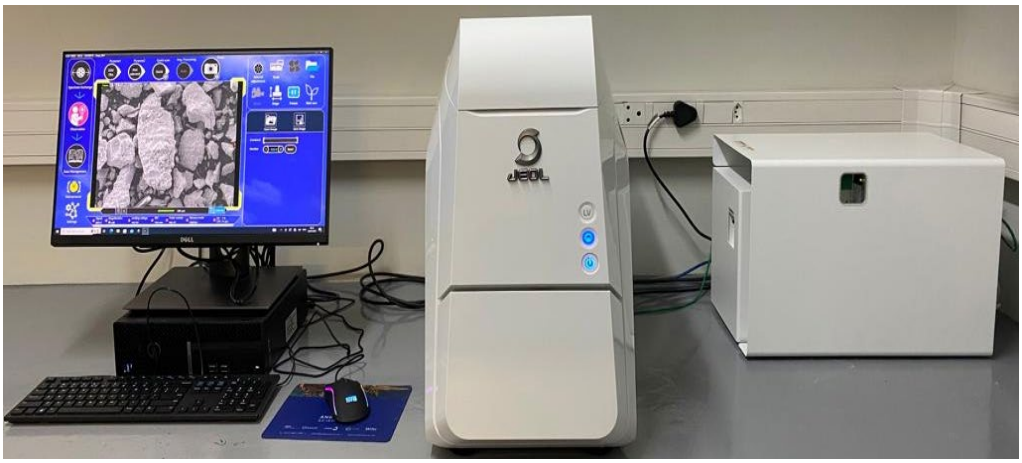

Figure 3.17: Jeol SEM apparatus

XRD is used to characterise the mineralogical composition of specimens and materials thereby providing insights into their structural properties and potential applications. XRD was done in accordance with ASTM D3906. The detailed procedure for XRD is presented in Appendix B.14.2. Figure 3.20 shows the X-ray diffractometer assembly that was used in this study.

Figure 3.18: D2 PHASER XRD apparatus

A Rigaku NEX DE High-Resolution Energy Dispersive X-ray Fluorescence (EDXRF) Spectrometer (Figure 3.21) was used to determine the elemental composition of materials. Pulverised glass specimens were first crushed and ground into a fine powder using a laboratory mill until they passed through a 75-µm sieve. This ensured that the specimens were uniform and suitable for testing. The powder was then dried in an oven at 105 °C for 24 hours to remove any

moisture. About 5 g of the dry powder was pressed into a flat pellet using a laboratory hydraulic press, preparing it for analysis.

Figure 3.19: Rigaku NEX DE High-Resolution Energy Dispersive X-ray Fluorescence (EDXRF) Spectrometer (UWC laboratory)

The spectrometer was calibrated before testing, using reference materials with known compositions to ensure accuracy. A blank specimen was also tested to confirm the absence of contamination. The pellet was carefully placed in the spectrometer's sample holder, ensuring it was flat and centred. The machine was set to high-resolution mode to detect the elements present in the specimen. The X-ray beam was directed at the pellet, and the detector captured signals from the elements in the glass. Each specimen analysis took 5 minutes. Three scans were undertaken to improve accuracy of the analysis. Utmost care was taken throughout the process to avoid contamination by using clean tools and handling specimens with gloves. The spectrometer was regularly calibrated, and testing was conducted in a controlled environment to prevent external factors from affecting the results. This method ensured reliable and accurate results for the analysis of the glass specimens. After completion, the spectral data obtained from the EDXRF measurement was retrieved and analysed. The results were compared against calibration standards to determine the elemental concentrations in the glass specimens.

3.6 Chapter summary

This chapter presented the detailed experimental methodology that was adopted in this study. Aspects such as the testing philosophy, test variables, material selection, list of materials and

equipment and a summary of the testing procedure were discussed. The next chapter presents results and discussion.

Chapter 4 - Results and discussion

This chapter presents the results of the tests that were conducted. An in-depth discussion and analysis of the test results is also presented.

4.1 Material characterisation

The concrete mix design constituents were characterised with regards to their chemical composition, and physical characteristics such as particle sizes, mass, density and water absorption. The results of tests on the aforementioned characteristics are presented in the subsequent subsections within this chapter.

4.1.1 Chemical composition

The chemical composition of cement, dune sand, and waste glass, as determined by X-ray fluorescence (XRF), reveals important insights into their potential use in concrete applications. It can be seen in Table 4.1 that waste glass contains the highest composition of silicon dioxide (SiO_2) at approximately 70%. This high silica content is a key requirement for materials that exhibit pozzolanic properties, meaning they can react with calcium hydroxide ($Ca(OH)_2$) produced during the hydration of cement to form additional compounds that enhance strength. The combined percentage of SiO_2, aluminium oxide (Al_2O_3), and iron oxide (Fe_2O_3) in waste glass is 72%, indicating potential for significant pozzolanic activity when incorporated into cement-based systems.

Table 4.1: Chemical characteristics of cement, dune sand and waste glass

Chemical composition	Cement (CEM II 42.5 N)	Dune sand	Waste glass
	Quantity (%)		
CaO	57.20	31.30	0.44
SiO_2	16.80	51.00	69.70
Al_2O_3	3.40	1.08	2.40
Fe_2O_3	2.81	0.17	0.08
MgO	1.68	0.72	0.97
Na_2O + 0.658 K_2O	0.98	0.49	15.78
SO_3	3.71	0.44	0.25

In contrast, the chemical composition of cement shows a high calcium oxide (CaO) content at approximately 57%, which is essential for hydration reactions that contribute to the overall strength and durability of concrete. Dune sand also has a considerable amount of SiO_2 at 51%, which supports its role as an aggregate in concrete mixtures. Additionally, the presence of alkalis,

specifically sodium oxide (Na_2O) and potassium oxide (K_2O), in waste glass – amounting to approximately 16% – is noteworthy as it may influence the overall properties of concrete.

4.1.2 Physical characteristics

The physical properties of cement, aggregates (stone, crusher dust, dune sand and waste glass) are presented in Table 4.2. The waste glass aggregates exhibited distinctive properties compared to conventional aggregates, particularly in terms of fineness modulus (FM). The waste glass showed a notably higher FM of 4.34 compared to the Philippi dune sand at 1.27 and crusher dust at 3.55. This higher FM value aligns with findings by Ling and Poon (2012), who reported typical FM values from 3.47-4.51 for recycled glass aggregates. The higher FM of waste glass indicates a coarser particle distribution, which Olofinnade et al. (2018) found to significantly influence the fresh properties of concrete, often resulting in harsher mixes requiring additional water for adequate workability.

Table 4.2: Physical characteristics of materials

Description	Specific gravity	Fineness modulus	Water absorption (%)	CBD (kg/m³)	Nominal size (mm)
Water	1.00	-	0	1000	-
Cement (PPC CEM II 42.5 N)	3.15	-	0.10	1440	-
20 mm stone (hornfels)	2.74	-	0.64	1420	20
Crusher dust (hornfels)	2.74	3.55	1.0	1650	7.1
Philippi dune sand (natural fine aggregate)	2.58	1.27	1.5	1623	2
Sand-Crusher dust	2.64	2.11	0.27	1657	7.1
Waste glass (fine aggregate)	2.53	4.34	0.40	1580	2

The specific gravity results show that waste glass (2.53) had a lower specific gravity compared to both the crusher dust and Philippi dune sand (2.74 and 2.58 respectively). This property, as noted by Ismail and Al-Hashmi (2009), affects the overall density and proportioning of concrete mixes. The water absorption indicate that waste glass has the lowest absorption at 0.40%, considerably

lower than crusher dust (1.0%) and Philippi dune sand (1.5%). Elavarasan and Dhanalakshmi (2016) suggest that the low water absorption in glass aggregates could improve workability due to reduced water absorption during mixing, though it may influence the interfacial transition zone between paste and aggregates in the hardened state. The compacted bulk density (CBD) of waste glass (1580 kg/m³) is lower than that of the crusher dust (1650 kg/m³) and Philippi dune sand (1623 kg/m³). This variation in CBD, according to Olofinnade et al. (2018), necessitates careful consideration during mix design to ensure proper proportioning and to achieve desired concrete properties.

4.1.3 Particle size distribution

The particle size distribution of the waste glass and fine and coarse aggregates is presented in Figure 4.1. It can be seen from the curve that the sand/crusher dust and waste glass are well graded. The waste glass, however, has a coarser distribution compared with sand/crusher dust and the grading limits.

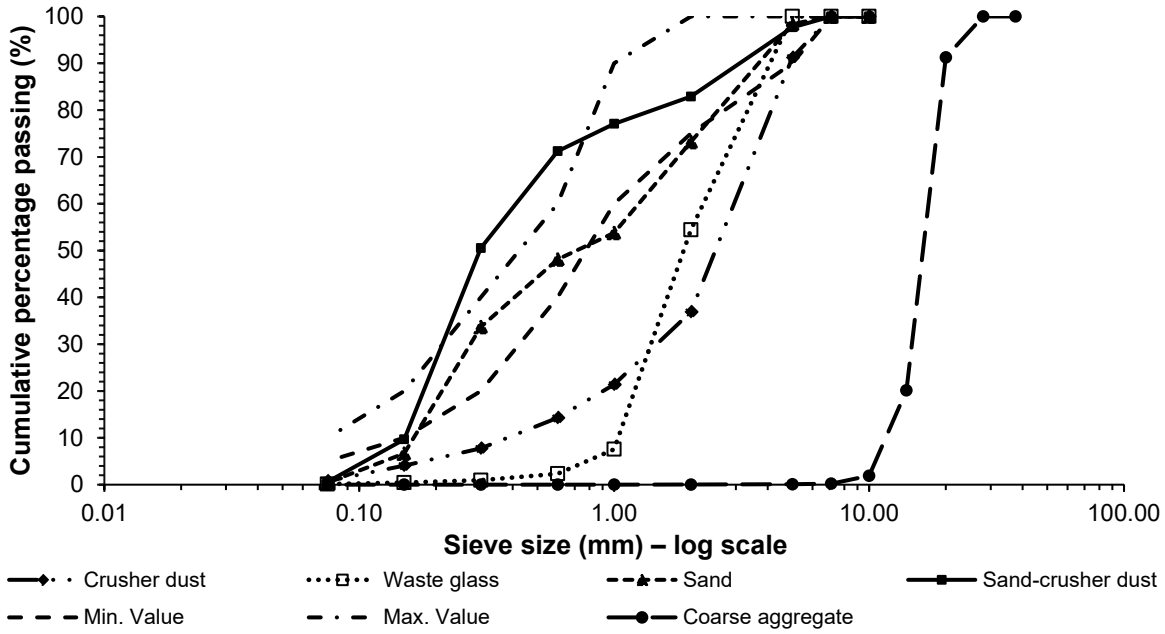

Figure 4.1: Particle size distribution of coarse and fine aggregates

It can be seen that sand-crusher dust presented a more homogeneous distribution across the sieves, while waste glass exhibited a predominance of particles within a specific size range. The portion of finer particles in waste glass was lower than in sand-crusher dust. Specifically, 58.04%

of waste glass was retained on the 2.00 mm sieve, 9.87% on the 1.00 mm sieve, and 3.28% on the 0.600 mm sieve. In contrast, sand/crusher dust retained 83.43% on the 2.00 mm sieve, 77.42% on the 1.00 mm sieve, and 71.61% on the 0.600 mm sieve. Waste glass showed a coarser distribution in the range of sieves from 0.300 mm to 2.00 mm, which is noteworthy compared to the lower limits of the SANS 1083:2013 specification. These finer particles are relatively negligible in the context of its use as a fine aggregate in concrete.

The effective size of the distribution of the waste glass and fine and coarse aggregates is presented in Table 3. The formulae for the calculated parameters in the Table 4.3 are presented in Appendix B.

Table 4.3: Material classification parameters for concrete specimens

Description	D_{10}	D_{30}	D_{60}	C_u	C_c	Material gradation
Waste glass	1.2	1.4	2.2	1.8	0.5	Uniform
Sand	0.18	0.27	1.3	7.2	1.2	Well-graded
Crusher dust	0.38	1.6	3.45	9.1	1.2	Well-graded
Sand-crusher dust	0.15	0.23	0.4	2.7	3.8	Uniform

Where

C_u = coefficient of uniformity $C_u = \frac{D_{60}}{D_{10}}$

C_c = coefficient of curvature $C_c = \frac{D_{30}^2}{D_{10} \times D_{30}}$

D_{10} = the sieve size when 10% of the particles are still retained

D_{30} = the sieve size when 30% of the particles are still retained

D_{60} = the sieve size when 60% of the particles are still retained

The calculated material characteristics presented in Table 4.3 – especially the coefficients of uniformity (C_u) and curvature (C_c) – indicate that they are suitable for use in concrete production. Specifically, a C_u value greater than 4 for sand suggests that it is well-graded and would thus provide good packing and stability. The calculated C_c value between 1 and 3 further confirms its well-graded nature (Ontiveros-Ortega et al., 2016; Cayme and Asor, 2017). In contrast, the waste glass and sand-crusher dust mixtures exhibit uniformly graded characteristics with lower C_u values, indicating a lack of particle size diversity which may affect their performance in concrete

applications. Understanding these gradation parameters is crucial for optimising material selection and ensuring the desired mechanical properties in both fresh and hardened concrete.

4.2 Fresh concrete properties

The incorporation of glass in concrete affects fresh concrete properties such as workability. Studies by De Castro and de Brito (2013) have reported on waste glass properties such as particle size, shape and content on fresh concrete properties such as workability. The fresh concrete properties that have been presented in this subsection comprise slump, flow, and vebe time. Detailed results of each of the aforementioned tests are provided in Appendix C.

4.2.1 Slump

The results of tests for slump of concrete mixtures containing various waste glass contents and w/c ratios are presented in Figure 4.2 and in Appendix C.

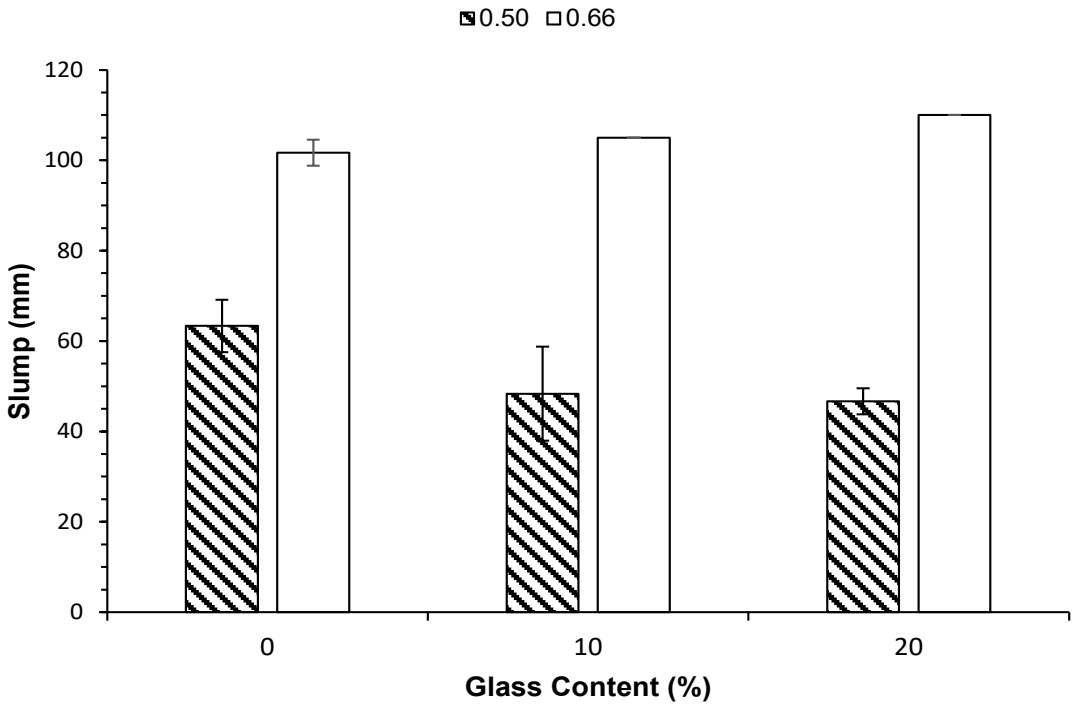

Figure 4.2: Slump test results.

It can be observed from Figure 4.2, despite the wide variability in the test results, that the effect of glass on slump is not well defined across the w/c ratios under investigation. An increase in

glass content resulted in a corresponding reduction in slump in the w/c = 0.50 mix. This reduction was statistically significant (at a level of significance of 5%) at a glass content of 20%. The reduction in slump in the w/c = 0.5 mix containing 10% glass was not statistically significant. Similarly, difference in slump between the w/c = 0.50 mixes containing 10% and 20% glass was not statistically significant at a level of significance of 5%. The incorporation of glass in w/c = 0.66 mixes resulted in a significant increase in slump at a level of significance of 5%. The increase in slump is directly proportional to glass content.

Analysis of variance (ANOVA) was conducted at a level of significance of 5% to evaluate the statistical significance of the aforementioned variations. The analysis confirmed that the effect of waste glass content on slump values was statistically significant, with a p-value of 2.00×10^{-8} ($p < 0.05$). This demonstrates that the observed changes in slump values are not due to random variation. Conversely, the w/c ratio did not significantly affect slump values at this level, as shown by a p-value of 0.555 ($p > 0.05$). This indicates that the reduction in workability is primarily driven by waste glass content, rather than the w/c ratio.

The observed effect of glass on slump is consistent with past studies. The reduction in slump of concrete mixes with a w/c ratio of 0.50 is consistent with studies by Tan and Du (2013) and Ismail and Al-Hashmi (2009), who attributed this reduction to the rough texture and angular geometry of waste glass particles. These characteristics increase internal friction within the concrete mixture, leading to decreased workability. Conversely, the observed increase in slump for concrete mixes with a w/c ratio of 0.66 aligns with the findings of Ahmad et al. (2022) and Fernandes et al. (2019), who noted that the smooth surface of waste glass particles enhances workability when sufficient water is available. The trends observed across all concrete mixes were corroborated by test results of flow and vebe time.

4.2.2 Flow

The results of tests for flow of concrete mixtures containing various waste glass contents and w/c ratios are presented in Figure 4.3 and in Appendix C. It can be seen that the effect of glass on flow is not well defined across the w/c ratios under investigation. An increase in glass content in w/c = 0.50 mixes resulted in a corresponding reduction in flow. This reduction is statistically significant at a level of significance of 5%. The difference in slump between the w/c = 0.50 mixes with 10% and 20% glass, however, was not statistically significant. These flow-related observations are similar to those of slump. An increase in glass content in w/c = 0.66 mixes

resulted in a corresponding increase in flow. The observed increase in w/c = 0.66 mixes was not statistically significant at a level of significance of 5%. Whereas glass affects flow, its overall effect on flow at the two w/c ratios used in this study is not statistically significant. An ANOVA of this effect yielded a p-value of 0.098 which is greater than the level of significance of 0.05.

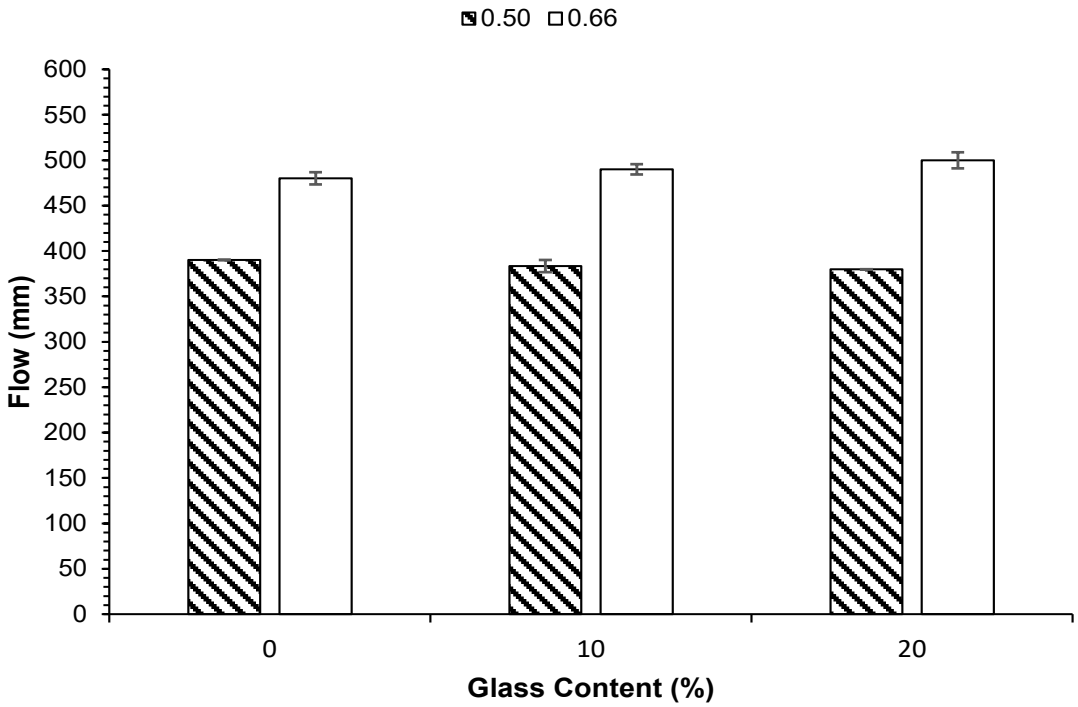

Figure 4.3: Flow test results.

The reduction in flow can be attributed to the angular and irregular shapes of waste glass particles which restrict easy movement within the mix and a consequent reduction in flow. The observed increase in flow with an increase in glass content is consistent with the findings from studies by Bahadur and Parashar (2023) and Hadi et al. (2022), and could be attributed to the smooth surfaces of waste glass particles, which reduce internal friction, and the higher water content, which provides additional free water for lubrication in the mix. The observed trends across, all concrete mixes under investigation, were corroborated with results of the tests for slump and vebe time.

4.2.3 Vebe time

The results of tests for the vebe time of concrete mixtures containing various waste glass contents and w/c ratios are presented in Figure 4.4 and in Appendix C. It can be observed that the effect

of glass on vebe time is not well defined across the w/c ratios under investigation. An increase in glass content resulted in a corresponding increase in vebe time for mixes with a w/c ratio of 0.50. However, an increase in glass content resulted in a reduction in vebe time in w/c = 0.66 mixes. The observed increase and reduction in vebe times are statistically significant at a level of significance of 5%.

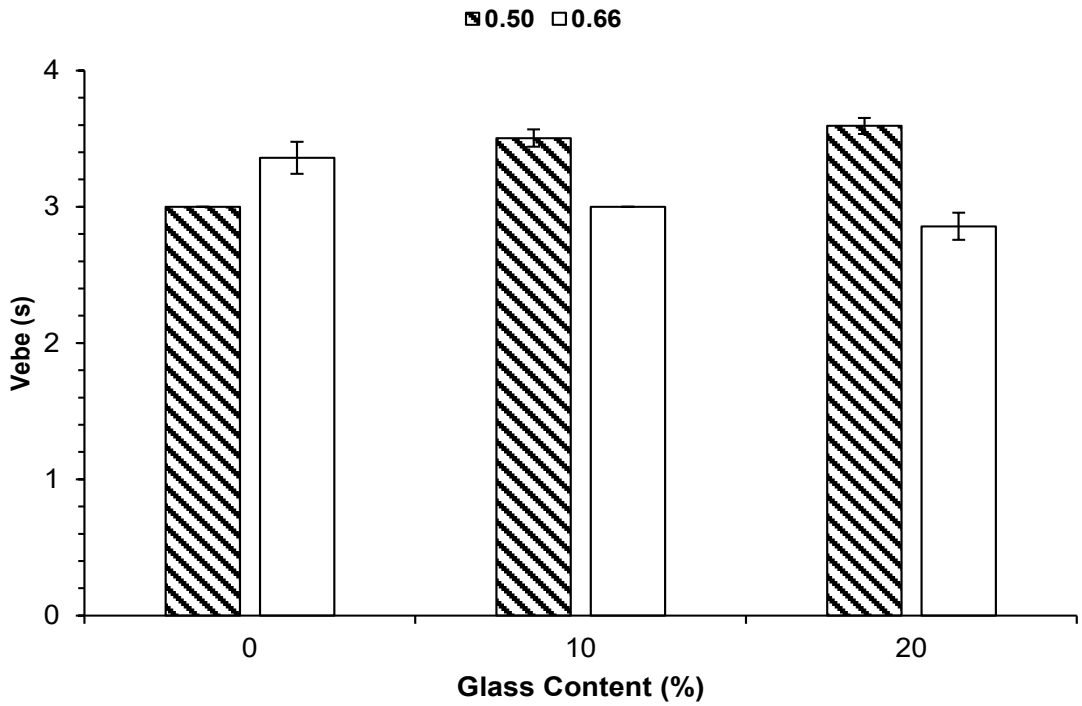

Figure 4.4: Vebe time test results.

The observed effect of glass on vebe time is consistent with the observation made on the effect of glass on slump and flow. The observed increase in vebe time resulting from the incorporation of waste glass in concrete signifies a reduction in workability (Topcu and Canbaz, 2004; Chilmon et al., 2023) and can be attributed to the enhanced internal friction caused by the angular and rough texture of waste glass particles. The observed reduction in vebe time with an increase in glass content at higher w/c ratios is consistent with literature. Upreti and Mandal (2021), for example, reported that the smoother surface of waste glass particles, combined with a greater amount of free water, enhances flowability and reduces internal friction. The enhanced flowability will manifest as a reduction in vebe time.

4.3 Fresh and hardened density

The effect of waste glass on the density (fresh and hardened) of concrete containing various waste glass contents and w/c ratios is presented in Figure 4.5, Figure 4.6 and Appendix D.

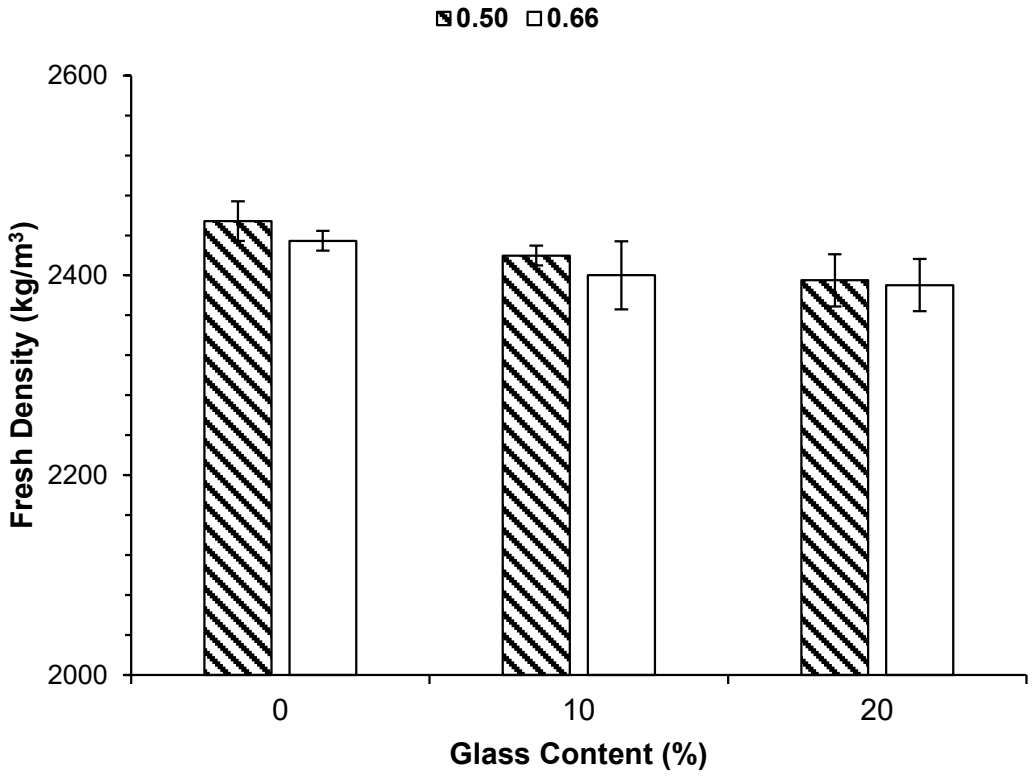

Figure 4.5: Fresh concrete density

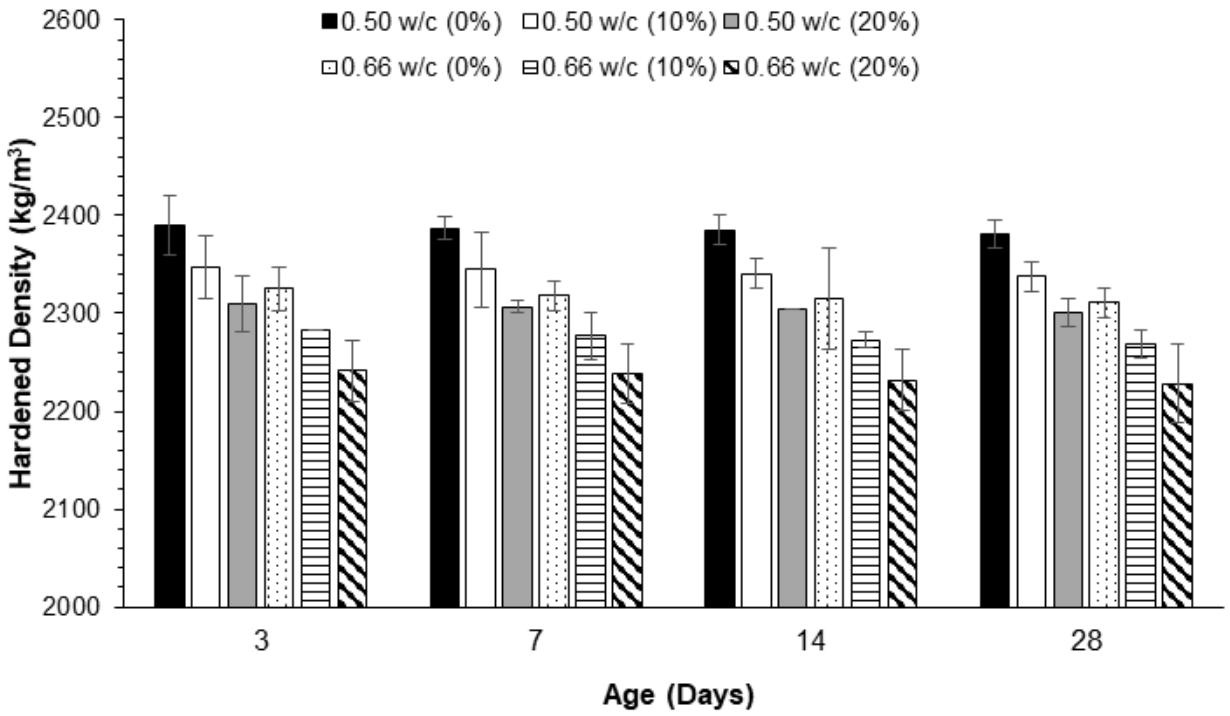

Figure 4.6: Hardened concrete density.

It can be observed that the partial replacement of dune sand with waste glass resulted in a reduction in fresh and hardened density throughout, irrespective of the w/c ratio. The reduction in density in mixes with a w/c ratio of 0.50 is statistically significant at a level of significance of 5%, and insignificant in mixes with w/c ratio of 0.66. In addition, the fresh and hardened density of mixes with a w/c of 0.66 were significantly lower than those for mixes with a w/c ratio of 0.50. The observed reduction in density due to the incorporation of glass is consistent with the findings of Ismail and Al-Hashmi (2009), Kou and Poon (2009) and Adaway and Wang (2015). The density of dune sand (2580 kg/m^3) is slightly higher than that of waste glass (2530 kg/m^3). Thus, the replacement of the dense material (dune sand) with a less dense material (waste glass) would result in an overall reduction in density. Mixes containing glass were characterised by high microporosity resulting from localised voids. The quantity of voids increased with an increase in glass content, thereby resulting in the observed reduction in density.

4.4 Compressive strength

The results of tests for compressive strength of concrete mixtures containing various waste glass contents and w/c ratios are shown in Figure 4.7 and Appendix E.

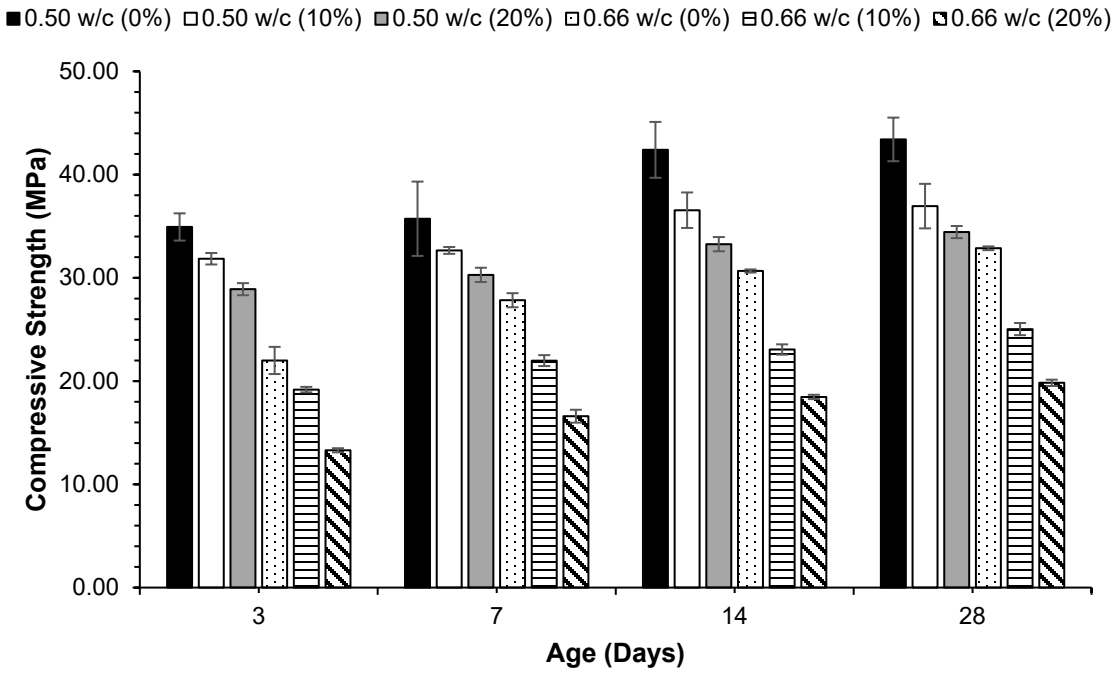

Figure 4.7: Compressive strength test results

Figure 4.7 indicates that an increase in glass content resulted in a reduction in compressive strength throughout the entire range of mixes under investigation. This reduction is statistically significant at a level of significance of 5%. The observed reduction in compressive strength is consistent with literature (Limbachiya, 2009; Gautam et al., 2012). The reduction in compressive strength can be attributed to the smooth surface texture of glass particles, which inhibits the formation of a strong bond at the interfacial transition zone (ITZ) between hardened cement paste and the aggregate. The percentage reduction in compressive strength across the w/c ratios in the study ranged between 15% and 24% at glass replacement levels of 10% and 20% respectively.

The reduction in compressive strength could also be attributed to the increased porosity (from the localised voids observed), microcracks and a weakened ITZ resulting from the smooth texture of glass particles as seen from the SEM micrographs presented in Section 4.8.1. Voids and microcracks reduce the degree of compactness of the microstructure and weaken the hardened cement paste, thereby reducing its ability to resist applied compressive stresses. An increase in glass content would result in a corresponding increase in localised voids and microcracks that would manifest as a reduction in compressive strength. As expected, mixes with a high w/c ratio (i.e., w/c = 0.66) exhibited lower strengths than those with a low w/c ratio (w/c = 0.50).

The reduction in compressive strength in mixes with high w/c ratio can be attributed to the increased porosity which increased the volume of capillary pores that compromise the overall integrity of the concrete matrix. Aliabdo et al. (2016) further report that the dilution of the cement paste in mixes with high w/c ratios may reduce its binding effectiveness, thereby affecting strength adversely despite localised improvements in microstructure. XRD results (See section 4.8.2) further show the alteration of the crystalline phases within the concrete as a result of increased glass content. This alteration would reduce hydration products and increase the proportion of amorphous silica, thereby resulting in a reduction in compressive strength, especially at high glass content.

4.5 Accelerated drying shrinkage

The results of tests for accelerated drying shrinkage of concrete mixtures containing various waste glass contents and w/c ratios are presented in Figure 4.8, Figure 4.9 and Appendix F. The incorporation of glass results in a reduction in drying shrinkage across the range of mixes and w/c ratios under investigation. The observed reduction in shrinkage was statistically significant at a level of significance of 5% except for the w/c = 0.50 mix with a glass content of 10%. The drying shrinkage in mixes containing 10% and 20% waste glass were not significantly different from each other across the w/c ratios that were used in this study.

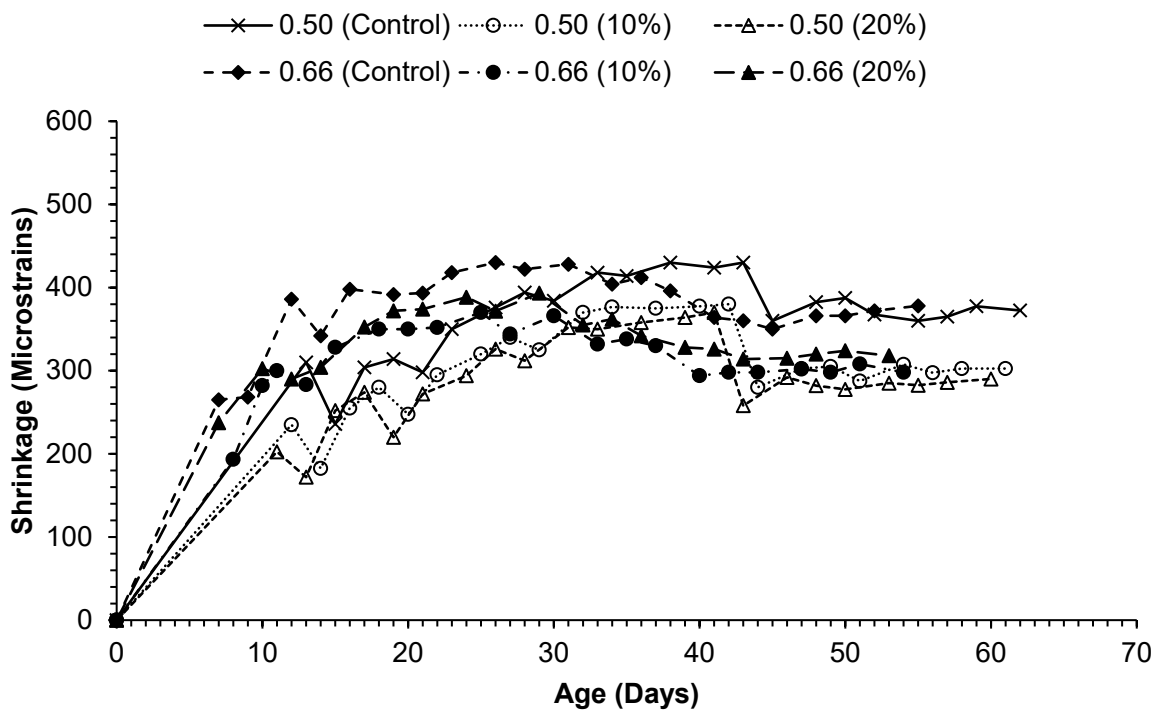

Figure 4.8: Shrinkage development in concrete mixes

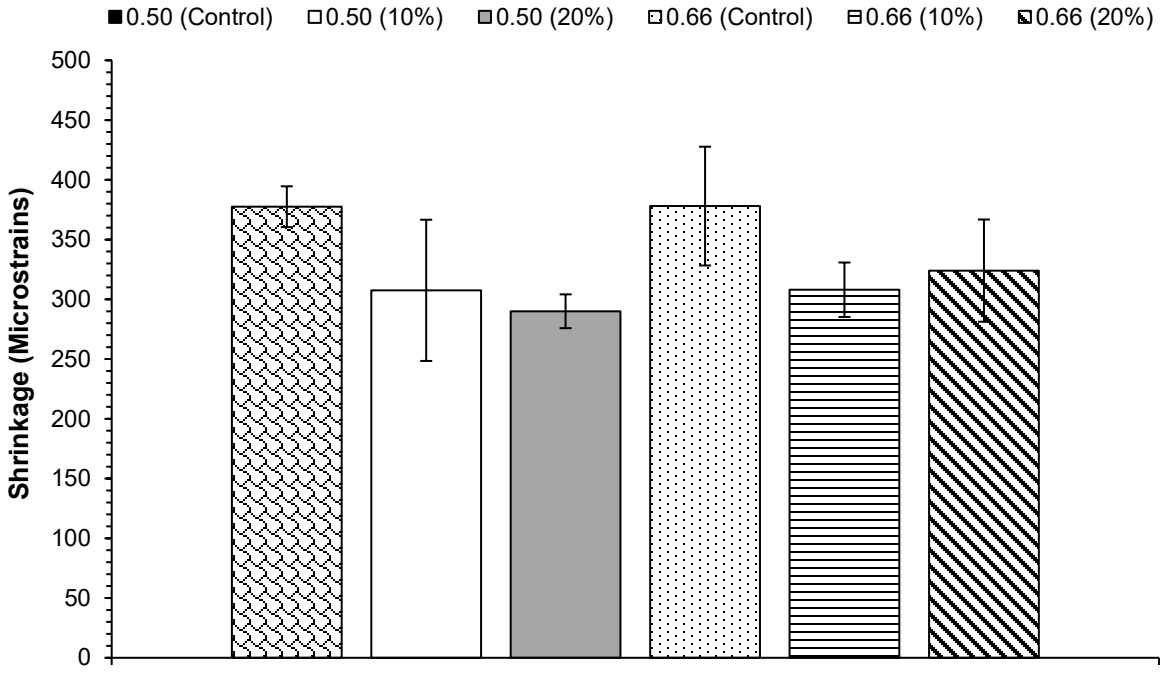

Figure 4.9: Drying shrinkage test results

The observed reduction in drying shrinkage is consistent with literature (Limbachiya, 2009; De Castro and de Brito, 2013; Hunag et al., 2015). Limbachiya (2009) reports that the reduction in shrinkage is not significant in concrete mixes with glass contents less than 20%. The observed reduction can be attributed to the additional restraint provided by larger glass particles compared to smaller sand particles (Zhao et al., 2022). It can be inferred, from particle size distribution and fineness modulus (FM) test results, that glass particles were larger and coarser (FM = 4.34) than dune sand (FM = 1.27). The coarse glass particles are thus expected to increase the degree of restraint to shrinkage within the concrete matrix because of the increased mechanical interlock within the coarse glass particles. An increase in the degree of restraint manifests as a reduction in shrinkage strain.

The water absorption of crushed glass (0.4%) is less than that of dune sand (1.5%). Mixes containing glass particles are thus expected to contain less water bound within their capillary pores and are thus less susceptible to shrinkage deformations that would result from the loss of water from the concrete matrix to the environment. The incorporation of glass in concrete resulted in an increase in localised voids as revealed by the SEM micrographs. These voids, however, are not interconnected. The addition of glass in concrete improved the density of the Interfacial Transition Zone (ITZ, and the overall microstructure of the concrete matrix. XRD analysis provides further specifics regarding phase composition changes due to waste glass inclusion. The prominent SiO_2 peak at approximately 26.6° 2θ indicates substantial quartz presence across all specimens, while the main $CaCO_3$ peak around 29.4° 2θ shows intensities varying from 25,000 to 45,000 cps, with higher intensity observed at w/c = 0.66. Notably, Portlandite peaks around 18° 2θ indicate a decrease in $Ca(OH)_2$ content from 5.3% to 0.5% as waste glass content increases; this supports findings by Idir et al. (2011), who noted that silica-rich materials lead to reductions in calcium hydroxide due to their reaction with silica, forming additional C-S-H gel. The formation of additional C-S-H gel, especially within the ITZ would thus densify the ITZ. The densification of the ITZ would reduce the ease with which moisture is lost to the environment. The absence of interconnected voids and the improved ITZ density would reduce the susceptibility to shrinkage due to the lack of direct pathways through which moisture can be lost from the concrete matrix to the environment.

4.6 Concrete surface resistivity

The results of tests for the surface resistivity of concrete mixtures containing varying waste glass contents and w/c ratios are presented in Figure 4.10 and Appendix G.

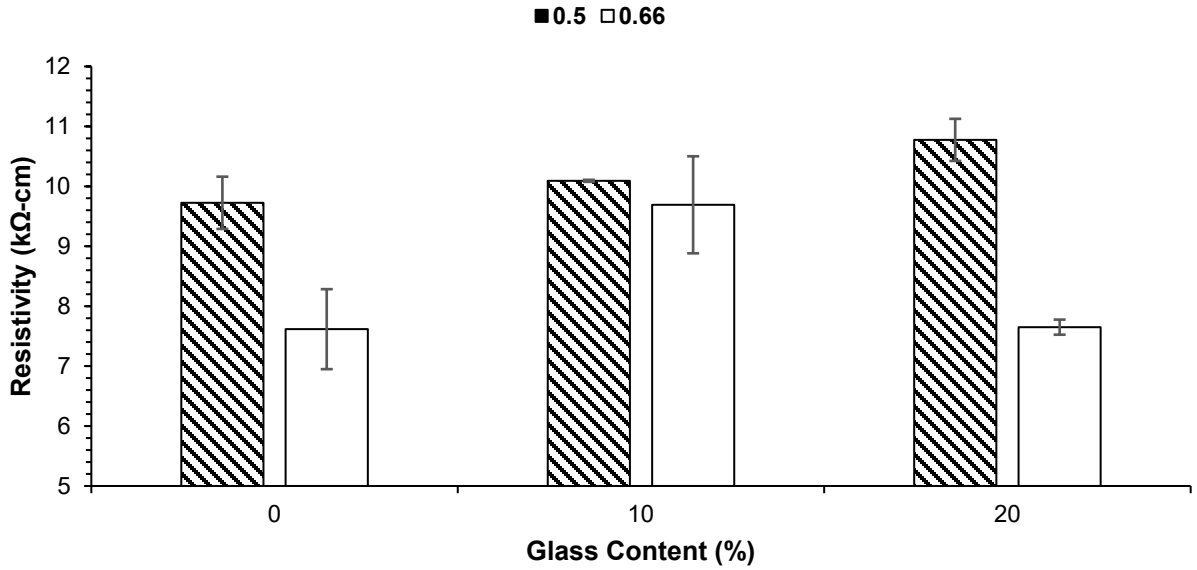

Figure 4.10: Surface resistivity test results

It can be seen in Figure 4.10 that the effect of waste glass on the surface resistivity of concrete is not clearly defined across the range of mixes and w/c ratios under investigation. Generally, the increase in surface resistivity, with respect to the control mix, was marginal except for the w/c = 0.50 mix at a glass content of 20% and the w/c = 0.66 mix at a glass content of 10%. The marginal increase was statistically significant in mixes with w/c = 0.50 at a level of significance of 5%. The observed increase in surface resistivity, though marginal, implies that glass could potentially reduce the susceptibility to corrosion of steel in concrete. In addition, it is important to note that the surface resistivity of concrete mixes is less than 20 kΩ-cm, thereby signifying that the susceptibility to corrosion of reinforcing steel embedded in any of these concrete mixes is within the range of moderate-high.

The observed increase in resistivity is consistent with literature (Saha, 2023). XRD analysis revealed that an increase in glass content resulted in a decrease in calcium hydroxide ($Ca(OH)_2$). The reduction in calcium hydroxide content can be attributed to the pozzolanic reaction between silica in the waste glass and the calcium hydroxide. This reaction forms additional calcium silicate hydrate (C-H-S) gel which enhances bonding and densifies ITZ and the concrete matrix. The densification of the concrete matrix and the ITZ reduces porosity, thereby reducing the ease with which ions and electrical current can flow in concrete. Whereas the incorporation of glass

enhances the density of the ITZ and the overall microstructure, as inferred from SEM and XRD tests, it can also be inferred that the benefits of the densification are counteracted by the localised voids and increased microcracks that form in concrete containing glass. These voids and microcracks facilitate the flow of current and ions, thereby counteracting the benefit of the densification of the ITZ, consequently resulting in the observed marginal increase in resistivity. Glass has a low water absorption (0.4%) in comparison to natural sand (1.5%). The concrete matrix of mixes containing glass are thus expected to contain additional free water – above that required for full hydration of cement grains – than the control specimen. The free water would increase the voids and facilitate the flow of ions and current within the concrete, thereby resulting in an increase in surface resistivity.

As expected, mixes with high water-to-cement ratios (w/c = 0.66) exhibited lower surface resistivity than those with low water-to-cement ratios (w/c = 0.55) (Topcu and Canbaz, 2004). Similar observations have been recorded by Ghosh and Ganesan (2022) and Wong et al. (2020). The inverse relationship between resistivity and glass content can be attributed to the increased number and interconnectivity of voids within the concrete matrix – resulting from a high w/c ratio – that facilitate the ease with which current and ions flow within the concrete matrix. An indirect assessment of the macroporosity of the mixes under investigation – see Section 4.7.3 – confirmed that the macroporosity of mixes with w/c = 0.66 were significantly higher than those with w/c = 0.50 mixes. SEM micrographs of the mixes further revealed that mixes with w/c = 0.50 had a denser ITZ and lesser voids in comparison to w/c = 0.66 mixes.

4.7 Durability indexes

Durability index (DI) testing comprised standard laboratory tests for oxygen permeability index (OPI) and water sorptivity index (WSI). The macroporosity of the mixes was also determined indirectly through these tests

4.7.1 Oxygen permeability index

The results of tests for OPI of concrete mixtures containing varying waste glass content and w/c ratios are presented in Figure 4.11 and Appendix H.

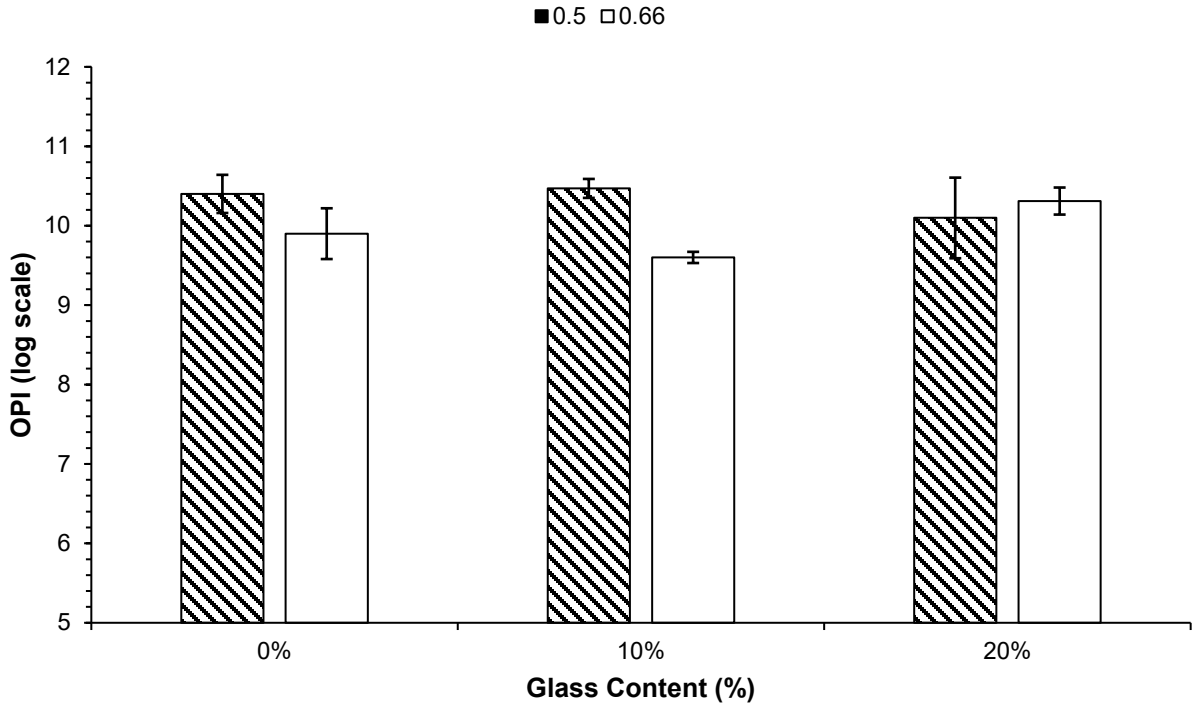

Figure 4.11: OPI test results

It can be observed in Figure 4.11 that the effect of glass content on OPI is not clearly defined across the range of w/c ratios and mixes under investigation. It is equally important to note that the OPI is measured on a logarithmic scale. Thus, a small change in OPI corresponds to a large change practically. However, it can be seen that the differences in the OPI of mixes with 20% glass class across the two w/c ratios used in this study were statistically significant in comparison to the control specimen at a level of significance of 5%. Further research on the effect of glass on OPI across a wider range of w/c ratios is needed to identify clear trends and the nature of the relationship between glass content and OPI. As expected, the OPI of mixes with w/c = 0.50 were significantly higher than those of w/c = 0.66 mixes, except for the mixes with 20% glass content. The observed increase in OPI in mixes with low w/c ratio were consistent with literature (Alexander and Beushausen, 2009; Mardani-Aghabaglou et al., 2015; Kim et al., 2018) and can be attributed to the high porosity that is characteristic of concrete with high w/c. SEM micrographs (see Section 4.8.1) and macroporosity tests results (see Section 4.7.3) further confirmed the high porosity of w/c = 0.66 mixes in comparison to the w/c = 0.50 mixes. The increased voids in w/c = 0.66 mixes would enhance the ease with which gases such as oxygen permeate the concrete matrix, thereby resulting in a reduction in OPI. Furthermore, the OPI values that were recorded for the mixes under investigation show that the quality of the concrete is within the range of “good” to “excellent”

based on the classification system provided by Alexander and Beushausen (2009). The recorded OPI values also fall within the range commonly used in South African concretes.

4.7.2 Water sorptivity index

The results of tests for WSI of concrete mixtures containing varying waste glass content and w/c ratios are presented in Figure 4.12 and Appendix H.

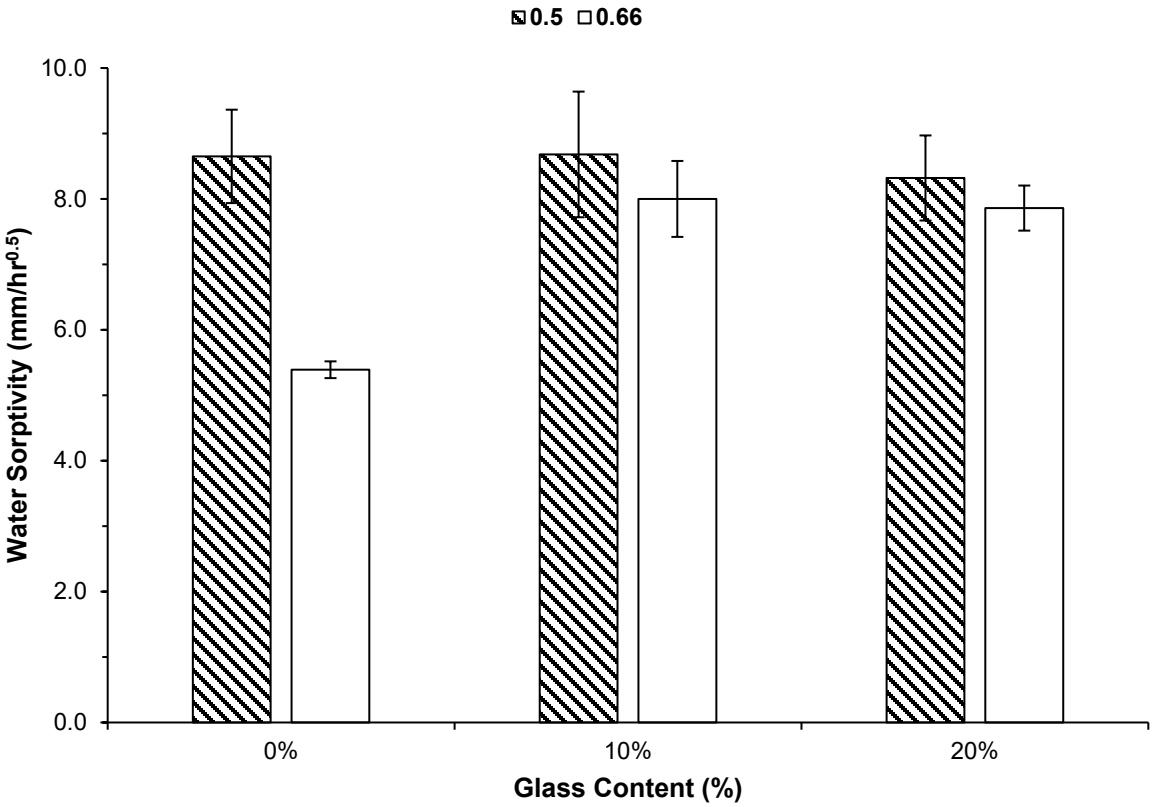

Figure 4.12: WSI test results

It can be observed in Figure 4.12 that the effect of glass on WSI is not clearly defined across the range of w/c ratios and glass contents under investigation. Specifically, it can be seen that glass increased the WSI of w/c = 0.66 mixes. This increase is statistically significant at a level of significance of 5%. Concrete mixes containing 10% glass content exhibited the highest WSI values across the w/c ratios under investigation. The increase in WSI could be attributed to the microcracks within the concrete matrix. Mixes containing glass were characterised by microcracks. These microcracks would thus facilitate the movement of water within the concrete matrix, thereby increasing the WSI. The effect of glass on w/c = 0.50 mixes, however, was not

statistically significant. The lack of a clearly defined relationship between glass content and WSI highlights the need for further research on the effect of glass on WSI across a wider range of w/c ratios than the one used in this study. The increase in WSI in w/c = 0.66 mixes can be attributed to the increased voids in these mixes as discussed in the previous subsections within this subsection. The increase in voids enhances the sorption within the concrete, thereby resulting in high WSI values.

The difference in WSI of w/c = 0.50 and w/c = 0.66 concrete mixes were not statistically significant at a level of significance of 5% except for the control mixes. This observation, though unexpected, could have resulted from the wide variability that was generally observed in the reported results. The presence of random microcracks within the concrete matrix of concrete mixes containing glass, as evident from the SEM micrographs, might be responsible for this observation. Microcracks enhance the sorption of water in a concrete mix, irrespective of the w/c ratio, due to their interconnectivity. The quality of the concrete, based on its WSI values, can be deemed as good as per the evaluation criteria used in South Africa (Alexander and Beushausen, 2009; Alexander et al., 2017).

4.7.3 Macroporosity

The results of indirect tests for macroporosity of concrete mixtures containing varying waste glass content and w/c ratios are presented in Figure 4.13 and Appendix H. It can be observed in Figure 4.13 that the relationship between glass content and macroporosity is not clearly defined across the range of w/c ratio and glass contents under investigation. As expected, the macroporosity of w/c = 0.66 mixes is higher than that of w/c = 0.50 mixes throughout. The observed difference in macroporosity across the w/c ratios under investigation was statistically significant at a level of significance of 5%. The observed increase in macroporosity is consistent with literature (Kim et al., 2018; Mehta and Monteiro, 2014) and can be attributed to the porous microstructure resulting from increased capillary pores at high w/c ratios. Specifically, Mehta and Monteiro (2014) state that excess mixing water – beyond the quantity required for hydration – creates a network of capillary pores which result in increased porosity and permeability in the hardened concrete microstructure.

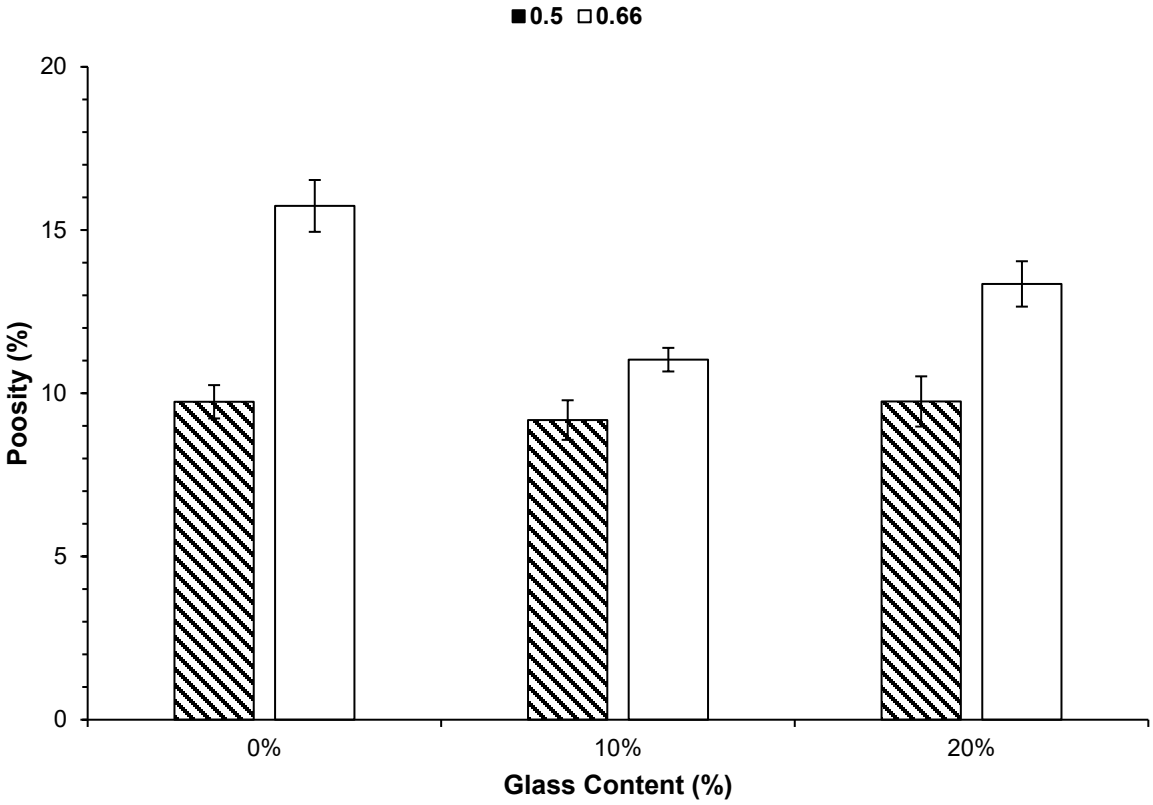

Figure 4.13: Macroporosity test results

It can also be observed that the incorporation of glass did not result in any significant change in the macroporosity of w/c = 0.50 mixes. However, the addition of glass in w/c = 0.66 mixes was accompanied by a reduction in macroporosity. This reduction is statistically significant at a level of significance of 5%. A relationship between glass content and the reduction in macroporosity in w/c = 0.66 could not be established. However, it can be hypothesised from the test results that the effect of glass on macroporosity is dependent on the w/c ratio and tends to be more pronounced in mixes with high w/c than in mixes with low w/c. Further research is needed to verify this claim. The observed reduction in macroporosity in mixes with high w/c ratios is consistent with the findings of Du and Tan (2014) and Kamali and Ghahremaninezhad (2016). This reduction can be attributed to an improvement in particle packing and pozzolanic reactions between the cement and the silica in glass. Kamali and Ghahremaninezhad (2016) further attribute the reduction to the ability of glass particles to fill capillary pores in mixes with high w/c ratios.

4.8 Micro-structural and mineralogical analysis

Microstructural and mineralogical analyses play a crucial role in understanding the properties and performance of materials. Test results of SEM and XRD analyses are presented in subsequent subsections within this section.

4.8.1 Scanning electron microscopy

Scanning electron microscopy (SEM) was used to study the morphology and microstructure of the concrete mixes under investigation. SEM micrographs of these mixes are presented in Figure 4.14. Several key microstructural features can be observed from these micrographs: ITZ (narrow dark lines), voids (dark portions), calcium hydroxide (CH) in hexagonal crystals, C-S-H gel/paste as fine fibrous crystals, and ettringite in needle-like formations. The presence of C-S-H gel formation – particularly in waste glass-modified samples – correlates with the findings of Waghmare (2020) regarding pozzolanic reactions and their positive effect on mechanical properties.

Control specimens (Figure 4.14a and Figure 4.14b) exhibited a compact matrix comprising fewer voids and minimal microcracks, indicating a dense interfacial transition zone with strong cement-aggregate bonds. This structure shows better particle-to-particle contact and a more uniform phase distribution. Similarly, the addition of glass at a constant w/c ratio resulted in a dense microstructure, an observation that is consistent with the findings of Du and Tan (2014) and Upreti et al. (2021). Mixes containing 10% glass exhibited the best microstructure throughout and were characterised by a dense ITZ density, fewer microcracks, enhanced aggregate-paste bonding and voids that were small and fewer. The incorporation of glass generally resulted in microcracks. Critical hardened concrete properties and performance characteristics of the mixes that were under investigation can be explained from the SEM results.

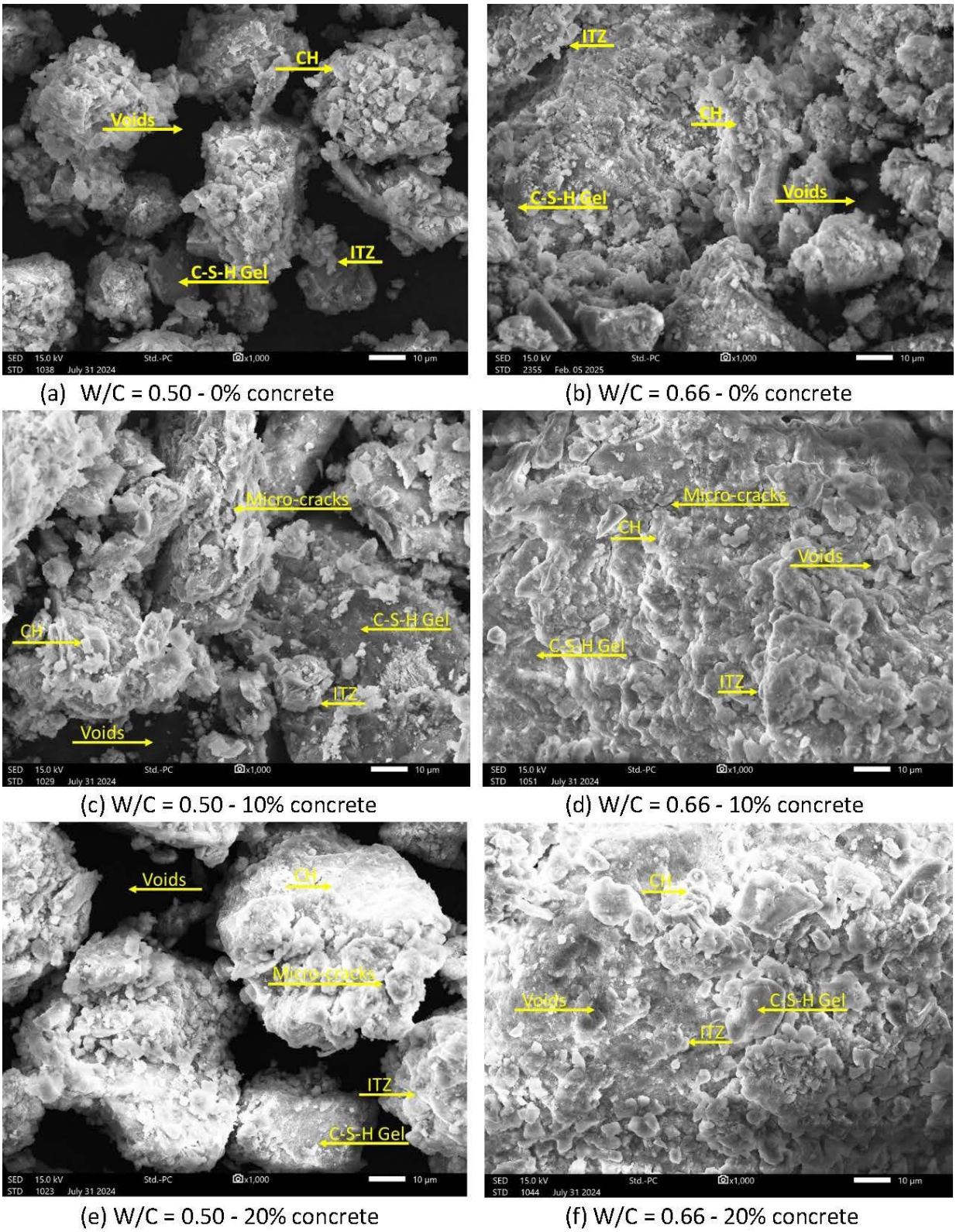

Figure 4.14: SEM micrographs

It can be seen, from Figure 4.14c, that the microstructure of the w/c = 0.50 mix containing 10% glass exhibited better glass-paste integration, which is indicative of efficient pozzolanic reactions and minimal microcracking. The microstructure of the w/c = 0.66 mix containing 10% glass (Figure 4.14d) – though better than the control mix – exhibited wider ITZ regions and increased microcracking along with hydration products that are scattered. Despite the observed microstructural enhancements, it is important to correlate these observations with the results of tests that were undertaken. It is expected that an improved ITZ density and a reduction in voids would produce concrete with high compressive strength and low macroporosity (Ibrahim, 2017). However, the test results show that an increase in glass content neither increased compressive strength nor decreased macroporosity as anticipated. It was inferred that the microcracks within the matrix of mixes containing glass might have countered the benefits of an improved microstructure and ITZ density, thereby resulting in a reduction in strength and an increase in macroporosity. Microcracks weaken the concrete and enhance the penetrability of concrete by fluids, thereby affecting critical durability-related properties such as OPI, WSI and macroporosity (Olofinnade et al., 2018). The overall effect of glass on the mechanical and durability performance of concrete should therefore consider, inter alia, the improved microstructure, ITZ density, degree of restraint, microcracking, the interactions among these microstructural parameters and their relative degrees of importance.

It can also be observed that the effect of glass on the microstructure is more pronounced on the w/c = 0.66 mix than the w/c = 0.50 mix. The microstructure of mixes with w/c = 0.66 was denser than those for w/c = 0.50. Thus, it can be inferred that glass could potentially be used to improve the microstructure of mixes with high w/c ratio, thereby improving their overall performance. Figure 4.14e and Figure 4.14f present the micrographs for concrete mixes containing 20% waste glass replacement at w/c = 0.50 and w/c = 0.66 respectively. The observed microstructural features align with the observations by Bisht and Ramana (2018) who observed an enhanced concrete microstructure at glass contents up to 21%. Figure 4.14e shows compact regions with minimal voids and improved ITZ structure characterised by better waste glass particle distribution and more uniform reaction products with limited microcracking; in contrast, Figure 4.14f exhibits increased porosity at the higher w/c ratio accompanied by more scattered waste glass particles and notable microcracks. The scattered waste glass particles in Figure 4.14f may indicate insufficient integration within the concrete matrix resulting from challenges in particle packing and bonding when the glass content exceeds the optimal content. Insufficient integration of glass within the matrix may lead to stress concentrations that enhance microcracking.

4.8.2 X-ray diffraction analysis

XRD analysis was used to study the crystalline phases and the effect of glass on the concrete mixes under investigation. These results are presented in Figure 4.15.

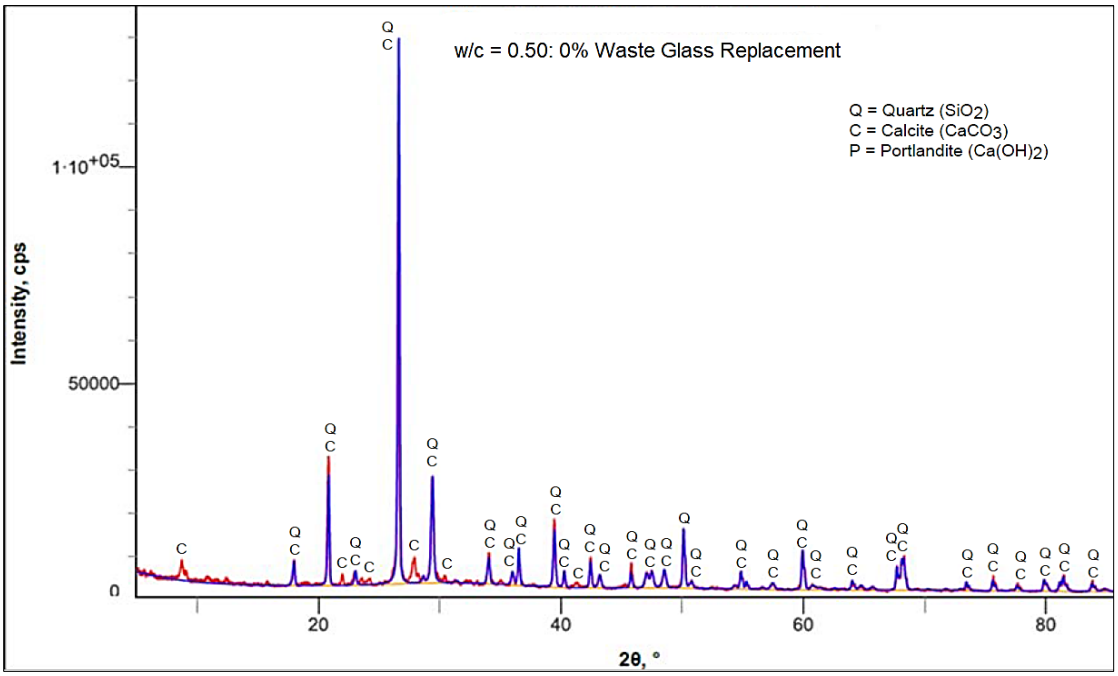

(a) w/c = 0.50 - 0% concrete

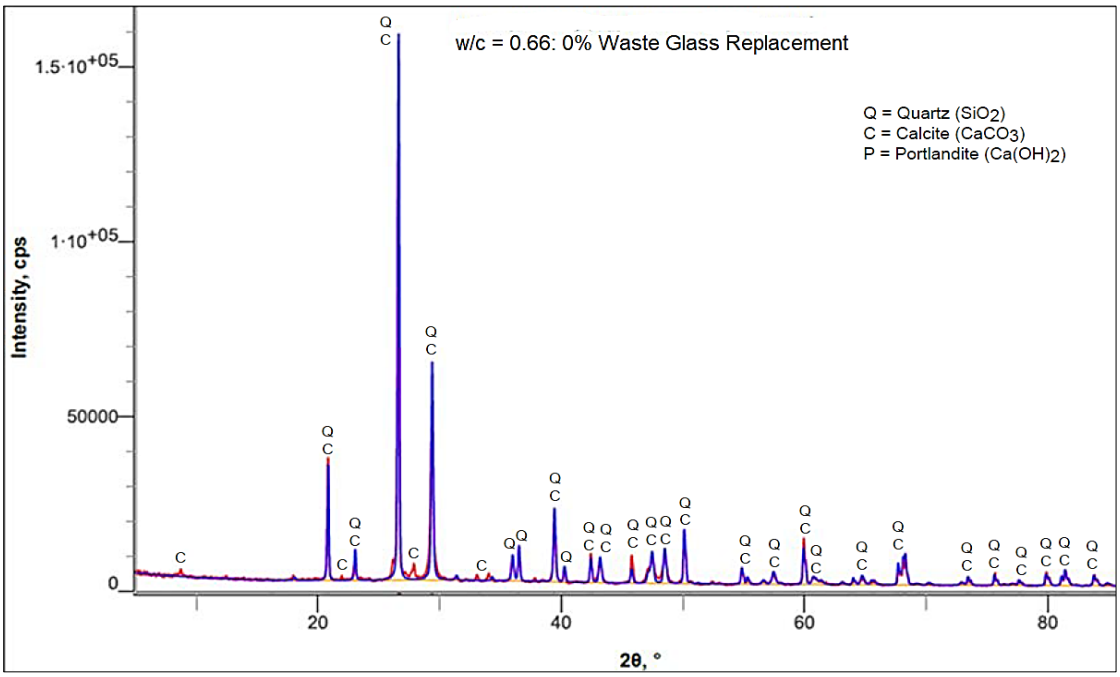

(b) w/c = 0.66 - 0% concrete

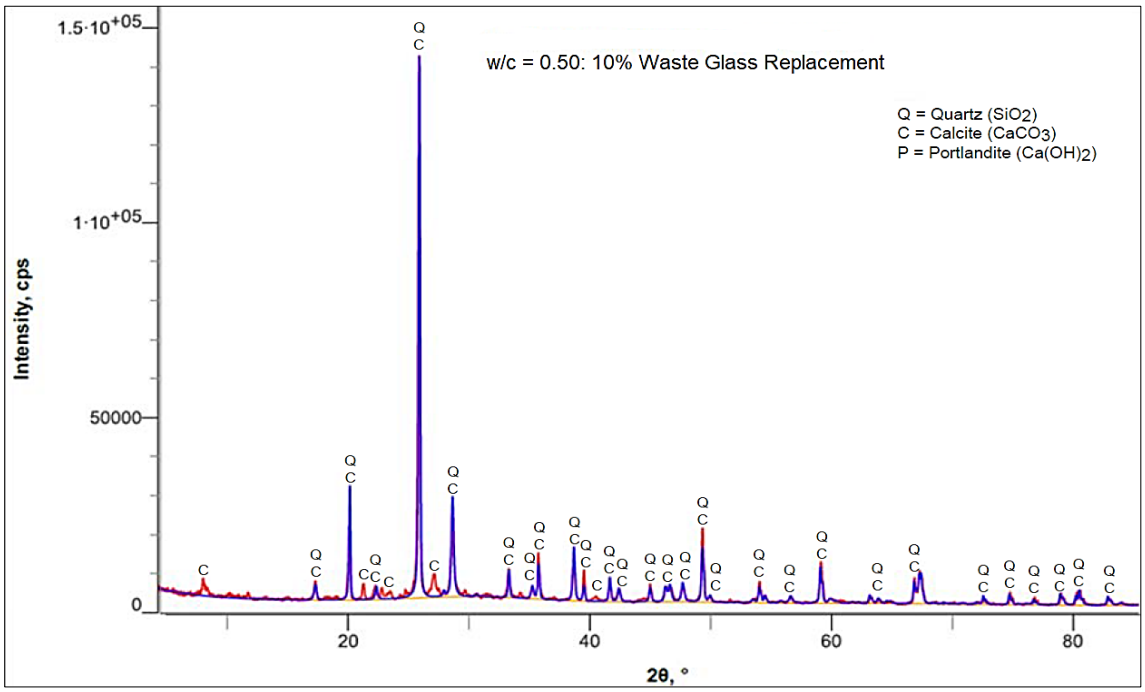

(c) w/c = 0.50 - 10% concrete

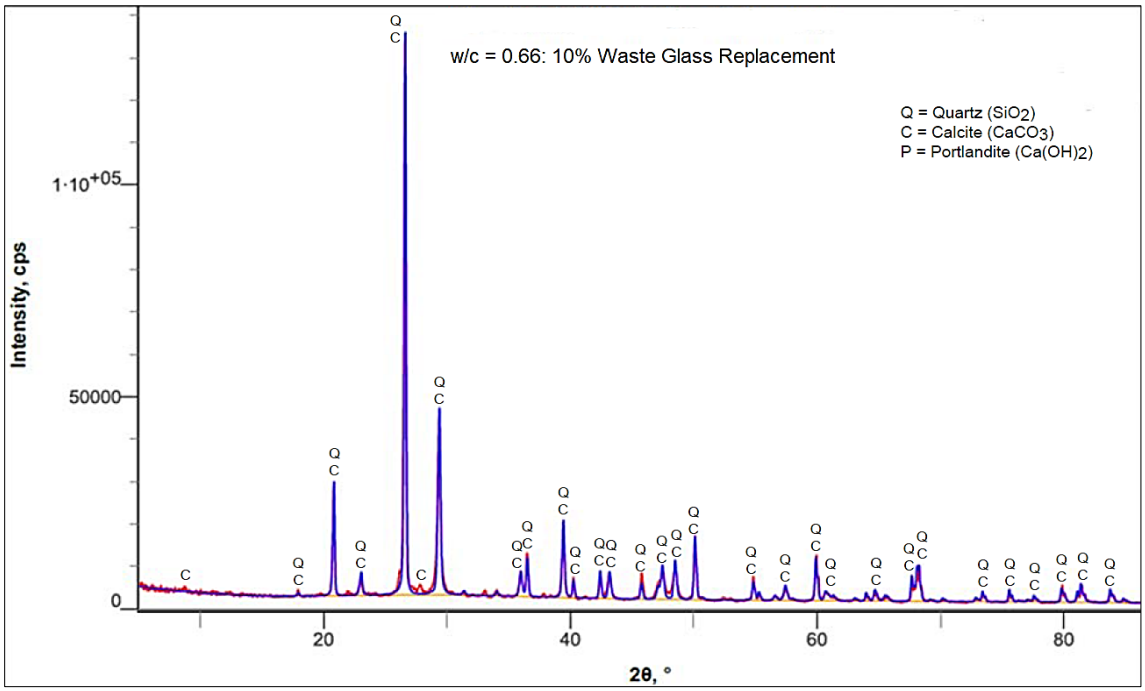

(d) w/c = 0.66 - 10% concrete

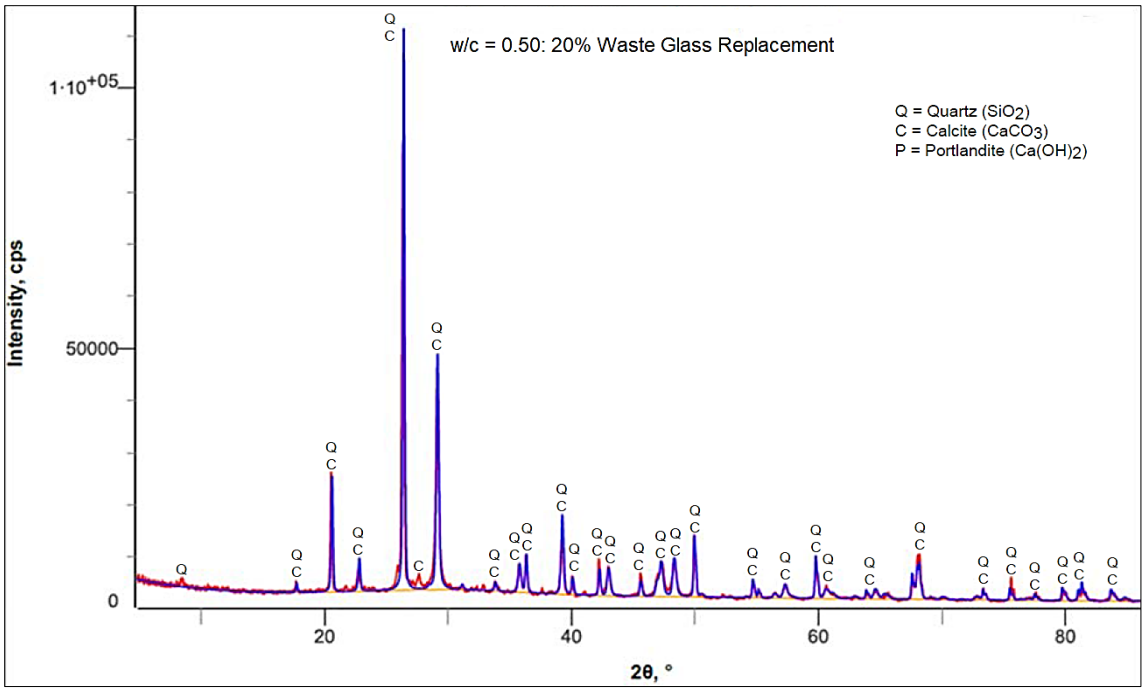

(e) w/c = 0.50 - 20% concrete

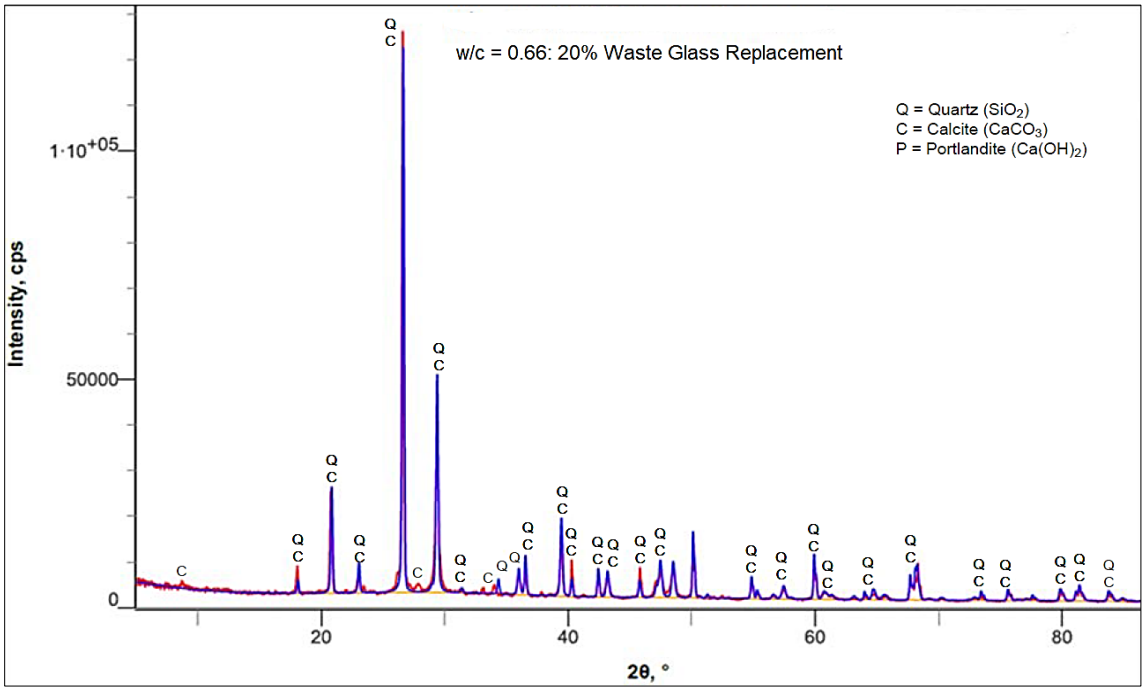

(f) w/c = 0.66 - 20% concrete

Figure 4.15: XRD results.

Note: Portlandite ($Ca(OH)_2$), although detected in low quantities by Rietveld refinement, is not visibly resolved in the diffractogram due to its trace content and possible peak overlap with major phases.

The XRD results in Figure 4.15 show peaks corresponding to crystalline phases, particularly SiO_2 (quartz), $CaCO_3$ (calcite) and $Ca(OH)_2$ (portlandite) throughout. SiO_2 peaks – especially the prominent one at approximately 26.6° 2θ with intensity around 110,000 to 140,000 cps – were significant, thus indicating that quartz was present in substantial quantities across the w/c ratios under investigation. The silica content in w/c = 0.50 mixes, except for the w/c = 0.50 mix with 20% glass content, were higher than in the w/c = 0.66 mixes. Silica-rich glass can enhance pozzolanic reactions which lead to the gradual consumption of calcium hydroxide within the concrete matrix (Idir et al., 2011). The relationship between silica, calcite, portlandite and glass content is presented diagrammatically in Figure 4.16, Figure 4.17 and Figure 4.18 respectively.

The relationship between silica content and glass content was consistent throughout the mixes under investigation as observed in Figure 4.16. Specifically, an increase in glass content from 0% to 10% was accompanied by a corresponding increase in silica content. Silica content decreased when the glass content was increased from 10% to 20%. The highest silica content was observed at a glass content of 10% across all mixes under investigation. Interestingly, mixes with 10% glass content exhibited the best microstructure (as discussed in Section 4.8.1). The silica contents of w/c = 0.50 mixes, except for the w/c = 0.50 with a glass content of 20%, were generally higher than those of w/c = 0.66 mixes.

The incorporation of glass effectively alters the crystalline structure of concrete, as shown by the high-intensity SiO_2 peaks observed in XRD results and the systematic changes in phase compositions. This indicates that silica-rich glass contributes to pozzolanic reactions. Silica facilitates the production of calcium silicate hydrate (CSH) during cement hydration. CSH is critical for strength development, durability performance and the overall densification of the concrete microstructure. Concrete mixes containing high silica content are – ideally – expected to possess a dense microstructure and exhibit high strength, less shrinkage, high resistivity, low macroporosity, low WSI and low OPI. The observed performance of the mixes under investigation, however, did not match their expected behaviour. The inability of the concrete mixes to match the expected behaviour can be attributed to additional critical parameters other than their mineralogy such as microcracking. It is thus imperative that an evaluation and estimation of concrete performance ought to integrate aspects pertaining to their microstructure, mineralogy and physical and mechanical characteristics simultaneously.

.

A clear and well-defined relationship between calcite content, portlandite content and glass content could not be established from the results presented in Figure 4.18 and Figure 4.19. Figure 4.15 further shows that the main peak for $CaCO_3$ – around 29.4° 2θ, with intensities varying from 25,000 to 45,000 cps – exhibited notable intensity differences across the mixes. The w/c = 0.66 mixes, except for the w/c = 0.50 mix at 20% glass content, exhibited the highest intensity throughout. Portlandite peaks, most notably at around 18° 2θ with intensities varying between 8,000 and 15,000 cps, indicated a decrease in $Ca(OH)_2$ content. An increase in glass content resulted in a corresponding reduction in portlandite content in w/c = 0.50 mixes. A clear relationship between glass content and portlandite content could not be established for w/c = 0.66 mixes. The observed reduction in portlandite in mixes containing w/c = 0.50 is a potential durability concern. Portlandite is responsible for the protection of reinforcing steel against corrosion. Thus, a reduction in portlandite would increase susceptibility to reinforcement corrosion. Overall, it can be observed that the beneficial aspects of glass on concrete properties are more pronounced in mixes with w/c = 0.66 than in mixes with w/c = 0.50. A detailed exposition of the observed performance of the concrete mixes under investigation vis-à-vis the observed microstructural characteristics and mineralogy has been presented in the preceding subsections within this chapter.

4.9 Chapter summary

This chapter presented an in-depth discussion and analysis of the test results. The test results were presented in the form of graphs and images. A summary of the key insights gleaned from the analysed results comprises the following:

1. The effect of glass on the fresh and hardened concrete properties under investigation depends on the water/cement ratio.
2. The effect of glass on workability is dependent on the w/c ratio of the mix. Mixes with w/c = 0.50 exhibited a reduction in slump, a reduction in flow and an increase in vebe time with an increase in glass content. Mixes with w/c = 0.66 experienced an increase in slump, an increase in flow and a reduction in vebe time with an increase in glass content.
3. The incorporation of glass in concrete resulted in a reduction in fresh and hardened density.
4. The incorporation of glass in concrete resulted in a reduction in compressive strength at all ages and a marginal increase in surface resistivity.
5. The incorporation of glass in concrete resulted in a reduction in drying shrinkage.
6. The effect of glass on durability indexes (OPI and WSI) was not well-defined.

7. The incorporation of glass in concrete resulted in a general improvement in microstructure, with mixes containing 10% glass exhibiting the best microstructure.

Chapter 5 - Conclusions and recommendations

This study investigated the effect of waste glass on selected fresh and hardened properties of concrete, namely slump, flow, vebe time, compressive strength, surface resistivity, drying shrinkage and durability indexes. The mineralogy and microstructure of concrete containing waste glass was also investigated. The conclusions that were arrived at from this study and recommendations for further research are presented in the subsequent subsections within this chapter.

5.1 Conclusions

The effect of glass on selected fresh and hardened concrete properties are presented in the subsequent subsections, aligned with the research objectives outlined in Chapter 1.

5.1.1 Effect of glass on fresh concrete properties

5.1.1.1 Effect of glass on slump, flow, and vebe time

Workability-related indicators that were studied comprise slump, flow and vebe time. The incorporation of waste glass in concrete influences its workability. Specifically, the effect of glass on workability is dependent on the w/c ratio. An increase in glass content resulted in a corresponding reduction in slump, a reduction in flow and an increase in vebe time in mixes with a w/c ratio of 0.50 and an increase in slump, an increase in flow and a reduction in vebe time in mixes with a w/c ratio of 0.66. The observed effect of glass on slump, vebe time and flow can be attributed to the physical characteristics of the glass such as texture and geometry. Internal friction resulting from coarse glass particles with angular geometry and rough texture was responsible for the reduction in slump, reduction in flow and an increase in workability. The availability of sufficient water to lubricate the mix and smooth particles in w/c = 0.66 mixes contributed to their better workability (i.e., increased slump, increased flow and reduced vebe time).

5.1.1.2 Effect of glass on fresh density

The incorporation of glass in concrete reduced its fresh density irrespective of the w/c ratio. The reduction in density was statistically significant in w/c = 0.50 mixes and insignificant in w/c = 0.66 mixes at a level of significance of 5%. The average density of waste glass was 2530 kg/m³ while that of dune sand was 2580 kg/m³. The observed reduction in density is attributed to the partial replacement of the dense material (i.e., dune sand) with a less dense material (glass) and the increased porosity in concrete specimens containing glass.

5.1.2 Effect of glass on hardened concrete properties

5.1.2.1 Effect of glass on hardened density and compressive strength

The incorporation of glass in concrete reduced its hardened density irrespective of the w/c ratio. This reduction is statistically significant in w/c = 0.50 mixes and insignificant in w/c = 0.66 mixes at a level of significance of 5%.

The incorporation of glass in concrete resulted in a reduction in compressive strength at all ages and across the w/c ratios under investigation. This reduction is statistically significant at a level of significance of 5%. The reduction can be attributed to the smooth surface texture of glass particles, which inhibits the formation of a strong bond at the ITZ between hardened cement paste and the aggregate, microcracking, the alteration of the crystalline phases within the concrete and the increased porosity from the localised voids observed in concrete mixes containing glass.

5.1.2.2 Effect of glass on drying shrinkage

The incorporation of waste glass in concrete resulted in a reduction in drying shrinkage. The observed reduction in shrinkage was statistically significant at a level of significance of 5% except for the w/c = 0.50 mix with a glass content of 10%. The drying shrinkages in mixes containing 10% and 20% waste glass were not significantly different from each other across the w/c ratios that were used in this study. The observed reduction in shrinkage was attributed to the low water absorption of glass in comparison to the dune sand, the high degree of internal restraint from coarse glass particles, the densification of the interfacial transition zone and the localised microcracks that are discontinuous.

5.1.2.3 Effect of glass on surface resistivity, durability indexes and macroporosity

The effect of glass on the surface resistivity, OPI, WSI and macroporosity of concrete was not clearly defined across the range of w/c ratios under investigation. An increase in glass content resulted in a marginal increase in surface resistivity. The increase in surface resistivity, however, was not statistically significant at a level of significance of 5%. Whereas the resistivity of concrete increased, albeit marginally, the effect of glass on the long-term durability of concrete in service could not be determined from the test results.

The effect of glass on OPI was statistically significant at a glass content of 20%. The effect of glass was also significant in mixes with w/c = 0.66 and insignificant in mixes with w/c = 0.50. Glass

did not result in any significant change in macroporosity in mixes with w/c = 0.50. The macroporosity of mixes with w/c = 0.66, however, reduced significantly. The relationship between glass content and surface resistivity, OPI, WSI and macroporosity was attributed to the microstructure, microcracking and mineralogy of the concrete and the interactions among these parameters. Thus, an in-depth investigation into the highly complex interactions among the aforementioned parameters across a wide range of mixes is required to fully understand the long-term effect of glass on the durability performance of concrete, specifically with regards to surface resistivity, durability indexes and macroporosity.

5.1.2.4 Effect of glass on gradation and water absorption

Crushed glass exhibits uniform gradation unlike natural sands which are well graded. Most glass particles were coarse. The blending of crushed waste glass with natural fine aggregates (hornfels and dune sand) – up to glass replacement levels of 20% – improves the gradation of the aggregates, further contributing to conformity to SANS 1083 specifications. The incorporation of glass in concrete would thus contribute to the production of concrete conforming to South African specifications. The glass was also characterised by fine particles that act as fillers, thereby improving hydration, particle packing and the general porosity and microstructure of the concrete. Glass particles also exhibit low water absorption. The low absorption affects the workability of the concrete, and the interfacial transition zone of the hardened concrete.

5.1.3 Effect of glass on mineralogy and microstructure

Crushed glass is a potential pozzolanic material, with silica (SiO_2) being the predominant mineral. The combined percentage of SiO_2, aluminium oxide (Al_2O_3), and iron oxide (Fe_2O_3) in waste glass is 72%, indicating potential for significant pozzolanic activity when incorporated into cement-based systems. The silica content of waste glass (approximately 70%) was significantly higher than that of cement (approximately 17%) and dune sand (51%). The silica in glass plays a critical role in hydration and microstructural development. The high silica content of glass, however, can potentially increase the susceptibility to alkali silica reaction. Future reactions between the unreacted silica and calcium hydroxide would further increase the susceptibility of reinforcement in concrete containing glass to corrosion.

Furthermore, mineralogical analysis revealed the introduction of an amorphous silica phase from waste glass while maintaining essential crystalline phases, thereby suggesting potential long-term pozzolanic activity in the concrete matrix. Concrete mixes containing 10% glass exhibited the best

microstructure throughout and were characterised by a dense interfacial transition zone, fewer microcracks, an enhanced aggregate-paste bonding and fewer and smaller voids. The observed improvement in microstructure is consistent with literature. Most literature reports that glass enhances the microstructure of concrete at contents less than 21%. The beneficial effects of glass on the microstructure were more pronounced in the w/c = 0.66 concrete mix than the w/c = 0.50 mix. Additionally, the presence of alkalis, specifically sodium oxide (Na_2O) and potassium oxide (K_2O), in waste glass – amounting to approximately 16% – is noteworthy as it may influence the overall properties of concrete.

Concrete mixes containing glass were also characterised by microcracks within the concrete matrix. These microcracks countered the benefits of an improved microstructure and interfacial transition zone density, thereby resulting in reduction in strength and macroporosity. It is important therefore that the overall effect of glass on the mechanical and durability performance of concrete consider, inter alia, the improved microstructure, ITZ density, degree of restraint, microcracking, the interactions among these microstructural parameters and their relative degrees of importance.

5.2 Recommendations

The recommendations for future research are hereby listed:

1. The long-term durability performance of concrete mixes containing glass, especially with regards to alkali silica reaction, chloride conductivity index, restrained shrinkage cracking and corrosion of reinforcement, is required. Such a study would inform the adoption of concrete containing glass in practice in South Africa.
2. An in-depth microstructural and mineralogical analysis of concrete mixes over a wider range of w/c ratios than that used in this study is required. Such a study would identify the trends and complex interactions that exist between these parameters, thereby elucidating the true effect of glass on concrete performance.
3. The performance of concrete mixes subjected to abrasion and impact forces is required. Such a study would evaluate the suitability of such concrete mixes for use in concrete floors subjected to the loads.
4. An in-depth cost-benefit analysis, life cycle costing and life-cycle analysis of concrete containing glass is required to critically evaluate the economic and environmental benefits and impact of glass for use in concrete production.
5. An in-depth study on the hydration of concrete mixes containing glass and the corresponding kinetics and mechanics of hydration is recommended. Such a study would

provide knowledge that would inform the nature of the product forms and other important information that would facilitate the optimal use of glass in concrete.

References

AASHTO. 2021. Standard method of test for surface resistivity indication of concrete's ability to resist chloride ion penetration. AASHTO T 358-21. https://www.scribd.com/document/692568888/AASHTO-T-358-2021

Abdallah, S. and Fan, M. 2014. Characteristics of concrete with waste glass as fine aggregate replacement. *International Journal of Engineering and Technical Research*, 2(6): 11-17.

Abrananth, M.S. 2020. A Study on Partial Replacement of Fine Aggregates by Using Crushed Glass And M-Sand in Concrete.
www.ijcrt.org

ACI Committee 211. 2007. Guide for selecting proportions for high-strength concrete. American Concrete Institute.

Adaway, M. and Wang, Y. 2015. Recycled glass as a partial replacement for fine aggregate in structural concrete – Effects on compressive strength. *Electronic Journal of Structural Engineering*, 14(1): 116-123.

Addis, B. and Owens, G. 2024. *Fulton's concrete technology*. 10th ed. Cement and Concrete Institute.

AfriSam. 2008. *Your guide to the use of all purpose cement*. http://www.afrisam.co.za/media/13680/all_purpose_cement.pdf. [15 October 2023].

Afshinnia, K. and Rangaraju, P.R. 2021. Influence of recycled glass on the alkali-silica reaction in concrete. *Construction and Building Materials*, 81: 257-267.

Aggregate Industries. 2014. *Concrete workability*.
http://www.concrete2you.com/about-us/concrete-workability/. [15 November 2023]

Ahmad, J., Martinez-Garcia, R., Algarni, S., de-Prado-Gil, J., Alqahtani, T. and Irshad, K. 2022. Characteristics of sustainable concrete with partial substitutions of glass waste as a binder material. *International Journal of Concrete Structures and Materials*, 16(1): 21.

Ahmad, J. and Zhou, Z., Usanova, K.I., Vatin, N.I. and El-Shorbagy, M.A. 2022. A step towards concrete with partial substitution of waste glass (WG) in concrete: A review. *Materials*, 15(7): 2525.

Ahmed, A., Kuri, J.C., Hosan, A., Shaikh, F.U.A. and Biswas, W.K. 2023. The effect of recycled waste glass as a coarse aggregate on the properties of Portland cement concrete and geopolymer concrete. *Buildings*, 13(3): 586.

Alexander, M. and Beushausen, H. 2009. Fulton's concrete technology. *Cement and Concrete Institute*.Alexander, M. and Mindess, S. 2005. *Aggregates in concrete*. 13th ed. London: Taylor and Francis, London.

Alexander, M., Bentur, A. and Mindess, S. 2017. *Durability of concrete: Design and construction*. 1st ed. CRC Press.

Alexander, M.G., Ballim, Y. and Stanish, K. 2009. A framework for use of durability indexes in performance-based design and specifications for reinforced concrete structures. *Materials and Structures*, 42(4): 321-333.

Ali, E.E. and Al-Tersawy, S.H. 2012. Recycled glass as a partial replacement for concrete sand in self-compacting concrete. *Construction and Building Materials*, 35: 785-791.

Aliabdo, A.A., Abd Elmoaty, M. and Aboshama, A.Y. 2016. Utilization of post-consumer glass pozzolan in the production of cement and concrete. *Construction and Building Materials*, 124: 866-877.

Almesfer, N. and Ingham, J. 2014. Effect of waste glass on the properties of concrete. *Journal of Materials in Civil Engineering,* 26(11)*:* 06014022.

Al-Zubaid, A.B., Shabeeb, A.N. and Ali, A.I. 2017. Study on the mechanical properties of concrete by using glass waste powder as a partial replacement of cement. *Energy Procedia*, 119: 680-692.

Ametepay, S.O. and Ansah, S.K. 2014. Impacts of construction activities on the environment: The case of Ghana. *Journal of Construction in Developing Countries*, 19(1): 29-46.

Andrić, L., Zheng, K., Khayat, K., Istry, S. and Jolin, M. 2017. Adhesion of recycled glass aggregate to cement paste: A route towards sustainable concrete. *Journal of Cleaner Production*, 164: 1218-1227.

ASTM International. 2019. ASTM D3906-19: Standard Guide for X-Ray Diffraction (XRD) Analysis of Cementitious Materials. [15 July 2024], https://www.astm.org/Standards/D3906.htm

ASTM International. 2025. ASTM D3906-25: Standard Test Method for Determination of Relative X-Ray Diffraction Intensities of Faujasite-Type Zeolite-Containing Materials.https://www.astm.org/Standards/D3906.htm

ASTM International. 2025. ASTM C1723-25: Standard Guide for Examination of Hardened Concrete Using Scanning Electron Microscopy (SEM).
https://www.astm.org/Standards/C1723.htm

Atoyebi, O.D. and Sadiq, O.M. 2018. Experimental data on flexural strength of reinforced concrete elements with waste glass particles as a partial replacement for fine aggregate. *Data in Brief*, (18): 846-859.

Bahadur, R. and Parashar, A.K. 2023. An investigation of waste glass powder with the substitution of sand on concrete mix. *Materials Today: Proceedings*. In press, corrected proof.

Bisht, K. and Ramana, P.V. 2018. Sustainable production of concrete containing discarded beverage glass as fine aggregate. *Construction and Building Materials*, 177: 116-124.

Byars, E.A., Morales, B. and Zhu, H.Y. 2004. Waste glass as concrete aggregate and pozzolan. *Concrete*, 38(1): 41-44.

Cayme, J.M.C. and Asor, A.N. 2017. Calcium content of lime mortars from 9th-century church ruins in the Philippines using volumetric analysis. *Malaysian Journal of Analytical Sciences*, 21(5): 1080-1090.

Cement and Concrete Institute. 2009. Cementitious materials for concrete standards, selection and properties. http://www.cnci.org.za. [20 May 2024].

Cement and Concrete Institute. 2011. Sustainable Concrete. Midrand: Cement and Concrete Institute.

Chen, G., Lee, H., Young, K.L., Yue, P.L., Wong, A., Tao, T. and Choi, K.K. 2002. Glass recycling in cement production – an innovative approach. *Waste Management*, 22(7): 747-753.

Chilmon, K., Jaworska, B. and Kalinowski, M. 2023. Significance of vebe time in pervious concrete. *Materials*, 16(8): 6239.

Concrete Society of Southern Africa. 2023. Durability Index (DI) testing – Procedure manual (Version 5.0, 2023-11-06).
https://concretesocietysa.org.za/concretetools/durability-index/. [15 May 2024].

Corinaldesi, V., Gnappi, G., Moriconi, G. and Montenero, A. 2005. Reuse of ground waste glass as aggregate for mortars. *Waste Management*, 25(2): 197-201.

De Castro, S. and de Brito, J. 2013. Evaluation of the durability of concrete made with crushed glass aggregates. *Journal of Cleaner Production*, 41: 7-14.

Department of Environmental Affairs. 2018. *South Africa State of Waste Report.* https://sawic.environment.gov.za/documents/8635.pdf

Du, H. and Tan, K.H. 2014. Use of waste glass as sand in mortar: Part I – Fresh, mechanical and durability properties. *Cement and Concrete Composites*, 35(1): 109-117.

Elavarasan, D. and Dhanalakshmi, D.G. 2016. Experimental study on waste glass as a partial replacing material in concrete for fine aggregate. *International Journal of Advanced Research in Biology, Engineering, Science and Technology*, 2: 116-120.

Fernandes, S.C., Barros, L.M., Barros, R.P., Liotto, P.F. and Alencar, D.B. 2019. The use of waste glass as partial replacement of fine aggregates in concrete. *International Journal for Innovation Education and Research*, 7(11): 193-203.

Figg, J.W. 1981. Reaction between cement and artificial glass in concrete. *5th International Conference on Concrete Alkali Aggregate Reactions (ICAAR)*: 252-257.

Gagg, C.R. 2014. Cement and concrete as an engineering material: An historic appraisal and case study analysis. *Engineering Failure Analysis*, 40: 114-140.

Gautam, S.P, Srivastava, V. and Agarwal, V.C. 2012. Use of glass wastes as fine aggregate in Concrete. *Journal of Academic Industrial Research*, 1(6): 320-322.

Gebremichael, N.N. 2022. Effects of particle size and replacement proportion of post-consumer glass in concrete. Doctoral dissertation, University of Nevada, Las Vegas.

Ghosh, P. and Ganesan, R. 2022. Effect of w/c ratio on fresh electrical resistivity of various pumice-based HPC and computation of setting time. *Materials and Structures*, 55(3): 103.

Gupta, J., Lata, N. and Nagar, B. 2018. Strength of concrete partially replacing fine aggregates by glass powder. *Journal of Civil Engineering and Environmental Technology*, 5(4): 252-255.

Hadi, R.A., Abd, S.M., Najm, H.M., Qaidi, S.., Eldirderi, M.M.A and Khedher, K.M. 2022. Influence of recycling waste glass as fine aggregate on the concrete properties. *Journal of Renewable Materials*, 11: 2925-2940,

Harbec, D., Zidol, A., Tagnit-Hamou, A. and Gitzhofer, F. 2017. Mechanical and durability properties of high-performance glass fume concrete and mortars. *Construction and Building Materials*, 134: 142-156.

Holcim South Africa Ltd. 2006. Materials handbook of Holcim South Africa. 2nd ed. Johannesburg: Kamran Haydendry Afrika.

Hunag, L.J., Wang, H.Y. and Wang, S.Y. 2015. A study of the durability of recycled green building materials in lightweight aggregate concrete. *Construction and Building Materials*, 96: 353-359.

Ibrahim, K.I.M. 2017. The effect of using waste glass [WG] as partial replacement of sand on concrete. IOSR *Journal of Mechanical and Civil Engineering*, 14(2): 41-45.

Idir, R., Cyr, M. and Tagnit-Hamou, W. 2011. Potential pozzolanicity of glass cullet fines and aggregates. *Annales du Bâtiment et des Travaux Publics*, 1: 28-34.

Ismail, Z.Z. and Al-Hashmi, E.A. 2009. Recycling of waste glass as a partial replacement for fine aggregate in concrete. *Waste Management*, 29(2): 655-659.

Johnson, C.D. 1974. Waste glass as coarse aggregate in concrete. *Journal of Testing and Evaluation*, 2(5): 344-350.

Kamali, M. and Ghahremaninezhad, A. 2016. An investigation into the hydration and microstructure of cement pastes modified with glass powders. *Construction and Building Materials*, 112: 915-924.

Kavyateja, B.V., Reddy, P.N. and Mohan, U.V. 2016. Study of strength characteristics of crushed glass used as fine aggregates in concrete. *International Journal of Research in Engineering and Technology*, 5(6): 157-160.

Kim, I.S., Choi, S.Y. and Yang, E.I. 2018. Evaluation of durability of concrete substituted heavyweight waste glass as fine aggregate. *Construction and Building Materials*, 184: 269-277.

Kou, S.C. and Poon, C.S. 2009. Properties of self-compacting concrete prepared with recycled glass aggregate. *Cement and Concrete Composites*, 31: 107-113.

Lalitha, G., Sasidhar, C. and Ramachandrudu, C. 2017. A review paper on strength and durability studies on concrete fine aggregate replaced with recycled crushed glass. I*nternational Journal of Civil Engineering and Technology*, 8(2): 199-202.

Lalitha, M., Anuradha, R. and Mounika, S. 2020. Strength and durability studies on concrete containing waste glass powder. *Materials Today: Proceedings*, 43: 1642-1647.

Limbachiya, M.C. 2009. Bulk engineering and durability properties of washed glass sand concrete. *Construction and Building Materials*, 23(2): 1078-1083.

Ling, T.-C. and Poon, C.-S. 2012. A comparative study on the feasible use of recycled beverage and CRT funnel glass as fine aggregate in cement mortar. *Journal of Cleaner Production*, 29-30: 46-52.

López-Uceda, A., Ayuso, J., López, M., Jimenez, J.R., Agrela, F. and Sierra, M.J. 2016. Properties of non-structural concrete made with mixed recycled aggregates and low cement content. Materials, 9(2).

Małek, M., Łasica, W., Jackowski, M. and Kadela, M. 2020. Effect of waste glass addition as a replacement for fine aggregate on properties of mortar. *Materials*, 13(14): 3189.

Malvar, J.L. and Lenk, R.L. 2006. Efficiency of fly ash mitigating alkali-silica reaction based on chemical composition. *ACI Materials Journal*, 103(5): 319-326.

Mardani-Aghabaglou, A., Tuyan, M. and Ramyar, K. 2014. Mechanical and durability performance of concrete incorporating fine recycled concrete and glass aggregates. *Materials and Structures*, 48: 2629-2640.

Mehta, P.K. and Monteiro, P.J.M. 2014. *Concrete: Microstructure, properties, and materials*. 4th ed. New York: McGraw-Hill Education.

Meyer, C. 2001. Recycled glass – from waste material to valuable resource. *International Symposium on Recycling and Reuse of Glass Cullet*, University of Dundee, Scotland: 19-20.

Nawy, E.G. 2008. *Concrete construction engineering handbook*. 2nd ed. CRC Press.

Neville, A.M. 2011. *Properties of concrete*. Edinburgh Gate: Pearson Education Limited.

Oliveira, L.A., Castro-Gomes, J.P. and Santos, P. 2008. Mechanical and durability properties of concrete with ground waste glass sand. *Proceedings of the 11DBMC International Conference on Durability of Building Materials and Components, Istanbul, Turkey*: 1-14.

Olofinnade, O.M., Ede, A.N., Ndambuki, J.M., Ngene, B.U., Akinwumi, I.I. and Ofuyatan, O. 2018. Strength and microstructure of eco-concrete produced using waste glass as partial and complete replacement for sand. *Cogent Engineering*, 5(1): 1483860.

Ontiveros-Ortega, E., Rodríguez-Gutiérrez, O. and Navarro, A.D. 2016. Mineralogical and physical–chemical characterisation of Roman mortars used for monumental substructures on the Hill of San Antonio, in the Roman city of Italica. *Journal of Archaeological Science*, 7: 205-223.

Park, S., Lee, B. and Kim, J. 2004. Studies on mechanical properties of concrete containing waste glass aggregate. *Cement and Concrete Researc*h, 34(12): 2181-2189.

Patwary, M.Z. 2012. Physical and chemical properties of glass. *Textile Fashion Study*. https://textilefashionstudy.com/glass-fiber-physical-and-chemical-properties-of-glass-fiber/. [5 February 2024].

Pellegrino, C., Faleschini, F. and Meyer, C. 2019. Recycled materials in concrete. In Mindess, S. (ed.). *Developments in the formulation and reinforcement of concrete*. Woodhead Publications: 19-54.

Phillips, J.C., Cahn, D.S. and Keller, G.W. 1972. Refuse glass aggregate in Portland cement concrete. In Schwartz, M.A. (ed.) *Proceeding of the Third Mineral Waste Utilization Symposium*. Chicago: IIT Research Institute: 385-390.

Pike, R.G., Hubbard, N.D. and Newman, E.S. 1960. Silicate glasses in the study of alkali-aggregate reaction. *High Research Board Bulletin,* 275: 39-44.

Polley, C., Cramer, S.M. and de la Cruz, R. 1998. Potential for using waste glass in Portland cement concrete. *Journal of Materials in Civil Engineering*, 10(4): 210-219.

Poon, C.S. and Wong, Y.L. 2007. Properties of concrete produced with recycled glass aggregate. *Cement and Concrete Research*, 37(2): 292-298.

Prezzi, M., Monteiro, P.J.M. and Spozito, G. 1997. The alkali-silica reaction. Part 1. Use of double-layer theory to explain behavior of reaction-product gels. *ACI Materials Journal*, 94(1): 10-17.

Qaidi, S., Najm, H.M., Abed, S.M., Özkılıç, Y.O., Dughaishi, H.A., Alosta, M., Sabri, M.M.S,. Alkhatib, F. and Milad, A. 2022. Concrete containing waste glass as environmentally friendly aggregate. *Materials*, 15(8): 6222.

Rajabipour, F., Maraghechi, H. and Fischer, G. 2010. Investigating the alkali-silica reaction of recycled glass aggregates in concrete materials. *Journal of Materials in Civil Engineering*, 22(12): 1201-1209.

Rakshvir, B. and Barai, S.V. 2006. Recycling of waste glass as a sustainable construction material. *Waste Management*, 26(10): 1176-1184.

Romero, D., James, J., Mora, R. and Hays, C.D. 2013. Study on the mechanical and environmental properties of concrete containing cathode ray tube glass aggregate. *Waste Management*, 33(7): 1659-1666.

SABS Standards Division. 2006. SANS 5862-1.2006. South African Bureau of Standards, Consistency of freshly mixed concrete-Slump test. http://eresources.library.cput.ac.za.ezproxy.cput.ac.za:2048/sabs/SANS5862-1.pdf

SABS Standards Division. 2006. SANS 5862-2.2006. South African Bureau of Standards, Concrete tests — Consistence of freshly mixed concrete — Flow test. http://eresources.library.cput.ac.za.ezproxy.cput.ac.za:2048/sabs/SANS5862-2.pdf

SABS Standards Division. 2006. SANS 5862-3.2006. South African Bureau of Standards, Vebe Consistometer test for concrete. http://eresources.library.cput.ac.za.ezproxy.cput.ac.za:2048/sabs/SANS5862-3.pdf

SABS Standards Division. 2006. SANS 5863.2006. South African Bureau of Standards, Compressive Strength of hardened concrete. http://eresources.library.cput.ac.za.ezproxy.cput.ac.za:2048/sabs/SANS5863.pdf

SABS Standards Division. 2006. SANS 6085.2006. South African Bureau of Standards, Drying shrinkage of mortars and concretes. Test method for the determination of drying shrinkage under specified conditions. [15 July 2024]. https://store.sabs.co.za/catalog/6085-2006.

SABS Standards Division. 2006. SANS 6250:2006. South African Bureau of Standards, Density of freshly mixed concrete. [15 July 2024]. https://store.sabs.co.za/catalog/6250-2006.

SABS Standards Division. 2006. SANS 6251:2006. South African Bureau of Standards, Density of hardened concrete. [15 July 2024] https://store.sabs.co.za/catalog/6251-2006.

SABS Standards Division. 2024. SANS 3001 – Part PR5:2024. South African Bureau of Standards, Fineness Modulus (FM) of fine aggregate. [15 July 2024] https://store.sabs.co.za/catalog/3001-PR5-2024.

SABS Standards Division. 2014. SANS 3001 – Part AG21:2014. South African Bureau of Standards, Determination of the bulk density, apparent density and water absorption of aggregate particles passing the 5 mm sieve for road construction materials. http://eresources.library.cput.ac.za.ezproxy.cput.ac.za:2048/sabs/SANS3001-AG21.pdf

SABS Standards Division. 2014. SANS 3001 – Part AG23:2014. South African Bureau of Standards, Particle and relative densities of aggregates. http://eresources.library.cput.ac.za.ezproxy.cput.ac.za:2048/sabs/SANS3001-AG23.pdf

SABS Standards Division. 2014. SANS 3001-AG1:2014. South African Bureau of Standards, Sieve analysis, fines content, and dust content of aggregates. http://eresources.library.cput.ac.za.ezproxy.cput.ac.za:2048/sabs/SANS3001-AG1.pdf

SABS Standards Division. 2015. SANS 3001-CO3:2015. South African Bureau of Standards, Concrete durability index testing – Preparation of test specimens. http://eresources.library.cput.ac.za.ezproxy.cput.ac.za:2048/sabs/SANS3001-CO3-1.pdf

SABS Standards Division. 2021. SANS 3001-Part CO3-2 2021. South African Bureau of Standards, Water Sorptivity Index (WSI). Pretoria: Standard South Africa.

SABS Standards Division. 2022. SANS 3001-Part CO3-2 2022. South African Bureau of Standards, Oxygen Permeability Index (OPI). http://eresources.library.cput.ac.za.ezproxy.cput.ac.za:2048/sabs/SANS3001-CO3-2_2022_Ed1Am1.pdf

Saha, A. 2023. Effects of waste glass on concrete properties. *Journal of Sustainable Construction*, 15(2): 123-135.

Sasanipour, H. and Aslani, F. 2020. Durability properties evaluation of self-compacting concrete prepared with waste fine and coarse recycled concrete aggregates. *Construction and Building Materials*, 236: 117540.

Schmidt, A. and Saia, W.H.F. 1963. Alkali-aggregate reaction tests on glass used for exposed aggregate wall panel work. *ACI Materials Journal*, 60: 235-1236.

Shao, Y., Lefort, T., Moras, S. and Rodriguez, D. 2000. Studies on concrete containing ground waste glass. *Cement and Concrete Research*, 30(1): 91-100.

Shayan, A. and Xu, A. 2004. Value-added utilisation of waste glass in concrete. *Cement and Concrete Research*, 34(1): 81-89.

Shayan, A. and Xu, A. 2006. Performance of glass powder as a pozzolanic material in concrete: A field trial on concrete slabs. Cement and Concrete Research, 36: 457-468.

Shi, G and Zheng, K. 2007. A review on the use of waste glass in the production of cement and concrete. *Resources, Conservation and Recycling*, 52(2): 234-237.

Simnani, S.I. 2017. Effect of water-cement ratio on compressive strength of concrete. *Journal of Emerging Technologies and Innovative Research*, 4(10): 486-490.

Singh, S., Srivastava, V. and Agarwal, V.C. 2015. Glass waste in concrete: Effect on workability and compressive strength. *International Journal of Innovative Research in Science, Engineering and Technology*, 4(9): 8142-8150.

Singh, S.P., Gupta, A. and Kumar, V. 2017. Impact of waste glass on the properties of concrete: A review. *Journal of Materials in Civil Engineering*, 29(6): 04017006.

Sobolev, K., Türker, P., Soboleva, S. and Iscioglu, G. 2007. Utilization of waste glass in ECO-cement: Strength properties and microstructural observations. *Waste Management*, 27(7): 971-976.

Soliman, N.A. and Tagnit-Hamou, A. 2017. Using glass sand as an alternative for quartz in UHPC. *Construction and Building Materials*, 145: 243-252.

Steyn, Z.C., Babafemi, A.J., Fataar, H. and Combrinck, R. 2021. Concrete containing waste recycled glass, plastic and rubber as sand replacement. *Construction and Building Materials*, 269: 121242.

Taha, B. and Nounu, G. 2008. Properties of concrete containing mixed colour waste recycled glass as sand and cement replacement. *Construction and Building Materials*, 22(5): 713-720.

Tamanna, N., Sutan, N.M., Lee, D.T.C. and Yakub, I. 2013. Utilization of waste glass in concrete. *Proceedings of the 6th International Engineering Conference, Energy and Environment (ENCON 2013)*, Kuching, Sarawak, Malaysia: 2-4.

Tamanna, N., Tuladhar, R. and Sivakugan, N. 2020. Performance of recycled post-consumer glass sand as partial replacement of sand in concrete. *Construction and Building Materials*, 239: 117804.

Tan, K.H. and Du, H. 2013. Use of waste glass as sand in mortar: Part I – Fresh, mechanical and durability properties. *Cement and Concrete Composites*, 35(1): 109-117.

Tong, G., Pang, J., Shen, J., Tang, B., Jiang, Z., Li, B., Huang, J., Zou, J. and Wang, H. 2024. Response tests on the effects of particle size of waste glass sand on the mechanical and durability performance of concrete. *Scientific Reports,* 14(1): 25445.

Topcu, B. and Canbaz, M. 2004. Properties of concrete containing waste glass. *Cement and Concrete Research*, 34(2): 267-274.

Turgut, P. and Yahlizade, E.S. 2009. Research into concrete blocks with waste glass. *International Journal of Civil and Environmental Engineering*, 3(3): 186-192.

University of Cape Town and University of the Witwatersrand. 2017. *Durability Index Testing Procedure Manual, Part 3, Version 4.5.1*. Concrete Materials and Structural Integrity Research Unit (CoMSIRU), Department of Civil Engineering, University of Cape Town, Cape Town, South Africa.
https://www.scribd.com/document/455609588/Durability-Index-Testing-Procedure-Manual

University of Cape Town and University of the Witwatersrand. 2023. *Durability Index Testing Procedure Manual, Part 3, Version 4.5.1*. Concrete Materials and Structural Integrity Research Unit (CoMSIRU), Department of Civil Engineering, University of Cape Town, Cape Town, South Africa.
https://ebe.uct.ac.za/sites/default/files/media/documents/ebe_uct_ac_za/848/UCT-WITS%20DI%20Manual_2023%20Ver%205.0%202023-11-06.pdf

Upreti, B. and Mandal, S. 2021. Performance evaluation of concrete incorporating recycled glass: A review. *Materials Today: Proceedings*, 45: 1234-1240.

Waghmare, S., 2020. Microstructural Analysis of M30 Grade Concrete Using Scanning Electron Microscopy (SEM) Method. *International Journal of Engineering Research and Applications*, 10(5): 65-71.
https://www.ijera.com/papers/vol10no5/Series-1/K1005016571.pdf [2 April 2025].

Wong, H.S., Poole, A.B., Wells, B., Eden, M., Barnes, R., Ferrari, J., Fox, R., Yio, M.H.N., Copuroglu, O., Guðmundsson, G. and Hardie, R. 2020. Microscopy techniques for determining water-cement (w/c) ratio in hardened concrete: A round-robin assessment. Materials and Structures, 53: 25

Xie, Z. and Xi, Y. 2002. Use of recycled glass as a raw material in the manufacture of Portland cement. *Materials and Structures*, 35(8): 510-515.

Zhao, Y., Gao, J., Wu, S. and Li, Q. 2022. Strength development and microcosmic mechanism of waste glass powder cement mortar. *Journal of Experimental Nanoscience*, 17(1): 564-584.

Appendix A: Physical properties of materials

A. 1: Specific gravity (Philippi dune sand)

Particle specific gravity (G_s):	(Dune sand)		08/03/24
Sample	A (g)	B (g)	C (g)
Mass of jar	47	101.2	190.7
Mass of jar & water	146	360	723.5
Mass of jar & specimen	86.9	163.7	315.7
Mass of jar, specimen & water	171	398	799
Mass of soil (g)	39.9	62.5	125.00
Specific Gravity ($G_{s)}$	2.68	2.55	2.53
Average Specific Gravity ($G_{s),}$ (kg/m^3)		2.58	

A.2: Specific gravity (waste glass)

Particle specific gravity (G_s):	(Waste glass)		08/03/24
Sample	A (g)	B (g)	C (g)
Mass of jar	46.8	101.2	190.6
Mass of jar & water	146.6	361.1	725.2
Mass of jar & specimen	106.8	181.2	310.6
Mass of jar, specimen& water	181.4	410.4	799
Mass of soil (g)	60	80	120.00
Specific Gravity ($G_{s)}$	2.38	2.61	2.60
Average Specific Gravity ($G_{s),}$ (kg/m^3)		2.53	

A.3: Coarse aggregate specific gravity and water absorption (Trial 1)

Specimen	Mass of Saturated Surface-Dry Specimen, M1 (g)	Mass of Saturated Surface-Dry Specimen in Water at 25°C, M2 (g)	Mass of Oven-Dried Specimen, M3 (g)	Specific Gravity (SG)	Water Absorption (WABS %)
A	1400	886	1391	2.72	0.68
B	998	628	992	2.7	0.6
C	1500	966	1491	2.81	0.64
Average values				2.74	0.64

A.4: Coarse aggregate specific gravity and water absorption (Trial 2)

Specimen	Mass of Saturated Surface-Dry Specimen, M1 (g)	Mass of Saturated Surface-Dry Specimen in Water at 25°C, M2 (g)	Mass of Oven-Dried Specimen, M3 (g)	Specific Gravity (SG)	Water Absorption (WABS %)
A	1425	890	1405	2.74	0.7
B	1000	630	994	2.72	0.61
C	1520	970	1505	2.8	0.65
Average values				2.75	0.65

A.5: Uncompacted bulk density (dune sand)

Uncompacted bulk density (kg/m^3): Dune sand			
Sample	A (g)	B (g)	C (g)
Mass of mould	2950	2950	2950
Mass of glass plate	150	150	150
Mass of mould + glass plate +water	5750	5750	5750
Mass of water (l)	2650	2650	2650
Mass of mould + sand (g)	6700	6750	6800
Mass of sand (g)	3750	3800	3850
Uncompacted bulk density (kg/m^3)	1.42	1.43	1.45
Average uncompacted bulk density, (kg/m^3)			1.43
Percentage voids in aggregate (%)		46.82	

A.6: Compacted bulk density (dune sand)

Compacted bulk density (kg/m^3): Dune sand			
Sample	A (g)	B (g)	C (g)
Mass of mould	2950	2950	2950
Mass of glass plate	150	150	150
Mass of mould + glass plate + water	5750	5750	5750
Mass of water (l)	2650	2650	2650
Mass of mould + sand (g)	7250	7250	7250
Mass of sand (g)	4300	4300	4300
Uncompacted bulk density (kg/m^3)	1.62	1.62	1.62
Average compacted bulk density (kg/m^3)			1.62

A.7: Uncompacted bulk density (coarse aggregate)

Uncompacted bulk density (kg/m^3): Coarse aggregate			
Sample	A (g)	B (g)	C (g)
Mass of mould	10650	10650	10650
Mass of glass plate	0	0	0
Mass of mould + glass plate + water	24300	24300	24300
Mass of water (l)	13650	13650	13650
Mass of mould + Coarse aggregate (g)	29600	29550	29650
Mass of Coarse aggregate (g)	18850	18900	19000
Uncompacted bulk density (kg/m^3)	1.38	1.38	1.39
Average uncompacted bulk density (kg/m^3)			1.38
Percentage voids in aggregate (%)		49.64	

A.8: Compacted bulk density (coarse aggregate)

Compacted bulk density (kg/m^3): Coarse aggregate			
Sample	A (g)	B (g)	C (g)
Mass of mould	10650	10650	10650
Mass of glass plate	0	0	0
Mass of mould + glass plate + water	24300	24300	24300
Mass of water (l)	13650	13650	13650
Mass of mould + Coarse aggregate (g)	30150	30000	30050
Mass of Coarse aggregate (g)	19500	19350	19400
Compacted bulk density (kg/m^3)	1.43	1.42	1.42
Average compacted bulk density (kg/m^3)			1.42

Appendix B: Test procedures

B.1: Water absorption

Water absorption tests were performed as per SANS 3001- Part AG21(2014) by soaking aggregate samples in water for a specified duration (typically 24 hours). The detailed procedure was as follows:

i. Representative aggregate samples of approximately 2 kg were obtained using proper sampling techniques.
ii. The samples were thoroughly washed to remove fines and dust particles.
iii. The washed samples were placed in the oven at 110 ± 5°C until a constant mass was achieved (typically 24 hours).
iv. After cooling to room temperature in a desiccator, the dry mass (M3) was recorded to the nearest 0.1 g.
v. The samples were then completely submerged in clean water at 25 ± 1°C for 24 hours.
vi. After the soaking period, the samples were removed from water and excess surface water was removed by blotting with a damp cloth until the sheen disappeared.
vii. The saturated surface-dry mass (M1) was immediately recorded to the nearest 0.1 g.
viii. The water absorption percentage was calculated using the formula:

$$W_{ABS} = 100 \times \left(\frac{M_1 - M_3}{M_3}\right)$$

Where

W_{ABS} = water absorption percentage

M_1 = mass of the saturated surface-dry sample

M_3 = mass of the oven-dried sample

B.2 Effective size of distribution

The parameters used for the classification of soils were computed from the logarithmic plot in Figure 4.1. These parameters include the uniformity coefficient (C_u) and coefficient of curvature (C_c) which are computed from the extrapolation of the 10%, 30% and 60% materials passing the corresponding sieve sizes. The results for these parameters are presented in Table 4.3 for each mortar sample.

1. **Coefficient of uniformity**

The coefficient of uniformity (C_u) is a parameter used to assess the consistency of particle size distribution, as defined by Equation 4.1 (Ontiveros-Ortega et al., 2016; Cayme and Asor, 2017).

$$C_u = \frac{D_{60}}{D_{10}} \quad (4.1)$$

2. **Coefficient of curvature**

The coefficient of curvature (C_c) assesses the variation in the sizes of soil particles, thereby indicating the gradation across different particle size ranges, as expressed in Equation 4.2. A coefficient of uniformity (C_u) equal to 1 signifies that all grain sizes are the same, indicating poorly graded material. Conversely, a C_u value greater than 1 indicates a wide range of grain sizes, characterising uniform material. For soil to be classified as well-graded, it must satisfy the criteria: $C_u > 1 < C_c < 3$ (Ontiveros-Ortega et al., 2016; Cayme and Asor, 2017).

$$C_c = \frac{D_{30^2}}{D_{10} \times D_{60}} \quad (4.2)$$

Where

D_{10} = the sieve size when 10% of the particles are still being retained

D_{30} = the sieve size when 30% of the particles are still being retained

D_{60} = the sieve size when 60% of the particles are still being retained

B.3: Particle size distribution (PSD)

The grading of fine aggregates was conducted in accordance with SANS 3001-AG1 (2014) to determine the particle size distribution. The following detailed procedure was followed:

i. Representative samples were obtained through proper quartering and reduction methods.
ii. A sample of approximately 500 g of sand was oven-dried at 110 ± 5°C until constant mass.
iii. The sample was allowed to cool to room temperature and weighed to the nearest 0.1 g.
iv. A set of standard 300 mm diameter sieves was assembled in descending order: 37.5 mm, 28.0 mm, 20.0 mm, 14.0 mm, 10.0 mm, 5.0 mm, 2.0 mm, 1.0 mm, 600 µm, 300 µm, 150 µm, and 75 µm, with a pan at the bottom.
v. The dried sample was placed on the top sieve, and the stack was secured in the mechanical shaker.

vi. The mechanical shaker was operated for a duration of 10 minutes to ensure complete separation of particles.
vii. After shaking, the mass of material retained on each sieve was carefully transferred and weighed to the nearest 0.1 g.
viii. The total mass of all fractions was compared with the initial mass to ensure that material loss did not exceed 1%.
ix. The percentage of material retained on each sieve was calculated.
x. The cumulative percentage passing each sieve was determined and used to plot the particle size distribution curve.
xi. The results were used to classify the aggregate according to standard grading requirements.

B.4: Compacted bulk density

The compacted bulk density (CBD) of coarse aggregate was determined following SANS 5845:2006. The detailed procedure was as follows:

i. A cylindrical metal measure with a known volume (typically 10 litres for aggregate sizes up to 37.5 mm) was selected.
ii. The measure was cleaned, dried, and weighed to the nearest 10 g (mass M1).
iii. The measure was placed on a level, firm surface.
iv. The aggregate sample was oven-dried at 110 ± 5°C until constant mass was achieved.
v. The sample was allowed to cool to room temperature.
vi. The measure was filled approximately one-third full of aggregate.
vii. The layer was tamped with a tamping rod (16 mm diameter, 600 mm length) by giving 25 strokes evenly distributed over the surface.
viii. A second layer of approximately equal volume was added and tamped as before.
ix. The measure was filled to overflowing with a third layer and tamped again with 25 strokes.
x. After tamping, the surface was levelled using a straight edge, taking care to balance the voids at the surface with the aggregate projections.
xi. The filled measure was weighed to the nearest 10 g (mass M2).
xii. The test was repeated three times with fresh samples, and the average value was calculated.
xiii. The compacted bulk density was calculated using the formula:

$$\delta = \frac{m}{v}$$

Where

δ = bulk density, in (kg/m^3)

m = mass of the aggregate in the container, in kilograms (kg)

v = volume of the container, in grams (m^3)

B.5: Particle and relative densities

The particle and relative densities of aggregates were assessed according to SANS 3001 – Part AG23 (2014). The detailed procedure was as follows:

i. A representative sample of approximately 1 kg was obtained and washed to remove dust and impurities.
ii. The washed sample was placed in a container and covered with water for 24 hours to ensure saturation.
iii. After soaking, excess water was drained, and the sample was spread on a flat, non-absorbent surface.
iv. The sample was exposed to warm, circulating air to remove surface moisture, being stirred occasionally to ensure uniform drying.
v. The surface-dry condition was tested by filling a cone mould placed on a flat surface, tamping lightly 25 times, and lifting the mould vertically.
vi. When the sample slumped slightly but maintained some shape, it was considered to be in the saturated surface-dry (SSD) condition.
vii. A 500 g portion of the SSD sample was weighed to the nearest 0.1 g (mass M1).
viii. A pycnometer was filled with water at 25 ± 1°C to the calibration mark and weighed (mass M4).
ix. The water was poured out, and the SSD sample was carefully introduced into the pycnometer.
x. The pycnometer was filled with water to about three-quarters full, and entrapped air was removed by gentle agitation.
xi. The pycnometer was topped up with water to the calibration mark and weighed (mass M2).

xii. The sample was removed from the pycnometer, oven-dried at 110 ± 5°C until constant mass, cooled to room temperature in a desiccator, and weighed (mass M3).

xiii. The bulk density was calculated using the formula:

$$\mathrm{BD} = 997 \times \left(\frac{\mathrm{M_3}}{\mathrm{M_1} - \mathrm{M_2}}\right)$$

Where

BD = bulk density of the aggregate particles, expressed in kilograms per cubic meter (kg/m³).

M_1 = mass of the saturated surface-dry test sample, specified in grams (g).

M_2 = mass of the saturated test sample in water at 25 °C, denoted in grams (g).

M_3 = mass of the oven-dried test sample, expressed in grams (g).

B.6: Fineness modulus

The fineness modulus (FM) of fine aggregates was determined following SANS 3001 – Part PR5:2024. The detailed procedure was as follows:

i. A representative sample of approximately 500 g of fine aggregate was obtained through proper sampling methods.
ii. The sample was oven-dried at 110 ± 5°C until constant mass was achieved.
iii. After cooling to room temperature, the sample was weighed to the nearest 0.1 g.
iv. A set of standard 300 mm diameter sieves was assembled in descending order: 5.0 mm, 2.0 mm, 1.0 mm, 600 µm, 300 µm, 150 µm, and 75 µm, with a pan at the bottom.
v. The sample was placed on the top sieve, and the stack was secured in the mechanical shaker.
vi. The shaker was operated for 10 minutes to ensure complete separation of particles.
vii. The mass of material retained on each sieve was carefully transferred and weighed to the nearest 0.1 g.
viii. The percentage retained on each sieve was calculated.
ix. The cumulative percentage retained was determined for each sieve.
x. The fineness modulus was computed using the formula:

$$\mathrm{FM} = \frac{\mathrm{P_{CR(5mm)}} + \mathrm{P_{CR(2.0mm)}} + \mathrm{P_{CR(1.0mm)}} + \mathrm{P_{CR(0.60mm)}} + \mathrm{P_{CR(0.30mm)}} + \mathrm{P_{CR(0.15mm)}}}{100}$$

Where

P_{CR} = cumulative percentage retained

P_P = percentage passing

B.7: Consistence

The consistency of freshly mixed concrete was evaluated using three tests: the slump test, flow test, and vebe time test. Each of these methods is outlined in detail below.

B.7.1: Slump test

The slump test for freshly mixed concrete was conducted in accordance with SANS 5862-1:2006 to assess workability. The following procedure was followed:

i. A clean slump cone (height: 300 mm, base diameter: 200 mm, top diameter: 100 mm) was placed on a flat, rigid, non-absorbent surface.
ii. The interior of the cone was moistened with water to prevent adhesion.
iii. The cone was filled with freshly mixed concrete in three equal layers. Each layer was tamped 25 times with a standard tamping rod (16 mm diameter, 600 mm length, with a rounded end).
iv. The tamping was distributed uniformly over the cross-section of each layer, with the rod penetrating slightly into the underlying layer.
v. After the top layer was tamped, the surface was struck off level with the top of the cone using the tamping rod.
vi. Excess concrete was cleaned from around the base of the cone.
vii. The cone was carefully lifted vertically upward in a single steady motion, taking 5-10 seconds for the full removal.
viii. The cone was placed beside the slumped concrete for reference.
ix. The vertical distance from the top of the cone to the highest point of the slumped concrete was measured to the nearest 5 mm, providing the slump value.

x. The entire test was completed within 150 seconds from the start of filling the cone.

xi. If a shear slump or collapse slump occurred, the test was repeated with a fresh sample.

B.7.2: Flow test

The flowability of concrete was evaluated using a flow table test according to SANS 5862-2:2006. The procedure was as follows:

i. The flow table and flow mould were cleaned and moistened before testing.

ii. The flow table was placed on a level, firm surface free from external vibration.

iii. The flow mould (bottom diameter: 200 mm, top diameter: 130 mm, height: 200 mm) was centred on the table.

iv. The mould was filled in two equal layers, each layer being compacted with 10 tamps using a standard tamping rod.

v. Excess concrete was struck off level with the top of the mould using a straight edge.

vi. After a waiting period of 30 seconds, the mould was carefully lifted vertically in a single smooth motion.

vii. The flow table handle was immediately turned at a rate of one revolution per second for 15 complete revolutions.

viii. The concrete spread diameter was measured along two perpendicular axes with callipers to the nearest 1 mm.

ix. The average of these two measurements was calculated and recorded as the flow value in millimetres.

x. The entire procedure was completed within 2 minutes of obtaining the sample.

B.7.3: Vebe time test

The consistency of fresh concrete was measured using a Vebe consistometer according to SANS 5862-3:2006. The detailed procedure was:

i. The Vebe apparatus was assembled with the cylinder, disc, and funnel correctly positioned.
ii. The interior surfaces of the test container were dampened before use.
iii. The slump cone was placed inside the cylindrical container and filled in three equal layers.
iv. Each layer was compacted with 25 tamps of the standard tamping rod, ensuring even distribution.
v. Excess concrete was struck off level with the top of the cone.
vi. The cone was carefully lifted vertically, taking 5-10 seconds for complete removal.
vii. The transparent disc was lowered carefully until it made contact with the highest point of the concrete.
viii. The initial reading on the scale was recorded to the nearest 0.5 mm.
ix. The vibration table was switched on and a stopwatch started simultaneously.
x. The time was measured until the transparent disc's underside was completely in contact with the concrete (indicated by a complete coating of cement paste).
xi. This time, measured to the nearest second, was recorded as the vebe time.
xii. If the vebe time exceeded 30 seconds, the test was noted as having very low workability.
xiii. The entire test was completed within 5 minutes of obtaining the sample.

Table B. 1: Vebe time vs workability

Vebe time (seconds)	Workability
0 – 5	Very high
5 – 10	High
10 – 20	Medium
20 – 30	Low
>30	Very low

B.8: Density of fresh concrete

The density of freshly mixed concrete was determined following SANS 6250:2006 by measuring the mass of a known volume. The detailed procedure was as follows:

i. A cubical steel metal container with a volume of approximately 3.375 litres was selected.
ii. The empty container was cleaned, dried, and weighed to the nearest 10 g (mass M1).
iii. The volume of the container (V) was determined to the nearest 0.00001 m³.
iv. The container was placed on a level, firm surface.
v. The container was filled with freshly mixed concrete in three equal layers.
vi. Each layer was compacted by either rodding (25 strokes per layer with a standard tamping rod) or vibration (using an internal or external vibrator until no further settlement was observed).
vii. After compaction of the final layer, excess concrete was struck off level with the top of the container using a straight edge with a sawing motion.
viii. The sides of the container were cleaned to remove any adhering concrete.
ix. The filled container was weighed to the nearest 10 g (mass M2).
x. The test was performed within 20 minutes of mixing the concrete.
xi. The density was calculated using the formula:

$$\rho = \frac{m}{\nu}$$

Where

ρ = density of concrete in kg/m^3

m = mass of 150 mm × 150 mm ×150 mm cube in kg

ν = volume of cube in m^3

B.9: Density of hardened concrete

The density of hardened concrete specimens (cubes or cylinders) was tested according to SANS 6251:2006. The detailed procedure was as follows:

i. Concrete specimens (typically 150 mm × 150 mm × 150 mm cubes) were cast and cured under standard conditions.
ii. After the specified curing period, specimens were removed from the curing tank and surface water was wiped off.

iii. The dimensions of each specimen were measured to the nearest 0.5 mm at three locations for each dimension.
iv. The average length, width, and height were calculated and used to determine the volume of the specimen to the nearest 0.00001 m³.
v. Each specimen was weighed on a calibrated balance to the nearest 10 g.
vi. For water-cured specimens, measurements were taken within 30 minutes of removal from water.
vii. Three specimens were tested for each concrete mix, and the average value was reported.
viii. The density was calculated using the formula:

$$\rho = \frac{m}{\nu}$$

Where
ρ = density of concrete in kg/m^3
m = mass of 150 mm × 150 mm ×150 mm cube in kg
ν = volume of cube in m^3

B.10: Compressive strength

The compressive strength of concrete specimens (cubes or cylinders) was tested at specified curing intervals (3, 7, 14 and 28 days) following SANS 5863:2006. The detailed procedure was as follows:

i. Concrete specimens (typically 150 mm × 150 mm × 150 mm cubes) were cast in cubical steel moulds and properly compacted.
ii. The specimens were demoulded after 24 ± 2 hours and placed in a water curing tank maintained at 23 ± 2°C.
iii. At the specified testing age, specimens were removed from the curing tank and excess surface water was wiped off.
iv. The dimensions of each specimen were measured to verify compliance with tolerance requirements.
v. Each specimen was positioned in the compression testing machine such that the load was applied perpendicularly to the casting direction.

vi. The loading faces of the specimen were cleaned and aligned centrally with the platens of the testing machine.
vii. A uniform loading rate of 0.3 ± 0.1 MPa/s was applied continuously without shock until failure occurred.
viii. The maximum load at failure was recorded to the nearest 1 kN.
ix. The type of failure was noted and any unusual features recorded.
x. Three specimens were tested for each age and mix design, and the average value was reported.
xi. The compressive strength was calculated using the formula:

$$f_{cu} = \frac{\mathrm{F}}{\mathrm{A}}$$

Where

f_{cu} = compressive strength MPa

F = load at failure (N)

A = cross-sectional area of test cube (mm^2)

B.11: Accelerated drying shrinkage

Drying shrinkage tests were performed on concrete specimens following SANS 6085:2006. The detailed procedure was as follows:

i. Freshly cast prism specimens (100 × 100 × 500 mm) were covered with an impervious plastic sheet and stored for 20 to 24 hours in a vibration-free environment with a temperature range of 22°C to 25°C and a relative humidity of at least 90%.
ii. Specimens were removed from the mould after 24 hours.
iii. Strain targets were attached to two opposite faces of each specimen along the longitudinal direction.
iv. Specimens were cured in potable water at a temperature between 22°C and 25°C for six days after demoulding.
v. Specimens were removed from the water bath after approximately seven days. Excess water was wiped off, and the distance between strain targets was measured to the nearest 2 µm. Each specimen was marked to ensure consistent orientation.

vi. Specimens were placed in an environmental room with controlled conditions: temperature at 23 ± 2°C and relative humidity at 50 ± 4%, matching those used for ring tests.
vii. The distance between strain targets was measured every two days using a strain gun. The measurements for accelerated shrinkage were monitored at 2-day and 3-day intervals over a duration of 61 days.
viii. Three specimens were tested for each mix design, and the average value was reported.
ix. Accelerated drying shrinkage was calculated using the formula:

$$\varepsilon = \frac{(L_0 - L)}{G}$$

Where

ε = drying shrinkage strain (microstrain)

L_0 = initial length of the specimen after curing (mm)

L = length of the specimen at the measured age (mm)

G = gauge length (distance between studs or measurement points) (mm)

B.12: Surface resistivity

Electrical resistivity testing on concrete samples was conducted according to AASHTO T 358. The detailed procedure was as follows:

i. Cylindrical concrete specimens of dimensions 100 mm diameter × 200 mm height were cast and cured under standard conditions.
ii. At the testing age, specimens were removed from the curing tank and surface-dried with a damp cloth.
iii. The specimens were placed on a non-conductive surface in a controlled environment of 23 ± 2°C.
iv. A four-point Wenner probe array with electrode spacing of 38 mm was used for measurements.

v. Eight measurements were taken around the perimeter of each specimen at equal intervals, with the probe aligned parallel to the longitudinal axis.
vi. The probe was firmly pressed against the concrete surface to ensure good electrical contact.
vii. A small amount of conductive gel was applied to the probe tips if needed to improve contact.
viii. The resistivity meter was set to apply a current of approximately 250 μA at a frequency of 13 Hz.
ix. The voltage drop and applied current were measured, and the resistivity value was recorded for each measurement position.
x. Three specimens were tested for each mix design, and the average of 24 measurements (8 per specimen) was reported.
xi. Surface resistivity was calculated using the formula:

$$\rho = 2\pi a \frac{V}{I}$$

Where

ρ = surface resistivity

a = spacing between the probes

V = measured voltage

I = applied current

B.13: Durability indexes

Two durability indexes were assessed: the oxygen permeability index and the water sorptivity index. Specific details regarding each of these tests are outlined in the subsections below. Four specimens were tested for each durability index measurement.

B.13.1: Specimen preparation

The preparation of specimens for durability index (DI) testing was conducted in accordance with the Durability Index Testing Procedure Manual (Version 5.0, November 2023). A summary of the sample preparation steps is provided below:

i. Circular discs were cored from 100 × 100 × 100 mm mortar cube specimens using a water-cooled diamond-tipped core barrel attached to a coring drill. The internal diameter of the coring barrel was 70 ± 2 mm, and coring was performed perpendicular to the casting direction.
ii. The cored cubes were subsequently cut into discs with a thickness of 30 ± 2 mm.
iii. Each disc was marked with the appropriate reference number on its original interior face for identification. Specimens that sustained damage during coring or cutting were not used for testing.
iv. The prepared discs were placed in an oven set at 50 ± 2°C for a period of 7 days ± 4 hours.
v. Following the oven-drying process, the specimens were cooled in a desiccator maintained at 23 ± 2°C for a duration ranging from 2 to 4 hours.
vi. Once cooled, the specimens were removed from the desiccator and tested for durability indexes.

B.13.2: Oxygen permeability index

The oxygen permeability index (OPI) tests for the mortar mixes were performed as follows:

i. The test specimens were prepared in line with the guidelines specified in the Durability Index Testing Procedure Manual (Version 5.0, November 2023) and as detailed in Appendix B.10.1.
ii. Specimens were retrieved from the oven and placed in a desiccator for a period ranging between 2 and 4 hours.
iii. Following desiccation, the diameter and thickness of each specimen were measured at four equidistant points along the perimeter using a vernier calliper, with readings recorded to the nearest 0.02 mm. The average of these four measurements was calculated and documented.

iv. Each specimen was positioned within the compressible collar inside the rigid sleeve of the permeameter, ensuring that the test face (outer face) was at the bottom. Care was taken to eliminate any visible gaps between the specimen and the collar.
v. The assembled specimen, collar, and rigid sleeve were placed on the test chamber, covering the designated hole. A solid ring was positioned on top of the collar, ensuring no visible gaps. The cover plate was then secured atop the solid ring.
vi. The top screw was slightly tightened to ensure the cover plate was centred.
vii. The oxygen inlet and outlet valves of the permeability cells were opened, followed by opening the valve of the oxygen supply tank to achieve a pressure of 100–120 kPa. Oxygen was allowed to flow through the permeameter for 5 seconds.
viii. Subsequently, the oxygen outlet valve of the permeability cells was closed. The inlet valve was shut once the permeability cell's pressure gauge indicated a value exceeding 100 kPa.
ix. The gauge was tapped to confirm an accurate reading. The pressure was then adjusted to 100 ± 5 kPa by slightly opening the outlet valve.
x. Readings were recorded automatically using a data logger. The test concluded once the pressure dropped to 50 ± 2.5 kPa or after 6 hours ± 15 minutes, whichever occurred first.
xi. The collected data was subsequently downloaded from the data logger and analysed.

The slope of the linear regression line forced through the (0.0) point may be calculated from the following equation:

$$z = \frac{\sum[ln\,(\frac{P_0}{P_t})]^2}{\sum[ln\,(\frac{P_0}{P_t})t]}$$

Where

z = slope of the regression line

P_0 = pressure at time t_0 [kPa]

P_t = pressure reading taken at time t after t_0 [kPa]

t = time in seconds

The Darcy coefficient of permeability (k) can be determined by:

$$k = \frac{\omega V g d z}{R A \theta}$$

Where

$\boldsymbol{\omega}$ = Molar mass of Oxygen = 32 g/mol

V = Volume of Oxygen under pressure in the permeameter [m^3]

g = gravitational acceleration = 9.81 m/s^2

d = average specimen thickness [mm]

z = slope of the regression line

R = universal gas constant 8.313 Nm/K mol

A = cross-sectional area of the specimen in [m^2]

$\boldsymbol{\theta}$ = absolute temperature [K]

The oxygen permeability index of the specimens, can be determined by applying the following equation:

OPI = – log10 [¼ (k1 + k2 + k3 + k4)]

Where

k1, 2, 3, 4 = Darcy coefficients of sample disks 1, 2, 3 and 4.

The average of the four concrete disks tested for the OPI for the mixes at critical volume and mixed waste combinations were reported by Contest - Concrete Technology Services and used for this study.

B.13.3: Water sorptivity index

The water sorptivity index test was conducted in accordance with the Durability Index Testing Procedure Manual (Version 5.0, 2023). Four specimens were tested for each mix. The testing procedure is detailed below:

i. The vertical curved surfaces of the specimens retrieved from the desiccator were sealed with packaging tape, ensuring that the test face remained unobstructed.
ii. The diameter and thickness of each specimen were measured at four equidistant points along the perimeter using a Vernier calliper, with readings recorded to the nearest 0.02 mm. The average of these four readings was documented.
iii. A plastic tray was lined with ten layers of paper towel.
iv. A solution of water saturated with calcium hydroxide was poured into the tray, ensuring full saturation of the paper towel while maintaining visible water on the surface. Any air bubbles were removed by smoothing the paper pad towards the tray edges. The final solution level was slightly above the specimen's bottom edge, reaching a maximum of 2 mm up its sides. An additional dampened paper towel was kept nearby to absorb excess water from the specimen during testing.
v. Within 30 minutes of removal from the desiccator, specimens were placed with their test face on the wet paper pad, and a stopwatch was started. The initial time (t_0) was recorded.
vi. Each specimen was weighed at intervals of 3, 5, 7, 9, 12, 16, 20, and 25 minutes after briefly patting it with an absorbent paper towel to achieve a saturated surface dry (SSD) condition. Care was taken to prevent solution dripping onto other specimens during weighing.

vii. The mass was recorded to the nearest 0.01 g within 10 seconds of specimen removal from the tray. The specimens were then repositioned on the wet paper pad with the test face in contact. The stopwatch was not paused throughout the weighing process.

viii. Upon completion of the weighing process, specimens were placed inside a vacuum saturation tank with the packaging tape intact. They were arranged upright on their curved edges rather than their flat sides. The tank lid was sealed with petroleum jelly and closed.

ix. The tank was evacuated to a pressure of -75 to -80 kPa, maintaining this negative pressure for 3 hours ± 15 minutes. The pressure was not permitted to exceed -75 kPa during this period.

x. After 3 hours ± 15 minutes, the vacuum chamber was isolated, and calcium hydroxide-saturated water was introduced until it reached approximately 40 mm above the specimen tops. Care was taken to prevent air entry into the vacuum chamber.

xi. The vacuum was re-established at -75 to -80 kPa and maintained for an additional 1 hour ± 15 minutes. The pressure was kept below -75 kPa throughout.

xii. Following this, the vacuum was released, allowing air to enter, and the specimens were left to soak for a further 18 ± 1 hours.

xiii. After soaking, specimens were removed from the solution, dried to an SSD condition using a paper towel, and immediately weighed to an accuracy of 0.01 g. This mass was recorded as the vacuum-saturated mass (M_{sv}).

The water sorptivity (WS) was calculated using the prescribed equations in the Durability Index Testing Procedure Manual (Version 5.0, 2023).

Line of best-fit (*F*) by linear aggression analysis:

$$F = \frac{\sum\left[\sqrt{t_i} - T\right] - [M_{wti} - M_{wt}]}{\sum[\sqrt{t_i} - T]^2}$$

Where

M_{wti} = mass at any given time in grams

t_i = time in hours corresponding to the mass gain reading

$$M_{wt} = \frac{\sum M_{wti}}{n}$$

$$T = \frac{\sum \sqrt{t_i}}{n}$$

Where

n = number of data points

WS is calculated as follows:

$$WS = \frac{Fd}{M_{sv} - M_{s0}}$$

Where

WS = water sorptivity $\left[mm/\sqrt{h}\right]$

F = line of best-fit $\left[g/\sqrt{h}\right]$

d = average specimen thickness (mm)

M_{sv} = vacuum saturated mass (g)

M_{s0} = initial mass (g)

B.14: Microstructural and mineralogical analysis

Microstructural and mineralogical characteristics of concrete specimens were examined using scanning electron microscopy (SEM) and X-ray diffraction (XRD).

B.14.1: SEM

SEM analysis followed ASTM C1723-25:2022 standards:

i. Concrete samples were cut into small pieces (≤10 mm) and oven-dried at 60 ± 5°C for 24 hours.
ii. Samples were embedded in epoxy resin, cured, then ground with silicon carbide papers (120-1200 grit) and polished with diamond pastes (6 µm to 0.25 µm).
iii. After ultrasonic cleaning and vacuum drying, samples were coated with a conductive material.
iv. Images were acquired at 15-20 kV with 10-15 mm working distances, using both secondary and backscattered electron modes at magnifications from 20× to 100,000×.
v. Energy Dispersive X-ray Spectroscopy (EDS) was performed to determine elemental composition, with analysis focusing on cracks, voids, interfaces, and hydration products.

B.14.2: XRD

XRD analysis followed ASTM D3906-19:2019 standards:

i. Concrete samples were crushed, sieved (75 µm), and ground to <10 µm particle size.
ii. Analysis was performed using Cu Kα radiation (λ = 1.5406 Å) at 40 kV and 30 mA, scanning from 5° to 70° 2θ with 0.02° steps.
iii. Phase identification used the International Centre for Diffraction Data (ICDD) database, with semi-quantitative analysis by Rietveld refinement.
iv. Results were presented as diffractograms with identified phases marked.

Appendix C: Test results

C.1: Particle size distribution test results (waste glass)

Waste glass gradation test: SANS 3001-AG1:2014					SANS 1083:2013 Specification		
Sieve sizes (mm)	Sample A % Passing	Sample B % Passing	Sample C % Passing	Combined % Passing			
37.5	100.00	100.00	100.00	100.00	100	-	100
28.0	100.00	100.00	100.00	100.00	100	-	100
20.0	100.00	100.00	100.00	100.00	100	-	100
14.0	100.00	100.00	100.00	100.00	100	-	100
10.0	100.00	100.00	100.00	100.00	100	-	100
7.1	100.00	100.00	100.00	100.00	100	-	100
5.00	100.00	100.00	100.00	100.00	90	-	100
2.00	58.04	51.90	53.36	54.43	75	-	100
1.00	9.87	5.99	6.82	7.56	60	-	90
0.600	3.28	1.64	2.08	2.33	40	-	60
0.300	1.27	0.63	0.94	0.95	20	-	40
0.150	0.48	0.28	0.54	0.43	10	-	20
0.075	0.04	0.12	0.21	0.12	5	-	10
0.000	0.00	0.00	0.00	0.00			
Total Mass (g)	600.00	599.20	590.90	596.70			
Fineness Modulus (FM)	(4.27+4.40+4.36)/3 = 4.34						
Relative Density (RD), kg/m^3	2.53						

C.2: Particle size distribution test results (Philippi dune sand)

Philippi dune sand gradation test: SANS 3001-AG1:2014					SANS 1083:2013 Specification
Sieve sizes (mm)	Sample A % Passing	Sample B % Passing	Sample C % Passing	Combined % Passing	
37.5	100.00	100.00	100.00	100.00	100 - 100
28.0	100.00	100.00	100.00	100.00	100 - 100
20.0	100.00	100.00	100.00	100.00	100 - 100
14.0	100.00	100.00	100.00	100.00	100 - 100
10.0	100.00	100.00	100.00	100.00	100 - 100
7.1	100.00	100.00	100.00	100.00	100 - 100
5.00	100.00	100.00	100.00	100.00	90 - 100
2.00	100.00	100.00	100.00	100.00	75 - 100
1.00	99.00	99.53	98.78	99.11	60 - 90
0.600	94.36	94.35	93.86	94.19	40 - 60
0.300	69.49	68.41	68.11	68.67	20 - 40
0.150	10.11	13.73	10.19	11.34	10 - 20
0.075	0.42	0.50	0.37	0.43	5 - 10
0.000	0.00	0.00	0.00	0.00	
Total Mass (g)	600.00	599.20	590.90	596.70	
Fineness Modulus (FM)	(1.27+1.24+1.29)/3 = 1.27				
Relative Density (RD), kg/m^3	2.58				

C.3: Particle size distribution test results (Crusher dust)

Crusher dust gradation test: SANS 3001-AG1:2014					SANS 1083:2013 Specification		
Sieve sizes (mm)	Sample A % Passing	Sample B % Passing	Sample C % Passing	Combined % Passing			
37.5	100.00	100.00	100.00	100.00	100	-	100
28.0	100.00	100.00	100.00	100.00	100	-	100
20.0	100.00	100.00	100.00	100.00	100	-	100
14.0	100.00	100.00	100.00	100.00	100	-	100
10.0	100.00	100.00	100.00	100.00	100	-	100
7.1	100.00	100.00	100.00	100.00	100	-	100
5.00	91.74	91.29	90.68	91.24	90	-	100
2.00	38.44	36.79	35.46	36.90	75	-	100
1.00	22.93	20.96	20.23	21.37	60	-	90
0.600	15.57	13.89	13.36	14.27	40	-	60
0.300	8.55	7.52	7.20	7.76	20	-	40
0.150	4.58	3.95	3.72	4.08	10	-	20
0.075	0.80	0.77	0.74	0.77	5	-	10
0.000	0.00	0.00	0.00	0.00			
Total Mass (g)	600.00	599.20	590.90	596.70			
Fineness Modulus (FM)	(4.18+4.26+4.29)/3 = 4.24						
Bulk Relative Density (BRD), kg/m^3	2.74						

C.4: Particle size distribution test results (Sand-crusher dust)

Sand-crusher dust gradation test: SANS 3001-AG1:2014					SANS 1083:2013 Specification		
Sieve sizes (mm)	Sample A % Passing	Sample B % Passing	Sample C % Passing	Combined % Passing			
37.5	100.00	100.00	100.00	100.00	100	-	100
28.0	100.00	100.00	100.00	100.00	100	-	100
20.0	100.00	100.00	100.00	100.00	100	-	100
14.0	100.00	100.00	100.00	100.00	100	-	100
10.0	100.00	100.00	100.00	100.00	100	-	100
7.1	100.00	100.00	100.00	100.00	100	-	100
5.00	97.88	98.08	97.05	97.67	90	-	100
2.00	83.43	83.92	81.31	82.89	75	-	100
1.00	77.42	77.38	76.42	77.07	60	-	90
0.600	71.61	71.21	70.83	71.22	40	-	60
0.300	51.39	50.55	49.63	50.53	20	-	40
0.150	9.44	9.93	9.66	9.68	10	-	20
0.075	0.62	0.62	0.53	0.59	5	-	10
0.000	0.00	0.00	0.00	0.00			
Total Mass (g)	600.00	599.20	590.90	596.70			
Fineness Modulus (FM)	(2.09+2.09+2.15)/3 = 2.11						
Bulk Relative Density (BRD), kg/m^3	2.74						

C.5: Particle size distribution test results (Fine aggregate)

Fine aggregates gradation test: SANS 3001-AG1:2014					SANS 1083:2013 Specification		
Sieve sizes (mm)	Waste glass % Passing	Sand % Passing	Crusher dust % Passing	Sand-crusher dust % Passing			
37.5	100.00	100.00	100.00	100.00	100	-	100
28.0	100.00	100.00	100.00	100.00	100	-	100
20.0	100.00	100.00	100.00	100.00	100	-	100
14.0	100.00	100.00	100.00	100.00	100	-	100
10.0	100.00	100.00	100.00	100.00	100	-	100
7.1	100.00	100.00	100.00	100.00	100	-	100
5.00	100.00	98.37	91.24	97.67	90	-	100
2.00	54.43	73.22	36.90	82.89	75	-	100
1.00	7.56	53.79	21.37	77.07	60	-	90
0.600	2.33	48.12	14.27	71.22	40	-	60
0.300	0.95	33.71	7.76	50.53	20	-	40
0.150	0.43	6.67	4.08	9.68	10	-	20
0.075	0.12	0.43	0.77	0.59	5	-	10
0.000	0.00	0.00	0.00	0.00			
Total Mass (g)	600.00	599.20	590.90	596.70			

C.6: Particle size distribution test results (Coarse aggregate)

Coarse aggregate gradation test: SANS 3001-AG1:2014				
Sieve sizes (mm)	Sample A % Passing	Sample B % Passing	Sample C % Passing	Combined % Passing
37.5	100.00	100.00	100.00	100.00
28.0	100.00	100.00	100.00	100.00
20.0	89.66	92.89	91.24	91.27
14.0	17.93	19.16	23.33	20.14
10.0	1.71	1.73	2.30	1.91
7.1	0.21	0.20	0.23	0.21
5.00	0.02	0.02	0.06	0.03
2.00	0.00	0.00	0.00	0.00
1.00	0.00	0.00	0.00	0.00
0.600	0.00	0.00	0.00	0.00
0.300	0.00	0.00	0.00	0.00
0.150	0.00	0.00	0.00	0.00
0.075	0.00	0.00	0.00	0.00
0.000	0.00	0.00	0.00	0.00
Total Mass (g)	2367.80	2482.60	2487.60	2446.00
Fineness Modulus (FM)	(3.57+3.57+3.50)/3 = 3.55			
Bulk Relative Density (BRD), kg/m^3	2.74			

C.7: Slump test results

w/c ratio	Glass content (%)	Slump (mm)		
		Individual	Mean	Std. Dev
0.50	0	70	63.3	5.77
		60		
		60		
	10	60	48.3	10.41
		45		
		40		
	20	50	46.7	2.89
		45		
		45		
0.66	0	100	101.7	2.89
		100		
		105		
	10	105	105.0	0.00
		105		
		105		
	20	110	110.0	0.00
		110		
		110		

C.8: Flow test results

w/c ratio	Glass content (%)	Flow (mm)		
		Individual	Mean	Std. Dev
0.50	0	390	390.0	0.00
		390		
		390		
	10	380	383.3	5.77
		390		
		380		
	20	380	380.0	0.00
		380		
		380		
0.66	0	480	486.7	5.77
		490		
		490		
	10	490	495.0	5.00
		495		
		500		
	20	500	498.3	7.64
		490		
		505		

C.9: Vebe time test results

w/c ratio	Glass content (%)	Vebe time (s)		
		Individual	Mean	Std. Dev
0.50	0	3.00	3.0	0.00
		3.00		
		3.00		
	10	3.56	3.5	0.06
		3.50		
		3.45		
	20	3.65	3.6	0.05
		3.58		
		3.55		
0.66	0	3.25	3.4	0.10
		3.38		
		3.45		
	10	3.00	3.0	0.00
		3.00		
		3.00		
	20	2.78	2.9	0.09
		2.84		
		2.95		

C.10: Fresh density test results

w/c ratio	Glass content (%)	Fresh density (kg/m^3)		
		Individual	Mean	Std. Dev
0.50	0	2474	2454	17.11
		2444		
		2444		
	10	2430	2420	8.55
		2415		
		2415		
	20	2415	2395	22.63
		2370		
		2400		
0.66	0	2430	2435	8.55
		2430		
		2444		
	10	2370	2400	29.63
		2430		
		2400		
	20	2370	2390	22.63
		2415		
		2385		

C.11: Hardened density test results (w/c = 0.50)

w/c ratio	Glass content (%)	Age (days)	Hardened density (kg/m^3)		
			Individual	Mean	Std. Dev
0.50	0	3	2359	2390	30.96
			2421		
			2389		
		7	2390	2387	6.66
			2392		
			2380		
		14	2385	2385	14.81
			2370		
			2400		
		28	2382	2381	2.91
			2377		
			2382		
0.50	10	3	2347	2347	8.79
			2355		
			2338		
		7	2367	2345	24.48
			2348		
			2319		
		14	2350	2341	12.93
			2346		
			2326		
		28	2341	2338	2.41
			2338		
			2336		
0.50	20	3	2314	2310	4.46
			2305		
			2311		
		7	2311	2307	3.05
			2306		
			2305		
		14	2296	2304	7.72
			2306		
			2311		
		28	2311	2301	10.41
			2304		
			2290		

C.12: Hardened density test results (w/c = 0.66)

w/c ratio	Glass content (%)	Age (Days)	Hardened density (kg/m^3)		
			Individual	Mean	Std. Dev
0.66	0	3	2333	2325	7.73
			2318		
			2326		
		7	2326	2318	8.81
			2321		
			2309		
		14	2319	2315	4.10
			2315		
			2310		
		28	2316	2311	4.59
			2307		
			2309		
0.66	10	3	2290	2283	9.91
			2286		
			2271		
		7	2267	2277	9.87
			2278		
			2286		
		14	2278	2273	12.66
			2259		
			2283		
		28	2267	2269	13.55
			2257		
			2283		
0.66	20	3	2207	2242	30.84
			2267		
			2252		
		7	2222	2239	15.07
			2242		
			2252		
		14	2207	2232	30.84
			2222		
			2267		
		28	2252	2228	20.98
			2213		
			2219		

C.13: Compressive strength test results (w/c = 0.50)

w/c ratio	Glass content (%)	Age (days)	Compressive strength (MPa)		
			Individual	Mean	Std. Dev
0.50	0	3	33.4	34.9	1.32
			35.4		
			35.9		
		7	35.3	35.7	3.60
			39.5		
			32.3		
		14	43.0	42.4	2.71
			44.8		
			39.4		
		28	41.2	43.4	2.11
			43.7		
			45.4		
0.50	10	3	31.2	31.9	0.56
			32.3		
			32.0		
		7	32.6	32.7	0.33
			33.0		
			32.4		
		14	34.6	36.6	1.72
			37.6		
			37.5		
		28	39.4	37.0	2.16
			35.6		
			35.8		
0.50	20	3	28.6	28.9	0.58
			28.5		
			29.6		
		7	29.9	30.3	0.69
			31.1		
			29.9		
		14	33.1	33.3	0.69
			34.0		
			32.7		
		28	34.6	34.4	0.59
			34.9		
			33.8		

C.14: Compressive strength test results (w/c = 0.66)

w/c ratio	Glass content (%)	Age (days)	Compressive strength (MPa)		
			Individual	Mean	Std. Dev
0.66	0	3	20.9	22.01	1.32
			21.6		
			23.5		
		7	27.4	27.82	0.68
			28.6		
			27.5		
		14	30.7	30.68	0.15
			30.8		
			30.5		
		28	33.1	32.86	0.18
			32.7		
			32.8		
0.66	10	3	19.1	19.18	0.28
			19.5		
			19.0		
		7	21.6	21.99	0.53
			22.6		
			21.8		
		14	22.9	23.06	0.50
			22.7		
			23.6		
		28	25.6	25.04	0.59
			24.5		
			25.0		
0.66	20	3	13.5	13.3	0.21
			13.3		
			13.1		
		7	16.1	16.6	0.62
			16.4		
			17.3		
		14	18.7	18.5	0.20
			18.3		
			18.4		
		28	20.1	19.8	0.30
			19.5		
			19.9		

C.15: Accelerated drying shrinkage test results

Age (days)	Accelerated drying shrinkage (microstrains)					
	w/c ratio: 0.50			w/c ratio: 0.66		
	0%	10%	20%	0%	10%	20%
0	0	0	0	0	0	0
7	-	-	-	265	-	237.5
8	-	-	-	-	193	-
9	-	-	-	268	-	-
10	-	-	-	-	282	302.5
11	-	-	202.5	-	300	-
12	-	235	-	386	-	290
13	310	-	172	-	283	-
14	-	182.5	-	342	-	304
15	236	-	252	-	328	-
16	-	255	-	398	-	-
17	304	-	274	-	-	352.5
18	-	280	-	-	350	-
19	314	-	220	392	-	372
20	-	247.5	-	-	350	-
21	298	-	272	393	-	374
22	-	295	-	-	352	-
23	350	-	-	418	-	-
24	-	-	294	-	-	388
25	-	320	-	-	370	-
26	376	-	326	430	-	372
27	-	340	-	-	344	-
28	394	-	312	422	-	-
29	-	325	-	-	-	393
30	384	-	-	-	366	-
31	-		352	428	-	-
32	-	370	-	-	-	355
33	418	-	350	-	332	-
34	-	377	-	404	-	362
35	414	-	-	-	338	-
36	-	-	358	412	-	342
37	-	375	-	-	330	-
38	430	-	-	396	-	-

C.16: Accelerated drying shrinkage test results continued

Age (days)	Accelerated drying shrinkage (microstrains)					
	w/c ratio: 0.50			w/c ratio: 0.66		
	0%	10%	20%	0%	10%	20%
39	-	-	364	-	-	328
40	-	377.5	-	-	294	-
41	424	-	370	364	-	326
42	-	380	-	-	298	-
43	430	-	258	360	-	314
44	-	280	-	-	298	-
45	360	-	-	350	-	-
46	-	-	292	-	-	315
47	-	302.5	-	-	302	-
48	382.5	-	282	366	-	320
49	-	305	-	-	298	-
50	387.5	-	277.5	366	-	324
51	-	287.5	-	-	308	-
52	367.5	-	-	372	-	-
53	-	-	285	-	-	318
54	-	307.5	-	-	298	-
55	360	-	282.5	378	-	-
56	-	297.5	-	-	-	-
57	365	-	286	-	-	-
58	-	302.5	-	-	-	-
59	377.5	-	-	-	-	-
60	-	-	290	-	-	-
61	-	302.5	-	-	-	-

C.17: Concrete surface resistivity test results

w/c ratio	Mix ID (%)	Specimen ID	Resistivity					Mix Mean	Resistivity Std Dev	Resistivity COV (%)	Chloride Ion Penetrability
			1	2	3	4	Mean				
0.50	0	1	9.5	9.3	9.2	9.3	9.3	9.7	0.38	4	Moderate
		2	10.3	10.2	9.9	9.9	10.1				
		3	9.7	10.4	9.6	9.4	9.8				
	10	1	10.5	10.7	9.5	9.7	10.1	10.1	0.01	0	Moderate
		2	9.9	10.4	10.5	9.6	10.1				
		3	10.4	10	10.2	9.7	10.1				
	20	1	10.9	9.5	11.1	10.2	10.4	10.8	0.30	3	Moderate
		2	10.8	10.5	10.4	12	10.9				
		3	11.3	11	10.3	11.3	11.0				
0.66	0	1	8.7	7.6	8	8.6	8.2	7.6	0.58	8	High
		2	6.9	8	7.4	7.9	7.6				
		3	6.9	7.4	7.2	6.8	7.1				
	10	1	9.6	10.9	10.4	11.1	10.5	9.7	0.70	7	Moderate
		2	8.7	9.4	9.7	9.5	9.3				
		3	9.4	8.6	9.3	9.7	9.3				
	20	1	7.1	7.5	7.6	7.9	7.5	7.7	0.11	1	High
		2	7.0	7.4	8.1	8.4	7.7				
		3	8.1	7.4	7.9	7.4	7.7				

C.18: Suggested ranges of durability index value (Alexander et al., 2009a)

Durability Class	OPI (Log scale)	Sorptivity (mm/H)	Chloride Conductivity (mS/cm)
Excellent	> 10	< 6.0	< 0.75
Good	9.5 – 10	6.0 – 10	0.75 – 1.5
Poor	9.0 – 9.5	10 – 15	1.50 – 2.5
Very poor	< 9.0	> 15	> 2.5

C.19: OPI test results (cut surfaces): 7 days values only compared

OPI values (7 days values only compared): w/c = 0.50w/c ratio	Glass content (%)	Disk number	k (m/s)	OPI (Log scale)
0	0	1	6.485E-11	10.19
		2	6.190E-11	10.21
		3	2.737E-11	10.56
		4	2.210E-11	10.66
		Mean	4.405E-11	10.40
		Std dev.	2.244E-11	0.24
		Standard Error	1.122E-11	0.12
		95% Confidence Interval	2.244E-11	0.24
		COV (%)	51	2.31
	10	1	3.012E-11	10.52
		2	2.507E-11	10.60
		3	3.585E-11	10.45
		4	4.748E-11	10.32
		Mean	3.463E-11	10.47
		Std dev.	9.632E-12	0.12
		Standard Error	4.816E-12	0.06
		95% Confidence Interval	9.632E-12	0.12
		COV (%)	28	1.13
	20	1	2.470E-11	10.61
		2	1.537E-10	9.81
		3	3.720E-11	10.43
		4	2.909E-10	9.54
		Mean	1.266E-10	10.10
		Std dev.	1.240E-10	0.51
		Standard Error	6.199E-11	0.25
		95% Confidence Interval	1.240E-10	0.51
		COV (%)	98	5.00

C.20: OPI test results (cut surfaces): 7 days values only compared

OPI values (7 days values only compared): w/c = 0.66

w/c ratio	Glass content (%)	Disk number	k (m/s)	OPI (Log scale)
0.66	0	1	5.975E-11	10.22
		2	1.875E-10	9.73
		3	7.756E-11	10.11
		4	2.859E-10	9.54
		Mean	1.527E-10	9.90
		Std dev.	1.053E-10	0.32
		Standard Error	5.264E-11	0.16
		95% Confidence Interval	1.053E-10	0.32
		COV (%)	69	3.23
	10	1	2.855E-10	10.22
		2	2.500E-10	10.22
		3	1.991E-10	10.22
		4	2.767E-10	10.22
		Mean	2.528E-10	10.22
		Std dev.	3.888E-11	0.00
		Standard Error	1.944E-11	0.00
		95% Confidence Interval	3.888E-11	0.00
		COV (%)	15	0.00
	20	1	3.571E-11	10.45
		2	8.109E-11	10.09
		3	3.588E-11	10.45
		4	5.456E-11	10.26
		Mean	5.181E-11	10.31
		Std dev.	2.143E-11	0.17
		Standard Error	1.072E-11	0.09
		95% Confidence Interval	2.143E-11	0.17
		COV (%)	41	1.65

C.21: OPI test results (-log10k[m^2])

w/c Ratio	Glass content (%)	Disk 1	Disk 2	Disk 3	Disk 4	Mean
0.5	0%	10.19	10.21	10.56	10.66	10.40
0.5	10%	10.52	10.60	10.45	10.32	10.47
0.5	20%	10.61	9.81	10.43	9.54	10.10
0.66	0%	10.22	9.73	10.11	9.54	9.90
0.66	10%	10.22	10.22	10.22	10.22	10.22
0.66	20%	10.45	10.09	10.45	10.26	10.31

C.22: WSI test results (cut surfaces): 7 days values only compared

WSI values (7 days values only compared): w/c = 0.50

w/c ratio	Glass content (%)	Disk Number	Sorptivity (mm/hr$^{0.5}$)	Porosity (%)
0.50	0	1	9.54	9.27
		2	8.81	9.77
		3	7.84	9.49
		4	8.42	10.45
		Mean	8.65	9.74
		Std dev.	0.71	0.51
		Standard Error	0.36	0.26
		95% Confidence Interval	0.71	0.51
		COV (%)	8.25	5.24
	10	1	8.63	9.19
		2	7.45	9.67
		3	8.83	9.54
		4	9.79	8.32
		Mean	8.68	9.18
		Std dev.	0.96	0.61
		Standard Error	0.48	0.30
		95% Confidence Interval	0.96	0.61
		COV (%)	11.06	6.60
	20	1	8.97	9.72
		2	7.56	9.52
		3	8.74	8.97
		4	8.03	10.80
		Mean	8.32	9.75
		Std dev.	0.65	0.77
		Standard Error	0.32	0.38
		95% Confidence Interval	0.65	0.77
		COV (%)	7.81	7.89

C.23: WSI test results (cut surfaces): 7 days values only compared

WSI values (7 days values only compared): w/c = 0.66

w/c ratio	Glass content (%)	Disk Number	Sorptivity (mm/hr$^{0.5}$)	Porosity (%)
0.66	0	1	5.45	15.72
		2	5.40	15.68
		3	5.21	16.76
		4	5.51	14.82
		Mean	5.39	15.74
		Std dev.	0.13	0.79
		Standard Error	0.06	0.40
		95% Confidence Interval	0.13	0.79
		COV (%)	2.37	5.04
	10	1	8.10	10.98
		2	7.21	11.47
		3	8.61	10.59
		4	8.08	11.10
		Mean	8.00	11.03
		Std dev.	0.58	0.36
		Standard Error	0.29	0.18
		95% Confidence Interval	0.58	0.36
		COV (%)	7.25	3.28
	20	1	8.25	13.01
		2	8.04	13.95
		3	7.59	12.54
		4	7.55	13.90
		Mean	7.86	13.35
		Std dev.	0.34	0.70
		Standard Error	0.17	0.35
		95% Confidence Interval	0.34	0.70
		COV (%)	4.38	5.21

Appendix D: Technical data sheets

D.24: Product data sheet

Revision number: 2
Date: 2019/09/30
Supercedes: 2014/12/10

Technical data sheet

CHRYSO® Plast Omega 122

New generation, high range water reducing plasticiser

Description

CHRYSO® Plast Omega 122 is classified as a water reducing plasticiser. The admixture thus induces the following major effects in a concrete mix:

- Without affecting the consistence (workability), permits a reduction in the water content of a given concrete or
- Without affecting the water content, increases the slump/flow or
- Produces both of the above effects simultaneously.

Standards

- **CHRYSO® Plast Omega 122** conforms to the requirements of SANS 50934-2 (EN 934-2) Table 2). These requirements are approximate equivalents of ASTM C494 Type A.

Advantages

- **CHRYSO® Plast Omega 122** is a multi-dose admixture, allowing a wide range of dosages to be applied, without any excessive retardation at the higher dosages.
- The multi-dose characteristic of **CHRYSO® Plast Omega 122** allows concrete to exhibit extended workability characteristics.
- When used to reduce the water content of a concrete mix (lower the w/b ratio) **CHRYSO® Plast Omega 122** may potentially reduce the rate of bleeding.
- **CHRYSO® Plast Omega 122** improves the cohesion and lowers the viscosity of a concrete mix. This results in an improved homogeneity and compaction, allowing for superior off-shutter finishes.
- By reducing the need to add extra water, **CHRYSO® Plast Omega 122** increases the durability of concrete, by reducing permeability.

Physical and chemical properties

- Physical state(@25°C): liquid
- Specific gravity (@25°C): 1.010 (±0.020)
- Colour: brown
- pH: 8.0 (±1.0)
- Viscosity(@25°C): 10 -20 secs (ford#4 cup)
- Solubility in water: miscible

- **CHRYSO® Plast Omega 122** is robust to differences in cement characteristics. Based on aesthetic requirements, its suitability for use with white cement, should be ascertained prior to use.
- **CHRYSO® Plast Omega 122** may be used with in mixes extended with limestone and/or typically used SCMs - GGBS, GGCS, Fly Ash and Silica Fume.
- **CHRYSO® Plast Omega 122** does not undermine the early age strength of concrete and in certain cases, may be used to improve it.
- Depending on the dosage, **CHRYSO® Plast Omega 122** will cause a relative increase of mechanical strength after 24 hours.

Application guidelines

Use

- Typically ready-mix concrete and mechanically mixed site concrete.
- Low to high workability concrete.
- Conventionally placed concrete.
- Pumped concrete.
- Highly reinforced concrete.

CHRYSO Southern Africa (Pty) Ltd.
Gauteng (head office): 26 Malcom Moodie, Crescent, Jet Park
Sharecall facility: 0861 CHRYSO | T: +27(0)11 395 9700 | F: +27(0)11 397 6644 | W: za.chryso.com

CHRYSO INNOVATION IS OUR CHEMISTRY

Revision number: 2
Date: 2019/09/30
Supercedes: 2014/12/10

Technical data sheet

CHRYSO® Plast Omega 122

New generation, high range water reducing plasticiser

Dosage

- The optimum dosage of **CHRYSO® Plast Omega 122** can only be established by using trial tests, taking into account local conditions affecting the workability of the fresh mix and the mechanical properties required of the concrete.
- Range:
  - By volume: 0.3 to 1.0 litres per 100 kg of cementitious material (including extenders)
  - By weight: 0.33 to 1.1 kg per 100 kg cementitious material (including extenders)
- Typical:
  - By volume: 0.6 to 0.8 litres per 100 kg of cementitious material (including extenders)
  - By weight: 0.61 to 0.81 kg per 100 kg cementitious material (including extenders)
- Dosages approaching and over 1.5 litres per 100 kg of cementitious material (including extenders), may progressively retard the concrete.

Dispensing/mixing

- **CHRYSO® Plast Omega 122** is completely miscible in water.
- **CHRYSO® Plast Omega 122** should never be added to dry cement or to components of a mix that are dry.
- **CHRYSO® Plast Omega 122** can be added to concrete using one of the following methods:
  - To the gauge water before mixing: **CHRYSO® Plast Omega 122** should be added to approximately 90% of the concrete's total gauge water requirement (including admixture). The remaining 10% of the concrete's total gauge water requirement (without admixture) should be added in small increments until the target concrete workability is achieved.
  - As a component of the mixing process: Should be added simultaneously with approximately 90% of the concrete's total gauge water requirement.
  - To freshly mixed concrete in a ready-mix truck drum: Reverse the ready-mix truck drum to discharge at very slow revolutions. When the concrete reaches the mouth of the drum, stop the drum. Place **CHRYSO® Plast Omega 122** on the concrete and not onto any exposed surface of the drum interior. Change the direction of the drum to mixing and ensure that all material has moved to the bottom of the drum. Repeat a minimum of 2 more times (preferably 3), the reverse to discharge at very slow revolutions, until the concrete reaches the mouth of the drum and then change to mixing until the concrete has moved to the bottom of the drum - to ensure that all of the internal upper drum surfaces have been cleared of admixture and to ensure a more effective dispersion of admixture during actual mixing. When completed, thoroughly mix the concrete at maximum permissible drum rpm, in order to ensure effective dispersion of **CHRYSO® Plast Omega 135** throughout the concrete. (a minimum of 1minute per cubic metre of concrete; therefore 6 cubic metres = minimum 6 minutes). After completion of mixing at maximum rpm and before discharge, allow the concrete to agitate for 1 - 3 minutes at very low drum rpm (travel rpm).

Storage

- **CHRYSO® Plast Omega 122** has a shelf life of 18 months starting from the manufacturing date - provided no other chemicals are added to it.
- The product should be stored away from rain and frost in clean, dry tanks.
- After freezing, the properties of **CHRYSO® Plast Omega 122** can be recovered by controlled thawing and agitation.

CHRYSO Southern Africa (Pty) Ltd.
Gauteng (head office): 26 Malcom Moodie, Crescent, Jet Park
Sharecall facility: 0861 CHRYSO | T: +27(0)11 395 9700 | F: +27(0)11 397 6644 | W: za.chryso.com

Revision number: 2
Date: 2019/09/30
Supercedes: 2014/12/10

Technical data sheet

CHRYSO® Plast Omega 122

New generation, high range water reducing plasticiser

Packaging

- 25 ℓ jerry can
- 200 ℓ drum
- 1000 ℓ flow bin
- Bulk delivery on request

Health and safety

- This product is classified as harmless. CHRYSO will provide onsite assistance when requested.
- For more information, please refer to the material safety data sheet.

CHRYSO Southern Africa (Pty) Ltd.
Gauteng (head office): 26 Malcom Moodie, Crescent, Jet Park
Sharecall facility: 0861 CHRYSO | T: +27(0)11 395 9700 | F: +27(0)11 397 6644 | W: za.chryso.com

CHRYSO
INNOVATION IS OUR CHEMISTRY